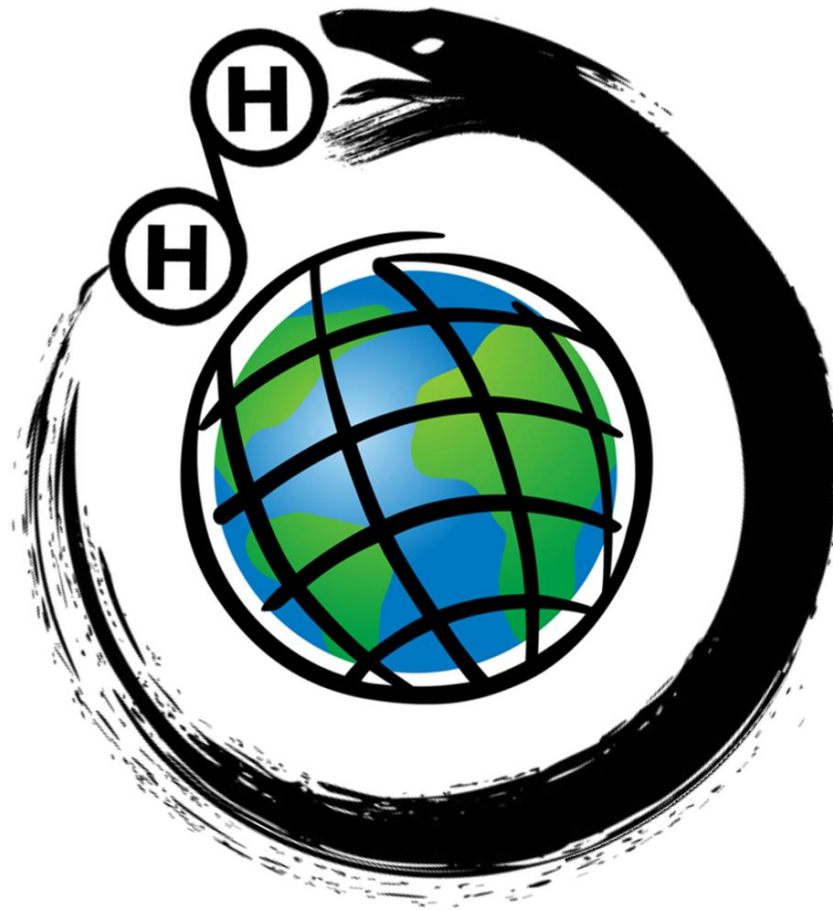


Exploring P2H futures in the North Sea using spatially explicit, techno-economic modelling



By
Daniel Fernandes

Exploring P2H futures in the North Sea using spatially explicit, techno-economic modelling

By

Daniel Xavier Fernandes

in partial fulfilment of the requirements for the degree of

Master of Science

in Sustainable Energy Technology

at the Delft University of Technology,
to be defended publicly on Monday November 30, 2020 at 1:00 PM.

Supervisor:

Thesis committee:

Prof. dr. Kornelis Blok

Chris Hellinga , TU Delft

Prof. dr. Ad. J. M. van Wijk , TU Delft

Dr. ir. Michiel. B. Zaayer , TU Delft

Contents

List of figures	5
List of Tables	8
Summary	10
Acknowledgements.....	12
1. Introduction	1
1.1. Context and relevance.....	1
1.2. Existing research	5
1.3. Problem definition.....	8
1.4. Work flow and report structure.....	9
2. Methodology	10
2.1. Configuration descriptions	11
2.2. Model overview.....	14
2.2.1. GIS inputs	14
2.2.2. Model working	20
3. Techno-economic module sizing and assumptions	22
3.1. Assumptions for the levelized cost.....	22
3.2. Component sizing and CAPEX cost assumptions.....	23
3.2.1. Generation	23
3.2.2. Conversion.....	28
3.2.3. Transmission.....	34
3.3. Other Capex	37
3.3.1. Installation.....	37

3.3.2.	Decommissioning	55
3.3.3.	Soft capex	56
3.4.	Operation and maintenance.....	57
3.5.	Lifetimes and losses	58
3.6.	Assumptions for future developments.....	60
4.	Results.....	62
4.1.	Configuration comparison (Hypothetical results).....	62
4.2.	LCOH distribution in the North Sea over time and space (Without spatial exclusions)	66
4.2.1.	Statistical LCOH distribution in the North Sea (Current prices – 2020)	66
4.2.2.	Supply curves.....	67
4.2.3.	Maps	68
4.3.	Exclusionary effects on supply pathways.....	72
4.4.	Spatial comparison between Electricity and Hydrogen production	76
5.	Discussion.....	79
5.1.	Limitations and Critique	79
5.2.	Sensitivity analysis.....	81
5.2.1.	Supply curve sensitivity to WACC rates.....	81
5.2.2.	LCOH sensitivity to WACC rates and capacity factors.....	82
5.2.3.	LCOH comparison sensitivity to cost of In-Turbine electrolyzer	83
5.3.	Model results in a wider context.....	84
6.	Conclusions	87
	Bibliography.....	89

List of figures

Figure 1.1 Future potential of hydrogen markets (IEA, 2019).....	1
Figure 1.2 Current hydrogen production costs (IEA, 2019)	2
Figure 1.3 Projected Hydrogen contribution to EU TFEC (Fuel Cells and Hydrogen Joint Undertaking (FCH), 2019)	3
Figure 1.4 (Peters et al., 2020)	6
Figure 1.5. Work flow of study.....	9
Figure 2.1 Study area	10
Figure 2.2 Schematic of Onshore configuration	11
Figure 2.3. Schematic of Offshore configuration	12
Figure 2.4. Schematic of the In-Turbine configuration.....	13
Figure 2.5 DOWA domains (Wijnant et al., 2019).....	16
Figure 2.6. Mean wind 7 year wind speed (m/s) at 10m height	17
Figure 2.7. Mean wind 7 year wind speed (m/s) at 100m height	18
Figure 2.8. North Sea bathymetric profile. Extracted from (EMODnet_bath, 2020)	19
Figure 2.9. Assumed onshore deliver/port locations.....	19
Figure 2.10. Model Algorithm.....	20
Figure 3.1. Power curve for 6MW turbine.....	24
Figure 3.2. Gross capacity factor map	24
Figure 3.3. Break-even distance between fixed and floating Total costs	27
Figure 3.4. Turbine details from (Musial et al., 2020)(Musial et al., 2019)	60
Figure 4.1. System comparison for Hypothetical cases- 2020.....	63
Figure 4.2. Levelized component cost comparison for Hypothetical cases - 2020.....	64
Figure 4.3. LCOH contour plots - Hypothetical - 2020.....	64

Figure 4.4. Temporal LCOH projection – Hypothetical	65
Figure 4.5. Statistical distribution of LCOH clusters in the North Sea - 2020	66
Figure 4.6. LCOH supply curves for the North Sea accross time	67
Figure 4.7. LCOH maps for the onshore configuration accross time	68
Figure 4.8. LCOH maps for the offshore configuration accross time	69
Figure 4.9. LCOH maps for the In Turbine configuration accross time	69
Figure 4.10. LCOH comparison maps for the offshore vs onshore configuration accross time	70
Figure 4.11. LCOH comparison maps for the In Turbine vs onshore configuration accross time	71
Figure 4.12. LCOH comparison maps for the In Turbine vs offshore configuration accross time	71
Figure 4.13. Pie chart of the maximum unrestricted GW capacity potentials in the North Sea	72
Figure 4.14. Exclusionary effects on the power capacity of each country - 2020	73
Figure 4.15. Effects of each exclusion on the theoretical yields for each country - 2020	74
Figure 4.16. Comparison between maximum restricted and unrestricted H ₂ yield potentials in the North Sea - 2020	74
Figure 4.17. Comparison between restricted and unrestricted supply curves for each configuration type - 2020	75
Figure 4.18. LCOE comparison maps for offshore P2H vs HVDC P2E accross time	76
Figure 4.19. LCOE comparison maps for In Turbine P2H vs HVDC P2E accross time	77
Figure 4.20. Yield comparison maps for offshore P2H vs HVDC P2E accross time	78
Figure 4.21. Yield comparison maps for In Turbine P2H vs HVDC P2E accross time	78
Figure 5.1. Supply curve sensitivity to WACC rates - 2020	81
Figure 5.2. LCOH sensitivy to gross capacity factor and WACC rates for the three configurations (Hypothetical cases - 2020)	82
Figure 5.3. Relative LCOH sensitivity comparison for variable In-Turbine electrolyzer costs	83
Figure 5.4. LCOH boxplot comparing the range of costs to satisfy 2050 H ₂ demands	84

Figure 5.5. LCOH boxplot comparing the range of costs to satisfy 2050 H₂ demands after competition with 212GW OWFs 85

Figure 5.6. LCOE boxplot comparing the range of costs to satisfy EU-2050 TFEC demand 86

Figure 5.7. LCOE boxplot comparing the range of costs to satisfy EU-2050 TFEC demand with all exclusions 86

List of Tables

Table 1.1 Hydrogen production routes in the North Sea.....	5
Table 1.2 Yield assessments for the North Sea	7
Table 2.1 System configurations.....	11
Table 2.2. List of GIS inputs.....	14
Table 3.1. Feasible depth ranges for each foundation type.....	27
Table 3.2. Offshore Substation electrical equipment and facilities costs (excluding substation structure) ...	28
Table 3.3. Material and manufacturing cost rates (dNVGL, 2018)(van Schot and Jepma, 2020).....	30
Table 3.4. DC cable options(Rubí and González, 2018)	34
Table 3.5. Inputs for the installation of fixed RNA and tower	39
Table 3.6. Transit faction calculation (Fixed turbine)	39
Table 3.7. Depth fraction calculation (Fixed turbine)	39
Table 3.8. Inputs for the installation of fixed foundations.....	41
Table 3.9. Transit faction calculation (Fixed turbine foundation).....	42
Table 3.10. Depth fraction calculation (Fixed turbine foundation).....	42
Table 3.11. Inputs for the installation of fixed foundations.....	44
Table 3.12. Transit faction calculation (Fixed offshore substation)	45
Table 3.13. Depth faction calculation (Fixed offshore substation)	45
Table 3.14. Inputs for the installation of floating technologies	47
Table 3.15. Transit fraction calculation (Floating offshore turbine and platform).....	48
Table 3.16. Transit faction calculation (Floating turbine platform mooring system).....	48
Table 3.17. Transit fraction calculation (Floating offshore turbine and platform).....	50
Table 3.18. Transit faction calculation (Floating turbine platform mooring system).....	50

Table 3.19. Inputs for the installation of AC and DC cables 52

Table 3.20. Length fraction calculation (DC cables) 52

Table 3.21. Transit and Length fraction calculation (DC cables) 53

Table 3.22. Decommissioning assumptions 55

Table 3.23. Soft CAPEX assumptions..... 56

Table 3.24. Operation and maintenance cost percentages 57

Table 3.25. Component lifetimes 58

Table 3.26. Component specific loss assumptions..... 59

Table 3.27. Assumptions for future developments 61

Table 5.1. Projected 2050 TFEC demands in Europe 84

Summary

Hydrogen, as a fuel, will soon play a key role in helping economies transition to more sustainable practices. Having always garnered attention due to its non-polluting nature, the costs associated with its production have stood in the way of it being more widely used in society. Since the cost of clean energy to produce hydrogen is one of the main reasons the current price is so high, locations with a high renewable potential are being looked at as a means to drive production prices down, benefiting from higher capacity factors at these locations. With near ideal offshore wind resources, the North Sea is one such location. This thesis aims to explore the potential of this resource to deliver future hydrogen and to a larger extent, EU TFEC demand in 2050. The main research question therefore asks:

“What is the future potential of P2H in the North Sea , from a spatially explicit, techno-economic perspective”

The analysis first explored the cost of different production configurations, mainly comparing the production of hydrogen onshore (via electricity transmitted over HVDC- high voltage direct current cables), offshore (after transmitting to shore via a pipeline) and in offshore wind turbines (again, after transmission to shore in a network of pipelines). The analysis then used GIS data to analyze the production potential in the North Sea by taking exclusion zones into account. A mapping model was therefore developed to estimate theoretical and practical yield potentials in steps of 5 years, until 2050. Supply curves and maps were then generated to paint a picture of P2H supply pathways in the North Sea.

One of the designated research goals in the thesis was to offer a comparative analysis between the three P2H configuration types, mentioned above. The results show a clear preference in favour of the In Turbine configuration which is followed by the offshore configuration and finally the onshore type. The hierarchy was mainly influenced by the conversion chain losses in the three configurations, with the In Turbine configuration having the lowest losses, followed by the offshore and then the onshore types.

Model results show a higher sensitivity to sea depth than transmission distance to shore for all three configuration types up till the fixed to floating transition point, after which the sensitivity to depth is reduced. The In Turbine and offshore configurations were however, predictably less sensitive to transmission distance than the onshore configuration since H₂ pipeline investment costs for large delivery capacities are almost negligible in comparison to HVDC electricity transportation.

Fishing zones, shipping zones, nature conservation zones and current wind farms were considered as exclusionary constraints in the model. This was done to test the influence of maritime spatial planning on both yield and costs in the North Sea. As far as country-specific yields to satisfy 2050 demands are concerned, only Germany, Belgium and France experience a lack of H₂ production capacities, owing to smaller and/or heavily restricted marine spaces. The four other countries have enough H₂ yield potentials that raise the possibility of not just completely satisfying national demands, but also extending that supply to both the EU and/or exporting H₂ as a commodity to the rest of the world. The exclusionary effects on costs are least felt by the In turbine configuration due to flatter supply curves while the Onshore configuration type is the most severely affected due to the loss of cheap near-shore locations. The total restricted and unrestricted yield potentials from the in-turbine configuration with the least losses were 15.8 and 24.18 EJ respectively. This represents 47% and 72% of EU total final energy consumption (TFEC) in 2050.

The (Power to Hydrogen) P2H supply pathways were finally compared to a conventional HVDC (Power to Electricity) P2E supply routes for the North Sea and interestingly, a few offshore and all in-turbine P2H locations become cheaper than P2E in the North Sea area between 2040-2050. This begs the question: 'What is the best/most cost effective supply pathway that leads us to a decarbonized energy system by 2050'. When the four supply pathways (3 P2H and 1 P2E) were viewed through the lens of supplying 50% of EU TFEC, the values reaffirm the previous results which indicate that between 2040-2050, the range of values needed to satisfy this future TFEC is cheaper for hydrogen than HVDC electricity.

The reality is that future sustainable energy generation capacities will be made up of a mix of sources and carriers that vary per country and region. However, the results in this study indicate that careful consideration needs to be given to the best possible production pathways, particularly, in the North Sea.

Acknowledgements

I would like to firstly thank my supervisor Prof. dr. Kornelis Blok for his guidance during this Master's thesis. I would also like to express my gratitude for giving me the opportunity to work on this thesis. When I was a little lost in terms of a future direction to head in, I was presented with a topic that would not only intrigue me in the present, but also shine a light on an area of research that will continue to intrigue me in the future, even though I did not realize it at the time. Working through this thesis and being allowed the freedom to express myself, for better or for worse, has shown me a potential path to walk on in my future career.

I would like to thank the members of the thesis committee. Dr. ir. Michiel. B. Zaayer, for always managing to take the time out when I was facing bottlenecks and providing keen, valuable advice. Prof. dr. Ad. J. M. van Wijk and Chris Hellinga for their critical but essential feedback that helped push me to challenge my-self and deliver meaningful results.

I would like to also express special gratitude to Maarten Verkou for helping me through this thesis, whose guidance allowed me to challenge myself with it's approach. Maarten, you are a madman. Never change.

Finally, I would like to thank my family for their endless love and support through all the years of my life, without whom I would not have had the opportunity to become the person I am today.

1. Introduction

1.1. Context and relevance

Hydrogen in the global context

1.1.1 Globally, around 115 million tons of hydrogen is consumed per year (IEA, 2019). Hydrogen today is mainly used in oil refining and in the production of ammonia. Other major uses include indirect uses of hydrogen in the production of methanol, and the direct reduction of iron ore to produce steel. This current hydrogen demand is projected to increase in both existing markets and potential future uses. Figure 1.1 below summarizes the IEA's findings on the potential prospects for hydrogen use in various sectors, in both the near and far term.

Type of application	Application	Size of the 2030 opportunity (ktH ₂ /yr)	Long-term potential scale
Major hydrogen uses today	Chemicals (ammonia and methanol)	Over 100	High
	Oil refineries and biofuels	Over 100	Medium
	Iron and steel (blending in DRI)	10-100	Low
New hydrogen uses for a clean energy system	Buildings (conversion to 100% hydrogen)	Over 100	High
	Road freight	Over 100	High
	Passenger vehicles	Over 100	Medium
	Buildings (blending in the gas grid)	Over 100	Low
	Iron and steel (conversion to 100% hydrogen)	10-100	High
	Aviation and maritime transport	Under 10	High
	Electricity storage	Under 10	High
	Flexible and back-up power generation	Under 10	Medium
	Industrial high-temperature heat	Under 10	Low

Figure 1.1 Future potential of hydrogen markets (IEA, 2019)

Hydrogen can be produced using different processes depending on the source of the energy or feedstock. Steam methane reforming (SMR), which uses natural gas, currently dominates the percentage of hydrogen produced, accounting for 75% of the total. Coal gasification accounts for a significant chunk of the remainder with 23%. Currently, electrolysis, which splits water into hydrogen and oxygen, only accounts for 2% of global dedicated hydrogen production (IEA, 2019).

Steam methane reforming which uses methane as both a fuel and feedstock in the ratio 3:7, is currently responsible for the consumption of 6% of global natural gas use. Meanwhile, 2% of the worlds coal is used to produce hydrogen. Due to the carbon intensive nature of these processes, around 830 MtCO₂/year is emitted as a result of dedicated hydrogen production worldwide, accounting for about 4% of global CO₂ emissions. This is roughly the equivalent to the emissions of Indonesia and the UK combined (IEA, 2019).

The costs associated with hydrogen production from renewable electrolysis is currently the main barrier to sustainable hydrogen production. On average, SMR with CCUS is the most cost effective clean production route. The cost of hydrogen production for different regions in the world is shown in Figure 1.2 below. The lower and upper bounds for conventional sources represent the costs in the near and long term. This reflects a CO₂ price of 25 \$/tCO₂ and 100 \$/tCO₂ in the near and long terms respectively. For renewables, the upper and lower bounds represent the costs in the near and long term respectively.

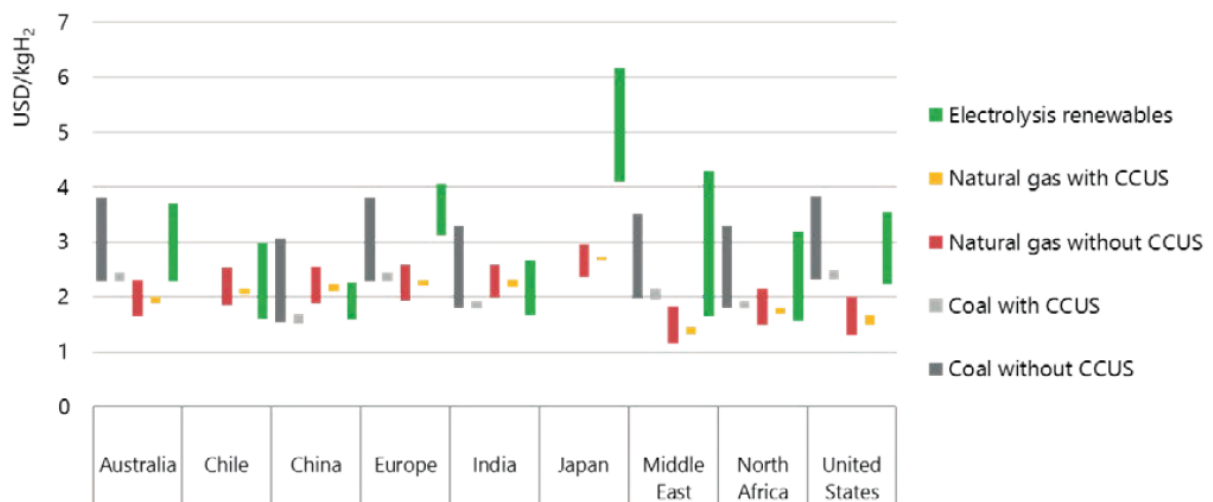


Figure 1.2 Current hydrogen production costs (IEA, 2019)

Hydrogen and Europe

The EU has expressed support for greater volumes of sustainably sourced hydrogen in the future (EU COM, 2020). This is in direct support of the 2x40 GW electrolyzer capacity envisioned by the hydrogen council by 2030 (Wijk and Chatzimarkakis, 2020). Hydrogen enables sector coupling by allowing electricity to be converted into fuels that offer more flexible decarbonization options for a variety of end use sectors. It could also serve as an essential buffer in the energy system, which enables higher penetrations of renewable generation capacities. A study conducted by the FCHJU on behalf of the EU commission, projected an H₂ contribution of 24% to EU TFEC in 2050. This amounts to 2251 TWh. The decomposition of demand per end use sector shown in Figure 1.3 below (Fuel Cells and Hydrogen Joint Undertaking (FCH), 2019). An older study called a clean planet for all, projected a hydrogen demand of 1932.57 TWh in its 1.5LIFE scenario which focused on both technological interventions, as well as interventions due to more sustainable consumption patters and business practices (EU COM, 2018). (Blanco et al., 2018) predicts an uptake of between 2364-5516 TWh, with the higher extreme being in a dedicated hydrogen scenario.

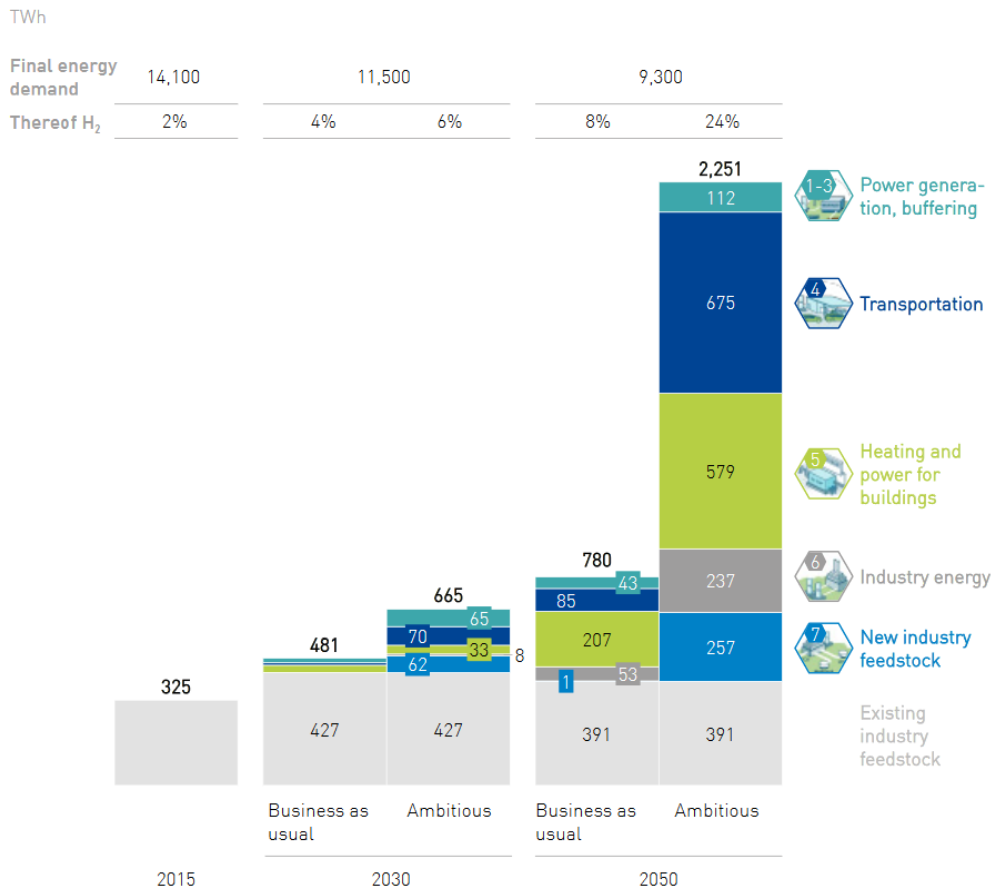


Figure 1.3 Projected Hydrogen contribution to EU TREC (Fuel Cells and Hydrogen Joint Undertaking (FCH), 2019)

Current discussions about sourcing gigawatt-scale renewable hydrogen for future EU energy systems have focused on either the North Sea or North Africa. Besides plummeting prices and making use of renewables with high capacity factors, this has to do with the fact that existing natural gas pipelines, which can be retrofitted to transmit hydrogen, already possess capacities greater than 10 times the electricity transmission capacities from said regions (Wijk and Chatzimarkakis, 2020).

Future P2H opportunities in the North Sea

There have been significant interests in the prospects of large interconnected energy systems in the North Sea. In the last decade, there have been commitments by countries that surround the North Sea to engage in a collaborative effort that aids large scale deployment of offshore wind farms in the region. More recently, this was reaffirmed by a joint statement by the North Sea countries and the European commission (NSEC, 2020). Wind Europe predicts as much as 212 GW worth of deployed capacity in the North Sea by 2050 (Wind Europe, 2019). This is a significant scale up from the current 17GW in 2019. This has resulted in a number of studies investigating potential deployment pathways for large scale interconnected hybrid projects that benefit the EU and the North Sea countries themselves (EU COM, 2019, 2016), (NSWPH, 2020).

Besides being a potential route to cost-effective hydrogen, large scale P2H deployment in the North Sea makes logical sense due to the high concentrated hydrogen demand from the countries that surround it. (Ebl, 2020). This is due to the dense clustering of industry in the region. Furthermore, the well-established Oil and gas industry in the North Sea, coupled with its proximity to salt caverns enables long term hydrogen and CO₂ storage.

The publication (van Wijk and Hellinga, 2018) posits that the true benefit of using hydrogen as the energy carrier of choice will be seen in transport over longer distances, i.e., further offshore in the North Sea .This essentially eliminates the higher costs and energetic losses associated with expensive electrical equipment, helping to drive down the cost of transported energy.

1.2. Existing research

P2G in the North Sea

As mentioned before, (van Wijk and Hellinga, 2018) note that it makes intuitive sense to opt for electricity to hydrogen conversion as close to the source as possible. When it comes to feasibility related P2H studies, this is an area that is being researched in current literature. For an offshore wind to hydrogen gas supply chain for distances below 2000 km, pipeline transmission is cheaper than transmission via ship (IEA, 2019). Therefore with the transmission options being either HVDC cables and pipelines, the alternatives that exist for the North Sea are shown in Table 1.1 below. The abbreviation OnG denotes Oil and Gas. The Oil and Gas industry has well established infrastructural assets in the North Sea. These assets, namely, platforms and pipelines, may be retrofitted and refurbished into both electricity and hydrogen production infrastructure.

Production	Offshore wind					
Conversion location	Offshore Platform		Onshore substation		Wind turbine	
	New	Reuse OnG	New	Reuse OnG	New platform	Reuse OnG platform
Transmission	Pipeline		HVDC cables		Pipeline	
	New	Reuse OnG	New		New	Reuse OnG

Table 1.1 Hydrogen production routes in the North Sea

P2G feasibility studies in the North Sea have so far, focused on site specific analyses. (dNVGL, 2018) performed a study on behalf of Gasunie and Tennet which compared onshore and offshore P2H hybrid systems for Ijmuiden Ver in the dutch North Sea. (Jepma et al., 2018) compared the production costs of P2H between dedicated offshore vs production within the turbine itself, for both new and re-utilized platforms. The study concluded with the production in the turbine being cheaper than the offshore case. (Crivellari and Cozzani, 2020) extended this analysis to include a comparison between H₂, SNG and methanol production routes for different end use sectors. However these analyses have not considered a generalized cost analysis over a larger study space, incorporating a wider range of factors that affect calculations. While the benefits of dedicated P2H systems that convert electricity to hydrogen as close to the source as possible have been analyzed before, it is unclear how this translates to the entire North Sea area.

Maritime spatial planning in the North Sea

Besides revealing possible benefits of long distance pipeline transmission, a spatially explicit yield assessment is crucial because any conversation about large volumes of offshore wind in the North Sea, raises questions about the availability of space, since the North Sea is one of the most heavily utilized marine spaces in the world. The need to address these conflicting uses and to find integrated solutions that benefit all economic sectors is made clear in the EU's Blue economy report (European Commission, 2019). Fishing, shipping, Oil and gas, and military activities, take up a significant portion of the available space.

These constraints have let to spatially explicit yield assessments being conducted, to quantify how these restrictions could affect the deployment of offshore wind in the future. To add to the competition for space

with human activities, natural habitats are significantly affected by both the construction and operation of wind farms. (European Commission, 2017) assessed how offshore wind farms affect the flora and fauna of a certain area. While activities such as foundation laying for example, do negatively affect the biodiversity that surround the farm, studies have also shown that wind farms could possibly lead to the formation of new ecosystems, benefitting some organisms while costing others. There are however, still unknowns in relation to the effects of offshore wind farms on the natural environment. This is highlighted by the fact that there exist no explicit laws that forbid the deployment of farms in a certain protected space (European Commission, 2017). The possibility of deployment in protected areas are subject to decisions following environmental impact assessments. Nevertheless, the possible negative consequences of human encroachment in the maritime space need to be taken into account and may possibly further restrict available areas for future development.

GIS based offshore wind analyses

The explicit accounting of space is a key feature of GIS based yield and Levelized Production Cost (LPC) assessments. It is mainly utilized during the pre-planning phase of project development such as in (Commission, 2019) when applied on a regional scale in the Baltic Sea. Its use in research though varies depending on the problem at hand. When it comes to energy system planning, GIS data is mainly used as a basis for resource assessments. However, other uses include infrastructure modelling and more recently, as a way to generate spatially explicit virtual environments in agent based modelling.

(Peters et al., 2020) performed a meta-analysis of GIS use in published offshore wind research. Figure 1.4 below shows the usage and number of occurrences of these studies.

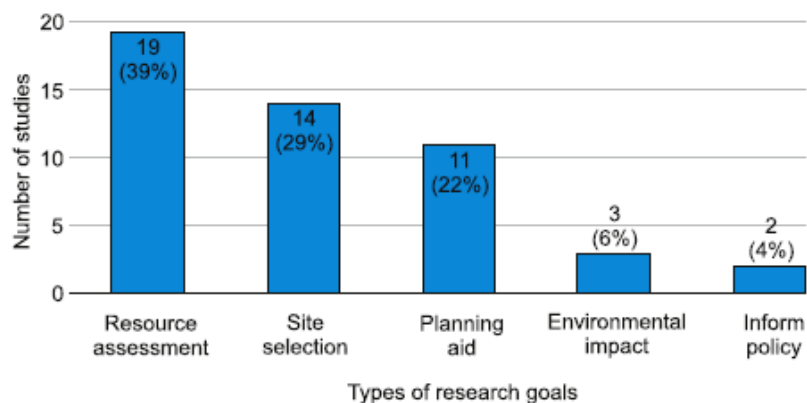


Figure 1.4 (Peters et al., 2020)

In the context of the North Sea and offshore wind research, GIS based yield assessments can be found going back as far as (Cockerill et al., 2001). Various studies have made spatially explicit assessments of yield potentials that cover the expanse of the North Sea with differing limiting conditions. (Schillings et al., 2012) does this with depths less than 50m. (Cavazzi and Dutton, 2016) developed a model for LCOE assessment for the UK EEZ with a consideration for floating offshore support structures. More recently, (NSWPH, 2019) makes an LCOE assessment for fixed bottom foundations. Almost all these studies take into account spatial exclusions and their effects on the yield. (NSWPH, 2019) even goes one step further and accounts for penalty functions that place a cost on OWF deployment in restricted areas. The studies that have performed resource/cost assessments of areas located within the North Sea have been tabulated in Table 1.2 below.

Author/Source	Spatial extent	Temporal forecasting	Spatial exclusions	Floating OWF
(Cockerill et al., 2001)	NSC except NO	No	No	No
(Cavazzi and Dutton, 2016)	UK EEZ	No	Yes	Yes
(Möller Bernd, 2011)	DK EEZ	No	Yes	No
(Schillings et al., 2012)	North Sea	No	Yes	No
(Möller et al., 2012)	DK EEZ	No	Yes	No
(NSWPH, 2019)	North Sea	Yes	Yes	No
(Wind Europe, 2019)	North Sea	Yes	Yes	Yes

Table 1.2 Yield assessments for the North Sea

1.3. Problem definition

While having been investigated on a sit-specific level, the spatial transmission benefits that could be gained due to H₂ pipeline transmission as opposed to conventional power transmission via cables have not been quantified over a larger study space. While significant interests in hydrogen value chains exist, there is currently no model to assess resource potentials to supply large volumes of future hydrogen demand. There currently exist no LCOH maps for hydrogen production in the North Sea. Being able to make spatially explicit assessments for cost-effective hydrogen production allows for security in investments, and future markets to develop in conjunction with large production volumes. Moreover, understanding conflicting industry interests in MSP and being able to put a monetary value on these conflicts enables long term multisectoral planning and damage mitigation. To bridge these gaps in understanding, the following research question and sub-questions will be investigated in this thesis:

“What is the future potential of P2H in the North Sea , from a spatially explicit, techno-economic perspective”

Sub-questions:

1. How do the system configurations for onshore, offshore and In-Turbine P2H production compare with each other?
2. How do the P2H supply paths vary in the North Sea over time and space?
3. Which geographic exclusionary constraints and human activities have the most impact on the cost of the transition?
4. How does P2H in the North Sea compare with conventional HVDC P2E supply pathways?

1.4. Work flow and report structure

The workflow of the study is depicted in Figure 1.5 below

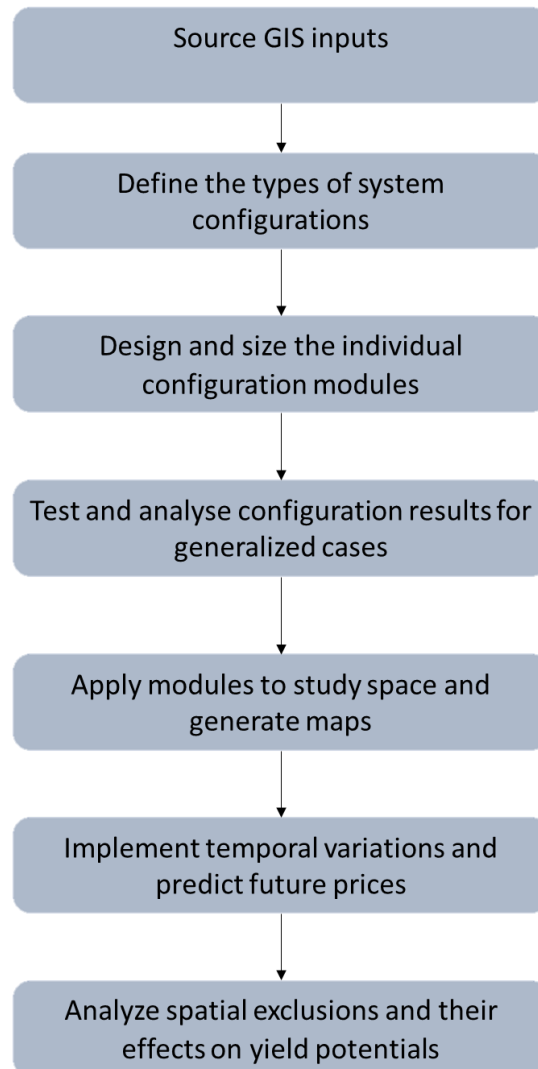


Figure 1.5. Work flow of study

Chapter 2 presents an overview of the model, its modules and the various GIS inputs. Chapter 3 documents the methodology and assumptions used for the sizing and cost analyses. Chapter 4 presents results which lay the basis for a discussion in chapter 5. Chapter 6 then summarizes the findings and aims to answer the research question and sub-questions.

2. Methodology

The methodology revolves around a mapping model that searches for least cost dedicated P2H locations over time and space. The aim of the analysis is therefore to perform a spatially explicit yield assessment and levelized cost assessment for hydrogen production in the North Sea. The model was developed in MATLAB and supplemented with the use of ArcGIS Pro wherever necessary.

The geographical scope of the analysis is the North Sea area as defined by the Exclusive economic zones of the countries that surround the North Sea, this is shown in Figure 2.1 below. The temporal scope extends to the year 2050.

Section 2.1 first describes the three system types and section 2.2 then presents an overview of the mapping model and its functions.

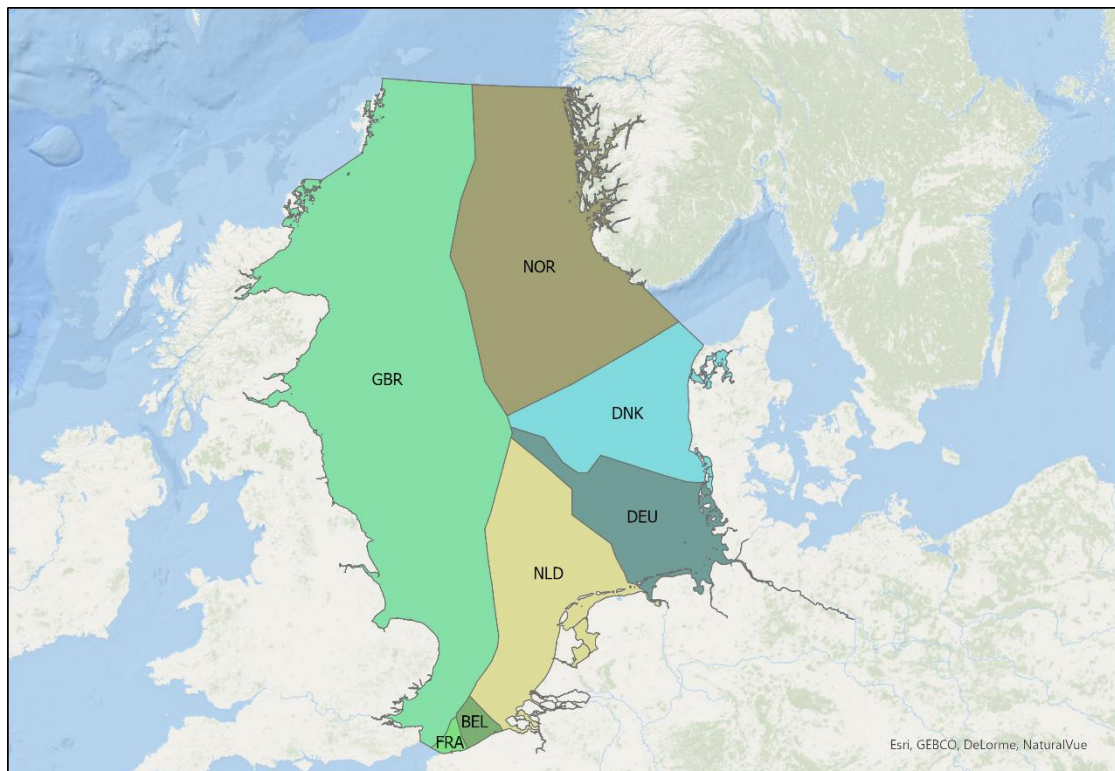


Figure 2.1 Study area

2.1. Configuration descriptions

Three main system configurations have been analyzed and implemented in the model. These have been tabulated in Table 2.1 below. Note that each configuration is assumed to be a cluster, which is comprised of smaller wind farms. These are connected to a platform at the center of the cluster.

Type	Conversion location	Transmission mediums
1	Onshore	AC inter-array/HVDC cables
2	Offshore platform	AC inter-array/H ₂ Pipeline
3	Inside wind turbine	H ₂ pipelines

Table 2.1 System configurations

The schematics of the systems and components are depicted below. The onshore configuration transmits the electricity to shore via HVDC cables after which it is converted to hydrogen. This therefore represents the conventional case for offshore to onshore electricity generation, conversion and transmission. AC export cables are currently the preferred transmission medium up to distances of 50-80km from shore (Legorburu et al., 2018) (NSWPH, 2019). The break-even distance at which HVDC cables become cheaper depends on losses per km, as well as the power that needs to be transmitted. This is a design choice that needs separate analysis but was not considered for simplicity. In any case, current industry practice favours the use of HVDC transmission for farms greater than 1GW, which is far smaller than the nominal capacities of the considered clusters. The simplification also enabled a consistent comparison between HVDC cables and H₂ pipelines over the study area.

The offshore configuration assumes that the conversion of electricity to hydrogen takes place on P2H platforms after which, a pipeline is used to deliver the produced gas to shore. The In-Turbine configuration considers a case where the electricity from the wind turbine is converted to hydrogen either within the turbine itself or on a platform located at the turbine location. A series of compressors and a network of pipelines then transmit the hydrogen to the central platform after which it is delivered to shore via a large pipeline.

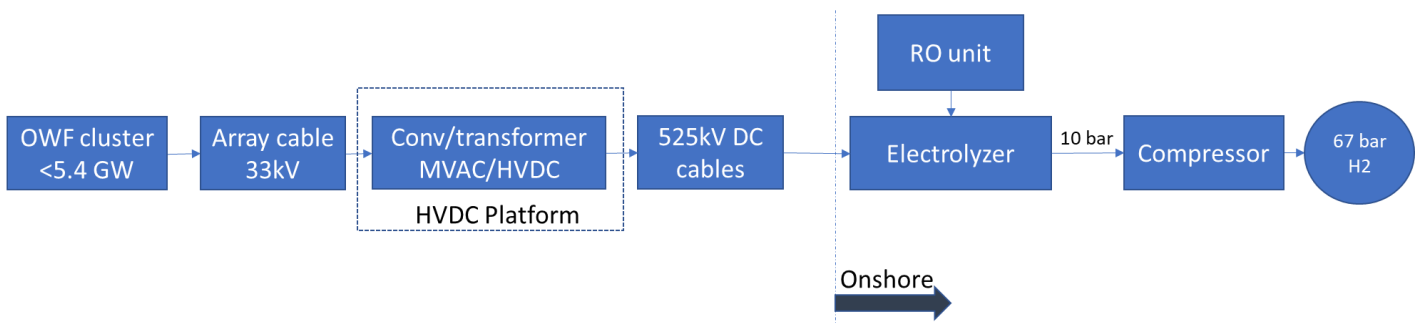


Figure 2.2 Schematic of Onshore configuration

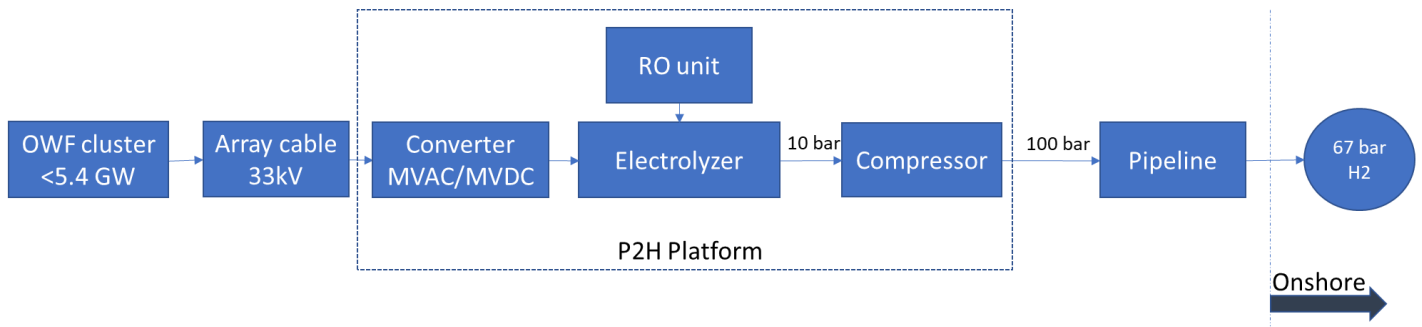


Figure 2.3. Schematic of Offshore configuration

The Onshore and Offshore configurations both use 33kV inter-array cables to collect the generated electricity and transmit it to the central platform. This is the current industry rating for array cables however, as wind turbines get larger, cable ratings of 66kV will soon become the standard. For the onshore configuration, the medium voltage AC (MVAC) power is converted to 525kV HVDC. The voltage is stepped up to reduce the losses incurred due to power transmission to shore. 525kV rated HVDC cables are used to transmit the power to shore after which the alkaline electrolyzer converts the electricity to hydrogen. A reverse osmosis unit treats seawater and delivers it to the electrolyzer located onshore. The Offshore configuration houses the RO unit and electrolyzer on the P2H platform along with the MVAC to medium voltage DC (MVDC) converter. A compressor is necessary to transmit the hydrogen to shore. Based on the assumptions in (Jepma et al., 2018), the output from the electrolyzer is assumed to be 10 bar and a pipeline transmission pressure of 100bar is deemed to be sufficient for delivery to shore. The compressor therefore compresses the produced hydrogen from 10 bar to 100 bar. The onshore delivery pressure is assumed to be 67 bar (Jepma et al., 2018). The delivery pressure of 67 bar is chosen since this is the operating pressure regime for most gas networks onshore, allowing the produced hydrogen to be fed into existing gas grids (Jepma et al., 2018). To allow for a fair comparison between the configurations, a compressor is added after the electrolyzer in the Onshore configuration which compresses the produced hydrogen from 10 bar to 67 bar. Although pressure drops along the pipeline are sensitive to the distance travelled and the flow rate of the fluid, this was not accounted for, for simplicity.

The conversion to hydrogen in the In-Turbine configuration is done in or at the turbine, shown in the blowout in the Figure 2.4 below. The conversion unit includes the RO unit, electrolyzer and compressor that compresses the hydrogen to 30 bar. This pressure regime was deemed to be sufficient for the distances that the hydrogen will have to travel to a centrally located platform (Jepma et al., 2018). Note that the number of 6MW bubbles are for representation only and are intended to reflect the same overall rated capacity clusters as the first two configuration types. The P2H platform in the In-Turbine configuration case is only used to house the compressor and other facilities necessary for the operation of the offshore wind farm cluster. A pressure drop of about 10 bar is assumed between the turbine and the platform. The compressor therefore compresses the H₂ from 20 bar to 100 bar for transmission via a pipeline to shore. Again, the delivery pressure on-shore is assumed to be around 67 bar. The layout for the pipeline network mentioned in the schematic for the In-Turbine config has been discussed in the pipeline section of 3.2.3.

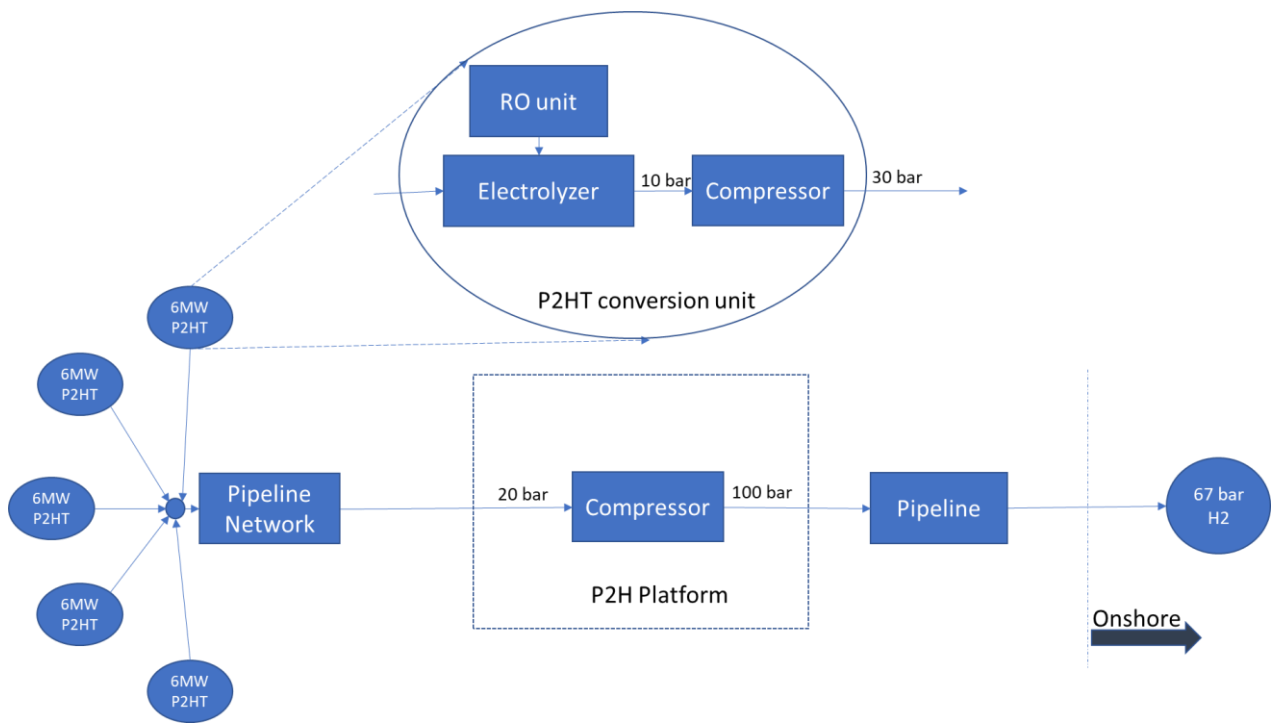


Figure 2.4. Schematic of the In-Turbine configuration

2.2. Model overview

Section 2.2.1. first discusses the various GIS inputs. Section 2.2.2. then presents a description of the model algorithm and space mapping functions

2.2.1. GIS inputs

The mapping model considers spatial exclusionary constraints as imposed by maritime human activities and also those imposed by marine flora and fauna. . Although a number of spatial datasets could be utilized as a hard input that directly affects calculated values, the exclusionary constraints were only utilized as a limiting factor to define feasible regions. In this sense, spatial inputs in the model can be divided into ones that serve as numerical inputs to the cost and sizing modules and ones that only serve to define go/no-go zones. For fishing and shipping zones, these are raster datasets that have values that represent the intensity of activity per unit area in either grid cells or pixels over the study space. For the rest of the exclusions, the datasets can only be turned on or off depending on the scenario considered.. Table 2.2 below lists all the GIS inputs to the model.

DATA	Format	Use	Limiting value/criteria	Source/Hosting server
Wind speed data	NetCDF	Input/calculation	-	(KNMI, 2020)
Bathymetry	NetCDF	Input/calculation	-	(EMODnet_bath, 2020)
Landing Points onshore	Shapefile	Input/calculation	-	Arbitrary choice
Nature zones	Shapefile	Exclusion	All	(EMODnet, 2020)
Fishing zones	Shapefile	Exclusion	>3 (SAR)	(EMODnet, 2020)
Shipping zones	Geotiff	Exclusion	>10hr/month	(EMODnet, 2020)
Current and planned OWFs	Shapefile	Exclusion	All	(EMODnet, 2020)
Estimated future OWF locations	NA	Exclusion	Cheapest locations	From model

Table 2.2. List of GIS inputs

Rationale behind the exclusion criteria

The spatial constraints that were considered were Fishing intensity (FI), shipping intensity(SI), nature conservation zones and current wind farms. For fishing intensity, locations with a swept area ratio (SAR) of >3 were excluded. OSPAR defines this variable as the fraction of a unit grid cell that has been covered by a fishing vessel over the course of a year (Gusatu et al., 2020). In this sense it represents the busyness of a certain area. For shipping intensity, locations with an intensity of >10 (hours/month) were excluded. This assumption was taken from (Wind Europe, 2019). It is believed that for intensities of less than 10 hours/month, multi-use of space is feasible. Nature and wind farm locations are polygons that can either be taken into consideration as a whole, or left out entirely. These therefore have no intensity value.

A host of other inputs could have been considered. Current intensities and wave heights affect the cost of foundation/substructure as well as the cost of installation and maintenance since unfavorable conditions result in smaller workable weather windows. The effects of these factors though were not considered mainly to simplify the analysis. (NSWPH, 2019) also notes that for the North Sea, the LCOE as a consequence of the variability of wave heights differed only marginally, by about 1-2 euro/Mwh, when calmer nearshore waters were compared to the costs incurred with deployment further offshore.

Locations which are licensed by Oil and Gas production companies take up a non-negligible amount of space but there is uncertainty about how this affects offshore wind farm development consent. Pipelines, and electricity and telecom cables litter the floor of the North Sea. Most spatial analyses implement a spatial buffer when incorporating these datasets in yield/cost assessment models. (NSWPH, 2019) also includes a penalty cost associated with possible cable crossings. This was not pursued in the analysis, for simplicity, but also since the data provider (EMODnet, 2020) notes that the polylines of the cables and pipelines are Hypothetical representative datasets, and may not always represent real layouts on the sea floor. Utilizing the network layouts as inputs to the model would therefore not improve the accuracy of the results.

The next 3 sections will discuss the three main inputs that affect the calculations in the model.

Wind speed

The wind speed dataset used in the model was sourced from the DOWA project of the Dutch Meteorological Institute (KNMI). The research was conducted by a consortium that comprised ECN, Whiffle and KNMI. The DOWA project utilizes the ERA5 10 year (2008-2017) global reanalysis dataset to provide downscaled and higher resolution regional reanalysis for the North Sea.

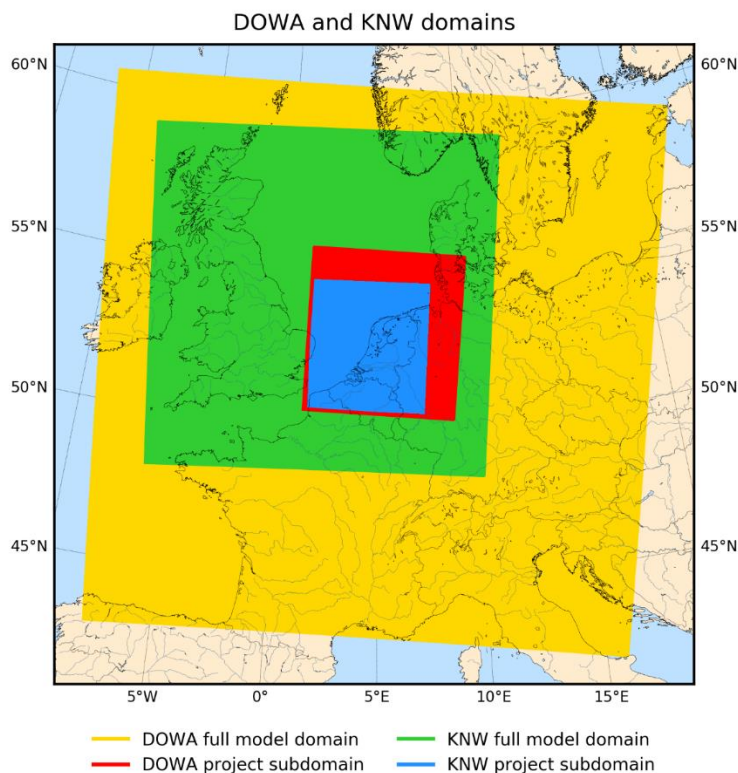


Figure 2.5 DOWA domains (Wijnant et al., 2019)

The yellow dataset was chosen in this report since it spans the entire expanse of the North Sea. The data from the KNMI data center for years 2011-2017 (inclusive) were extracted for the entire study space. Issues with the hosting server meant that incomplete data was obtained for years 2008-2010 and was therefore discarded from the analysis. The full domain data was available as hourly u and v components (2D XY plane), for which the resultant was calculated for each point to generate a vector field.

The plot of the mean wind speed at 10m for all 7 years which was extracted from the full domain DOWA data is shown below in Figure 2.6.

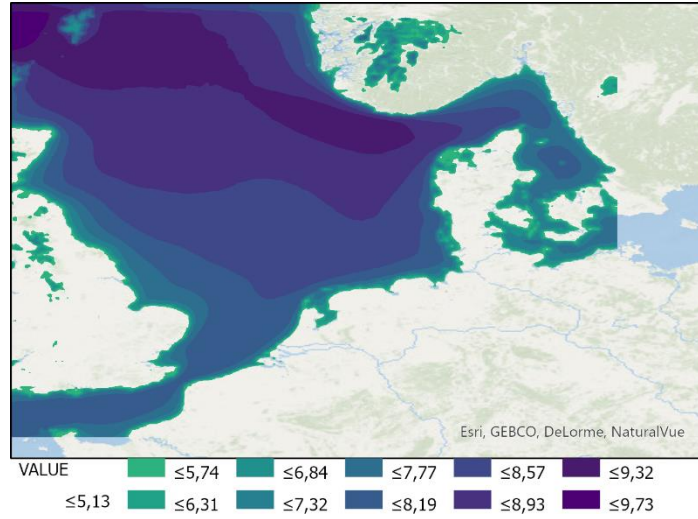


Figure 2.6. Mean wind 7 year wind speed (m/s) at 10m height

Wind turbine hub heights fall in between 100-150m for currently available 6MW to future 15MW turbines respectively. The 10m wind speed therefore needs to be translated to speeds at the hub height which are higher due to lower frictional effects from the surface of the water on the wind profile. The scaling was done using the log law up to a height of 60m and then using the power law up to the hub height, shown in equations 1 and 2 below. The rationale behind the choice for the turbine rating and corresponding hub height for the base case in 2020 will be discussed later in chapter 3. Figure 2.7 shows what the spatial variation of the wind dataset looks like at an altitude of 100m.

$$u_{60} = u_{10} * \frac{\ln\left(\frac{60}{Z_0}\right)}{\ln\left(\frac{10}{Z_0}\right)} \quad (1)$$

$$u_{hub} = u_{60} * \left(\frac{h_{hub}}{60}\right)^\alpha \quad (2)$$

Where:

$Z_0 = 0.0001$ (Assumed for offshore conditions)

$\alpha = \text{Wind shear coefficient} = 0.115$ (Musial et al., 2020)

$h_{hub} = \text{hub height (m)}$

$u_{10}, u_{60}, u_{hub} = \text{Wind speeds at 10, 60 and hub heights respectively } \left(\frac{m}{s}\right)$

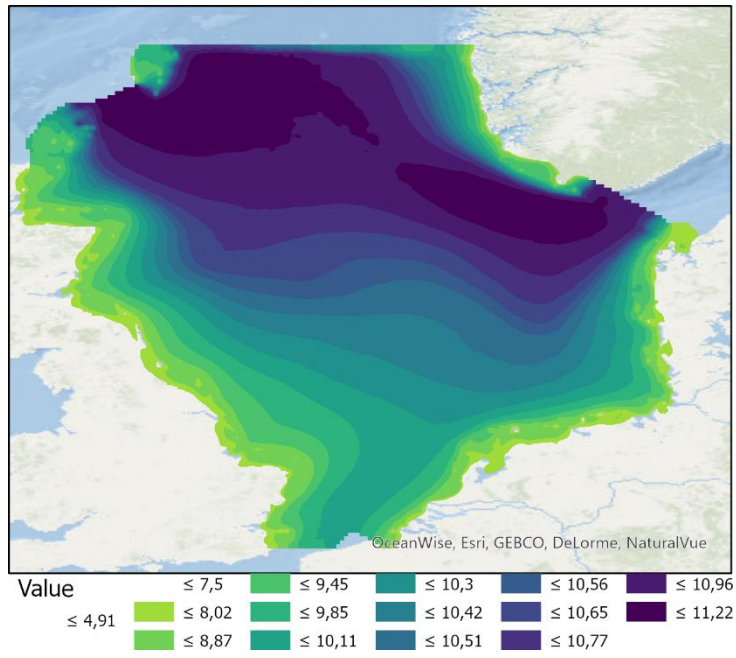


Figure 2.7. Mean wind 7 year wind speed (m/s) at 100m height

Bathymetry

The bathymetric data was extracted from (EMODnet_bath, 2020). The original dataset had a resolution of approximately 0.002x0.002 degrees or about 220m which was too fine for the analysis. The dataset was interpolated wherever necessary and assigned to the reference grid in the study. The input bathymetric dataset has been shown below for representation.

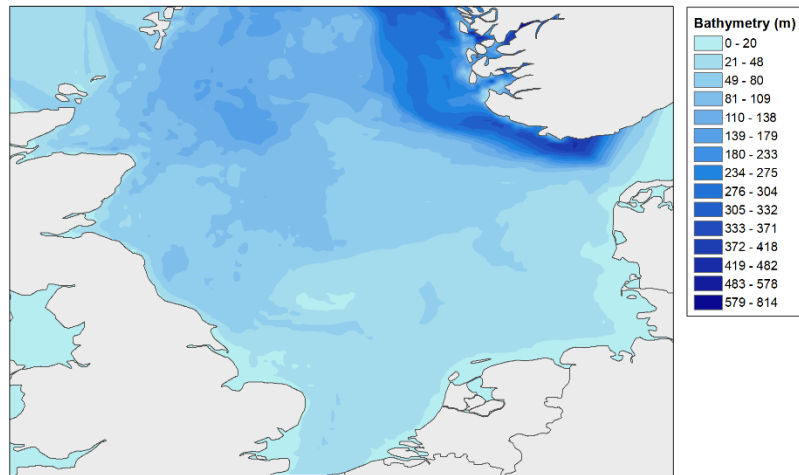


Figure 2.8. North Sea bathymetric profile. Extracted from (EMODnet_bath, 2020)

Onshore ports/delivery points

The landing points represent onshore connection points where either electricity or hydrogen is delivered to shore. These also represent the location of hypothetical ports or installation harbours. These points therefore also serve as a transit point from which installation vessels journey to a given site. These were chosen arbitrarily over the study space without any real-world consideration. The focus was on ensuring that delivery distances are not biased towards any particular region in the North Sea, which would affect transmission costs. The landing points are shown in figure 11 below.

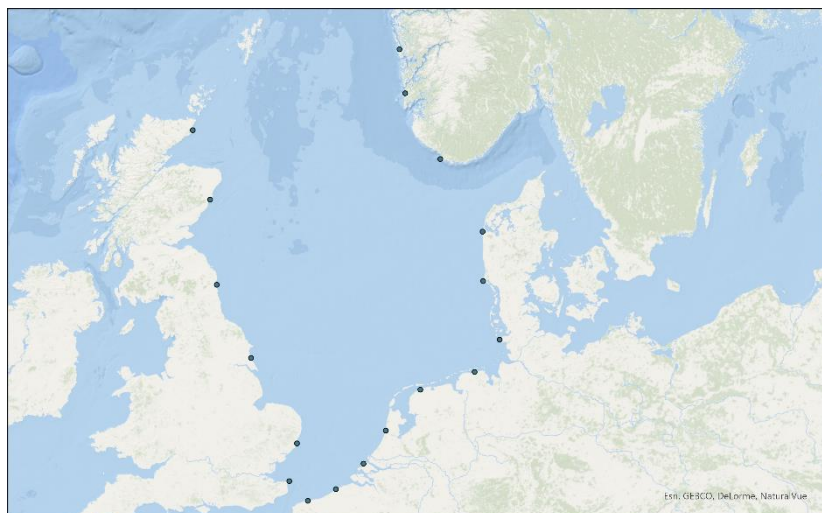


Figure 2.9. Assumed onshore deliver/port locations

2.2.2. Model working

The simplified model algorithm is shown in Figure 2.10 below. The simulation can be run from 2020 to 2050 in steps of 5 years, i.e., a total of 6 possible temporal states.

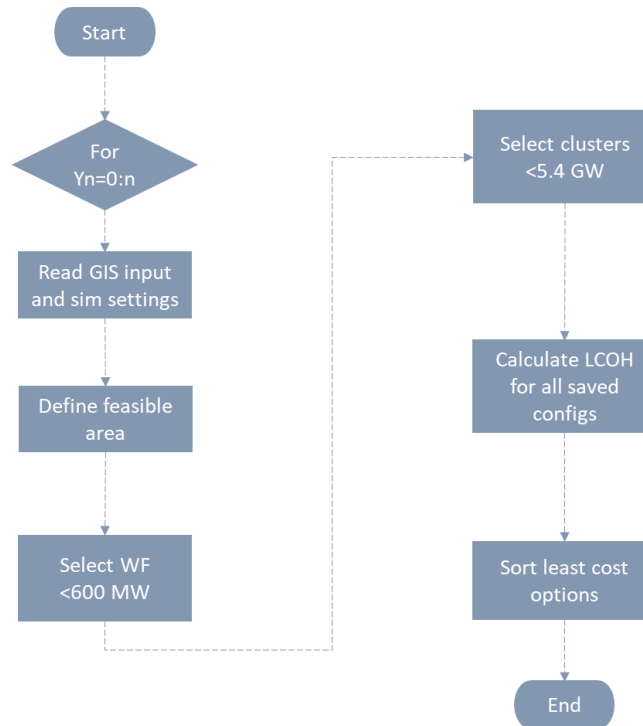


Figure 2.10. Model Algorithm

A reference grid first needed to be defined. It was assumed that each grid point represents the location of a single turbine. The grid spacing would therefore need to reflect the spacing between the turbines. The turbine spacing was chosen based on equation 3, which corresponds with a power density of 3.6 MW/km²(NSWPH, 2019). The chosen baseline turbine was rated at 6MW excluding generator losses. The choice will be elaborated on in section 3.1.1. This resulted in a spacing of 1.29 km, equalling a spacing of 8.6 times the rotor diameter of a 155m diameter baseline turbine.

$$Turbine\ spacing\ (km) = \sqrt{\frac{Turbine\ rating\ (MW)}{3.6}} \quad (3)$$

The spacing was assumed to be the same in both the dominant wind and crosswind directions. For simplicity, it was assumed that a certain base grid consists of a homogeneous rated wind turbine over the study space. A reference co-ordinate system also needed to be defined. Although most of the sourced input GIS datasets were referenced in geographic co-ordinate systems, a projected co-ordinate system, more specifically RDnew, was chosen. This decision was made since the modelling process which included defining a linear reference grid was done in MATLAB. The linear grid spacing would not translate to a uniform spacing in geographic co-ordinate systems. Keeping the turbine/grid spacing uniform was a necessary requirement which is why all input datasets were initially transformed to the chosen projected co-ordinate system.

Since the data source from KNMI consists of a grid with a 2.5x2.5 spacing, the values in the source grid were interpolated where necessary and assigned to the reference grid. Once the new grid is defined, the model then utilizes the GIS data and settings for exclusions to generate exclusionary masks. Depending on the setting, a new feasible grid is then cut out from the reference grid by removing turbines, or points, that fall within exclusion zones.

The mapping model then searches for eligible wind farms and uses those wind farms to build larger clusters, with a platform at its center. To do this, a rectangular search space was defined and made to move around the study space. The search space was used to identify the number of turbines that fall within it at any given time. Farms that were under 600 MW were saved in a database. The search space was dimensioned in such a way that at most, only 600MWs worth or 100 points could fall within it at any given time. No lower limit was set to prevent undervaluing the rated potential of the region. The upper limit was set to allow for direct array cable connections to the central platform in larger clusters without having to deploy an intermediate AC platform which steps up the array voltage to 270 kV. This was the assumption used in (NSWPH, 2019), with the caveat being that the maximum radial interconnection distance between an array string and the central cluster platform is less than 30km. This was to benefit from economies of scale. Beyond this point, the AC losses become high enough to necessitate the intermediate AC platform before connection to the platform in the center of the cluster. Although this restriction doesn't apply to a configuration with a pipeline network, the selection criteria for all configurations was assumed to be the same to allow for a fair comparison between system types.

Once the farms are mapped and saved in the database, a search space for a cluster is defined. This is similar to the farm search space but is larger in size. The search space is again, moved around the study area and saves configurations that are less than 5.4GW. Again, this selection ensures that, with the current turbine spacing, radial lengths do not exceed the 30km threshold to allow for the exclusion of the intermediate AC platform.

Once the configurations are saved, the radial distances to the nearest connection point to each country are calculated and saved in a database with all possible delivery options to each country, assuming a 100% capacity connection from each configuration to each country, regardless of EEZ restrictions.

Once the clusters are formed, the model generates layouts for the array cables in the onshore and offshore configurations, and the pipeline network for the In-Turbine case. These layouts are site specific and depend on the depth profile at the site. The configuration components are then sized and costs are evaluated using the techno-economic module.

3. Techno-economic module sizing and assumptions

The Techno-economic module comprises the sizing and cost functions for the components of the different configurations. This chapter documents the methodology for the sizing and the assumptions for the levelized cost that were adopted in the model. All cost assumptions documented in sections 3.1-3.5 assume baseline costs in 2020. Assumptions for future reductions in cost and efficiency improvements will be presented in section 3.6. Section 3.7 then presents preliminary results for the base-line LCOE as calculated by the model.

3.1. Assumptions for the levelized cost

The levelized cost of energy was calculated using equations 4 and 5. The CAPEX includes the costs of the components and the costs incurred due to installation and commissioning. The fixed OPEX includes the annual operations and maintenance costs. Each component has a specific annuity which depends on the lifetime of the component or sub-system. The WACC rate is assumed to be 3.1% which is the rate given by (Cleijne, 2021) as part of the SDE++ provision in the Netherlands.

$$LCOE = \frac{\sum_{i=1}^n (CAPEX_i * annuity_i + OPEX_i)}{E} \quad (4)$$

$$annuity_i = WACC * \frac{(1 + WACC)^{T_i}}{(1 + WACC)^{T_i} - 1} \quad (5)$$

Where:

LCOE = levelized cost of energy (€/MWh or €/kgH₂) ;

CAPEX_i = Capital expenditure of component (€);

OPEX_i = Yearly operational expenditure of component (€);

E = Yearly electricity or hydrogen produced (MWh or kgH₂);

WACC = Weighted average cost of capital = 3.1%

T_i = Lifetime of the component

3.2. Component sizing and CAPEX cost assumptions

This sub-section will present the costs for the production and acquisition of the components

3.2.1. Generation

Wind Turbines

- RNA and tower

The rated capacity of the turbines chosen for the baseline is 6MW excluding generator losses. Although turbines of larger rated capacities are available currently, the 6MW reference was chosen since this is the baseline turbine adopted in (Musial et al., 2020, 2019), and since the development of prices and technology improvements, which will be detailed in chapter 3.6, have been derived from these NREL studies. Choosing a turbine with a higher baseline capacity would therefore overestimate the projected yield and underestimate future LCOE/H. This is because larger nameplate capacities and lower specific powers would translate to turbine yields that are higher than those already projected for future 15MW turbines. This also applies to the future assumptions for efficiency improvements for other conversion technologies. The turbine designs for the rotor nacelle assembly (RNA) and tower are not site and configuration specific and will be a constant across the study space.

The cost of the RNA was calculated using the equation given in (Ioannou et al., 2018; Shafiee et al., 2016), shown below. Where $CRNA$ is in (£/Turbine) and PWT is the rated capacity of the turbine in MW. The conversion from pounds to euro was done using a factor of 1.1. The cost for the tower is assumed to be 50.751 €/kW (The Crown Estate, 2019). Again pounds have been converted to euros with a factor of 1.1.

$$CRNA = 3 * 10^6 * \ln(PWT) - 662400 \quad (6)$$

The reference power curve for the 6 MW turbine is shown below. Note that this refers to the rater power without considering losses. An aerodynamic efficiency of 0.45 and an air density of 1.225 kg/m³ was assumed.

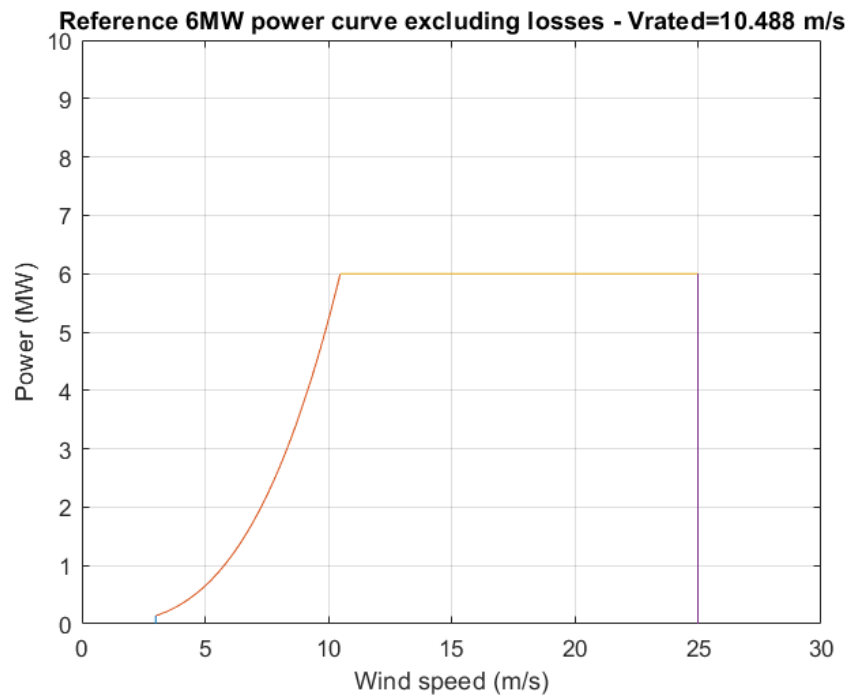


Figure 3.1. Power curve for 6MW turbine

The resulting gross capacity map which does not include losses and a consideration for inavailability is shown below. Note that some interpolation was necessary to generate this map.

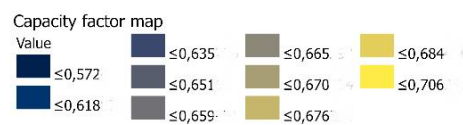
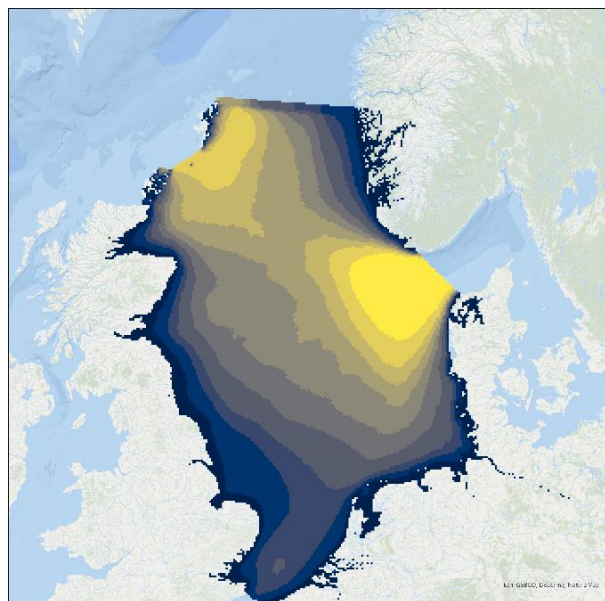


Figure 3.2. Gross capacity factor map

- Foundation

The model differentiates between fixed and floating foundation types. Fixed foundations are Monopile foundations.

For the fixed monopiles and transition piece costs, the scaling laws shown below were used (Maness et al., 2017). The cost of the monopile steel is 1912.5 €/tonne. The cost of the steel for the transition piece is 2745.5 €/tonne (Maness et al., 2017).

$$M_{RNA} = 2.082 * (T_{rated})^2 + 44.59 * T_{rated} + 22.48 \quad (7)$$

$$Monopile\ Mass = \frac{(T_{rated} * 1000)^{1.5} + \frac{(H_{hub})^{3.7}}{10} + 2100 * (D_T)^{2.25} + (M_{RNA} * 1000)^{1.13}}{10000} \quad (8)$$

$$Monopile\ Transition\ Piece\ Mass = e^{2.77+1.04*(T_{rated})^{0.5}+0.00127*(D_T)^{1.5}} \quad (9)$$

Where:

T_{rated} = Turbine rating (MW)

H_{hub} = Hub height (m)

M_{RNA} = RNA mass (tonnes)

D_T = Depth at turbine grid point (m)

Three main archetypes of floating platforms, namely, tension-leg platforms, spar-bouys and semi-submersibles, seem to be the most promising floating technology options. The semi-submersible type was chosen since it offers benefits that relate to ease of installation as well as maintenance. As of 2019, globally, 94% of floating projects use semisubmersibles (Musial et al., 2020). Although the choice for a suitable floating platform will depend on site-specific information and lowest project costs, the semi-submersible type was chosen since it can in theory, be deployed in waters greater than 40m depth, making its implementation in the model relatively simple. The equation for the cost of the floating substructure has been shown in equation 10 below. The costs of the platform, equalling 847 €/kW, was sourced from (Musial et al., 2020) and refers to the Aqua Ventus semi-submersible platform. The costs associated with mooring lines are the only costs that vary with the depth of the site. The total mooring length calculated by (Maienza et al., 2020a) for a comparable 5MW turbine at a reference depth at 135m equalled 450m for a 3 line catenary mooring system. (Myhr et al., 2014) make an assumption that the length required for a catenary mooring line increases by 150m per 100 meters of depth. This assumption was therefore utilized to calculate the slope of the equation that relates depth with the mooring line length of the platform. The slope was therefore 1.5. Although the mass and the radius of the mooring line will depend on the site location and the maximum tensile strength necessary to withstand hydrodynamic loads, an assumption was made that assumes a linear relationship between costs and the length and in turn, the depth of the site. The slope was therefore multiplied with the factor of 0.539 €/kW/m from (Maienza et al., 2020a), which represents the production and acquisition costs for the mooring lines for a 125 MW farm. Finally, anchoring costs of 7.56 €/kW) were added(Maienza et al., 2020a). The derived equation is shown below.

$$\text{Semi - sub (SS) foundation cost } \left(\frac{\text{€}}{\text{kW}} \right) = 854.56 + 0.81 * D_T \quad (10)$$

Where D_T is the depth at each turbine location (grid point) in meters.

To find the transition point between fixed and floating structures, the total costs for each foundation/substructure type were plotted against sea depth. This is seen in Figure 3.3 **Error! Reference source not found.** Note that these costs also include the costs for installation and decommissioning which will be discussed in section 3.3.1. The transition point occurs exactly at 40m. The assumed depth ranges have been tabulated in Table 3.1

Jacket structures are ususally deployed in waters between 30-50m and although having initially been incorporated into the model, lack of reliable jacket installation data for wind turbines meant that they needed to be removed from the analysis.

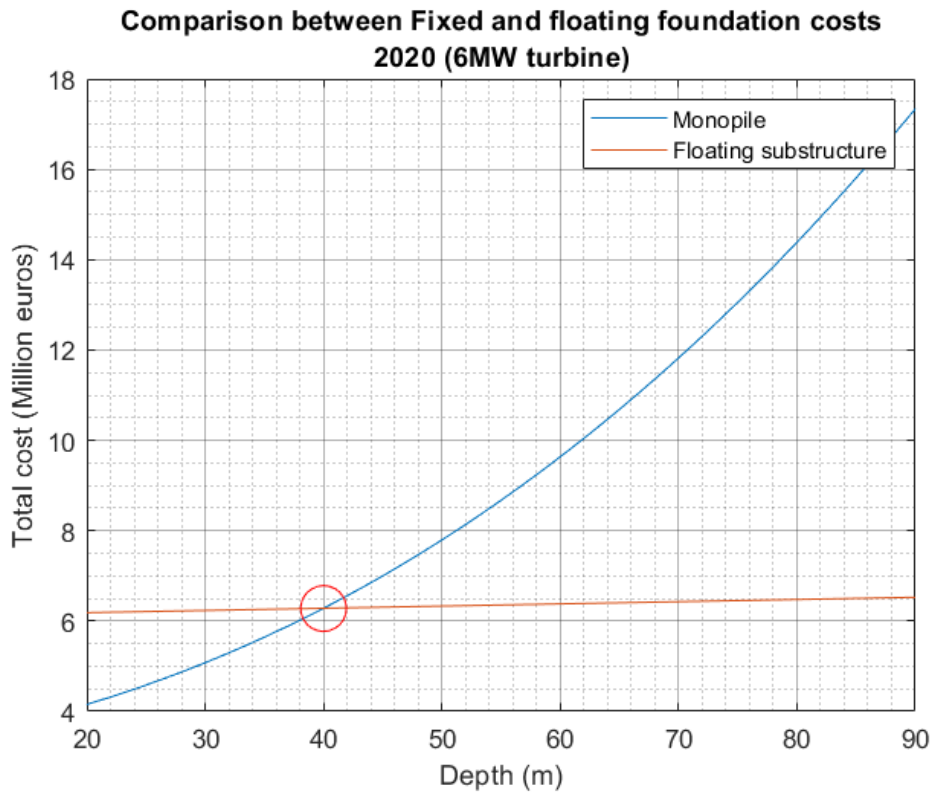


Figure 3.3. Break-even distance between fixed and floating Total costs
(incl Installation and Decommissioning)

Type	Assumed feasible depth ranges
Fixed (Monopiles)	0-40m
Floating (Semi-Submersible)	>40m

Table 3.1. Feasible depth ranges for each foundation type

3.2.2. Conversion

This section presents the assumptions for the costs and sizing of the components that relate to the conversion of electricity to hydrogen. The components have been presented in the following order:

- Fixed and floating offshore Substations (electrical equipment and facilities, excluding platform and structure)
- Fixed offshore substation platforms and structures (platform and jacket foundation)
- Onshore substation (including structure)
- Floating offshore substation platforms (including electrical equipment, facilities and semi-submersible platform and mooring system)
- Electrolyzers
- Compressors
- Reverse osmosis unit

Fixed and floating offshore Substations (Electrical equipment and facilities)

The offshore substation converts the power transmitted by the array cables to DC in the onshore configuration, converts electricity to hydrogen in the offshore case and houses the compressors and operational unit in the In-Turbine configuration.

The cost of the offshore HVDC substation equipment, is assumed to be 1.5 times the cost of an HVAC substation (Maienza et al., 2020a). The HVAC substation costs were sourced from (The Crown Estate, 2019). This includes the costs of the converter, transformers, power compensation, switchgears, auxiliary electrical equipment and the facilities on board the substation. The onshore substation is assumed to be half the cost of the offshore substation (Maienza et al., 2020a).

There is uncertainty about the costs for the equipment on the platform for the offshore and In-Turbine configurations. An assumption is made that the cost of electrical equipment for an offshore substation that converts electricity to hydrogen, costs half as much as that of an offshore HVDC substation. This was done to reflect the fact that the electrical equipment and the converter will need to operate at far lower voltage ratings compared to the conventional system while also eliminating the use of the MVAC-HVAC transformer. Previous results indicated that the transformers make up around 20%-30% of equipment costs while the HVDC converter makes up as much as 50% of the costs which is why this assumption was made. For the costs in the In-Turbine case, only the costs for facilities and operation on board the station were included. The costs for the hydrogen conversion units and compressors add to the costs in the offshore and In Turbine configurations separately. The assumptions are given in Table 3.2.

Config	Onshore	Offshore	In Turbine
Cost (€/kW)	107.25	53.625	22

Table 3.2. Offshore Substation electrical equipment and facilities costs (excluding substation structure)

Fixed offshore substation platforms and structures (Structural)

DNVGLs analysis on P2H feasibility at Ijmuiden was used to size the HVDC and P2H platforms. The equations presented in the report were based on industry expertise and were formulated as a function of the nominal power of the configuration connected to them and the depth of the location in question (dNVGL, 2018)(van Schot and Jepma, 2020). The equations from DNVGL first estimate the total topside mass and then assess the structural mass needed for the fixed jacket foundation. The equations estimating the topside and equipment mass, and coating and grating areas for both the HVDC and P2H platforms are shown in equations 9-21. The costs of the structures are then derived using the assumptions in Table 3.3.

- HVDC platform

$$HVDC\ Topside\ mass(tonnes) = 16.50 * Power(MW) \quad (11)$$

$$HVDC\ Topside\ volume\ per\ MW(m^3/MW) = 0.1395 * Power(MW) + 54.042 \quad (12)$$

$$HVDC\ Topside\ steel\ mass(tonnes) = 0.51 * HVDC\ Topside\ mass(tonnes) \quad (13)$$

$$HVDC\ Topside\ electrical\ equipment\ mass(tonnes) \quad (14)$$

$$= 0.22 * HVDC\ Topside\ mass(tonnes)$$

$$HVDC\ Topside\ Auxiliary\ equipment\ mass(tonnes) \quad (15)$$

$$= 0.27 * HVDC\ Topside\ mass(tonnes)$$

$$Topside\ coating\ area(m^2) = 12.74 * Steel\ mass\ (tonnes) + \quad (16)$$

$$Aux\ equipment\ mass\ (tonnes)$$

$$Grating\ area\ area(m^2) = 0.11 * volume(m3) \quad (17)$$

- P2H platform

$$P2H\ Electrical\ equipment\ mass(tonnes) = 5.65 * Power(MW) \quad (18)$$

$$P2H\ Processing\ plant\ mass(tonnes) = 5.65 * Power(MW) \quad (19)$$

$$P2H\ Cooling\ equipment\ mass(tonnes) = 1.5 * Power(MW) \quad (20)$$

$$P2H\ Steelwork\ mass(tonnes) \quad (21)$$

$$= 1.035 * (Electrical\ equipment + Processing\ plant$$

$$+ Cooling\ equipment) (tonnes)$$

$$Aux\ equipment, grating, cladding and control room mass(tonnes) \quad (22)$$

$$= 1.1689 * Electrical\ equipment\ mass$$

$$P2H\ Topside\ volume\ (m^3) = 193.55 * Power(MW) \quad (23)$$

The scaling equations for the jacket foundations for the platforms of both types are given in equations 22-25. The required mass for the 4 piles that fix the jacket lattice to the seabed are given in equation 25 (Maness et al., 2017).

$$Jacket\ mass(tonnes/m) = 0.018225 * topside\ mass - 15.7927 \quad (24)$$

$$Jacket\ anode\ mass\ (tonnes) = 0.0095 * jacket\ mass + 7.5265 \quad (25)$$

$$Jacket\ coating\ area = 1.0662 * jacket\ mass + 597.33 \quad (26)$$

$$Pile\ Mass\ (4\ piles)(tonnes) = 8 * (Jacket\ mass)^{0.5574} \quad (27)$$

Steel Rate (€/tonne)	3500
Cladding rate(€/tonne)	3000
Grating rate(€/tonne)	180
Coating rate(€/m ²)	120
Jacket steel rate(€/tonne)	2000
Jacket anode(€/tonne)	6500
Jacket Coating rate(€/m ²)	120
Pile steel rate(€/tonne)	1889.85

Table 3.3. Material and manufacturing cost rates (dNVGL, 2018)(van Schot and Jepma, 2020)

- Compression only platforms

The compression only platforms are utilized in the In-Turbine configuration. To calculate the costs of the compression only platforms, the mass of a corresponding HVDC platform and substructure were calculated from the formulae above and then multiplied with a factor of 0.285. This assumption was made based on the relative values of the two platforms in (Jepma et al., 2018) which quotes a cost of 72.128 million euros for an HVDC structure and a value of 20 million for a compression platform for the same reference site.

$$\begin{aligned} \text{Cost of fixed In – Turbine platform (incl foundation)} & \quad (28) \\ & = 0.285 * \text{Cost of HVDC platform} \end{aligned}$$

Onshore substation

The onshore configuration is the only case with an assumed onshore substation. For the offshore and In-Turbine cases, the needed facilities onshore would depend on the intended use and the intended destination of the produced gas. The cost of the onshore substation is assumed to be half the total cost of the offshore HVDC substation (Maienza et al., 2020b), shown in equation 29. This cost applies to both the fixed and floating cases for the Onshore configuration.

$$\begin{aligned} & \text{Cost of onshore substation (Onshore configuration)} \\ & = 0.5 * \text{Total cost of offshore HVDC substation (incl equipment and structure)} \end{aligned} \quad (29)$$

Floating offshore substation platforms

The cost of the semisubmersible HVDC substation was sourced from (Maienza et al., 2020a). The source gives costs in terms of the total for the equipment and the platform. The costs for mooring and anchoring which were discussed previously were added to the substation value following the same assumptions for mooring as before. For the offshore and In-Turbine configurations, the fixed cost for the substation is multiplied by 0.5; following on from the assumptions made for the fixed substation equipment discussed earlier, and since the equipment makes up the majority of the substation costs in the floating case. For the In-turbine case the costs for the fixed case were a factor of 19.4% of the whole HVDC substation. This was applied to the cost of the floating offshore substation for the In-turbine case

$$\text{Cost floating offshore substation (ON)} \left(\frac{\text{€}}{\text{kW}} \right) (\text{incl substructure}) \quad (30)$$

$$= 117.96 + 1.213 * D_T$$

$$\text{Cost floating offshore substation (OFF)} \left(\frac{\text{€}}{\text{kW}} \right) (\text{incl substructure}) \quad (31)$$

$$= 55.2 + 1.213 * D_T$$

$$\text{Cost floating offshore substation (IN)} \left(\frac{\text{€}}{\text{kW}} \right) (\text{incl substructure}) = 22.88 + 1.213 * D_T \quad (32)$$

Electrolyzers

The Alkaline electrolyzers are sized based on the (Rated power-losses) that are fed to them. A cost of 500(€/kW_e) is assumed for the baseline cost (IEA, 2019). Possible issues with costs as a function of scale for the In-turbine electrolyzer have been discussed in the chapter 5.

Compressors

The compressors are sized based on the rated production of hydrogen that is fed to it. The compressor is assumed to be a single stage mechanical compressor (for simplicity). The energy consumption of the compressor is given by the equation 31 below (Knoope, 2015) (Koornneef, 2020). The required rated capacity of the compressor is therefore calculated using the second equation. The cost for the compressors is assumed to be 2545 (€/kW_e). (Jepma et al., 2018).

$$E_{COMP} = \frac{Z * R * T * Y}{M * \eta_{ise} * \eta_{mech} * (Y - 1)} * \left[\left(\frac{P2}{P1} \right)^{\frac{(Y-1)}{Y}} - 1 \right] \quad (33)$$

$$W_{COMP} = E_{COMP} * \dot{m} \quad (34)$$

Where:

$$E_{COMP} = \text{Energy consumption of compression} \left(\frac{kJ}{kg} \right)$$

$Z = \text{compressibility factor for H}_2 = 1.04$

$$R = \text{Universal gas constant} = 8.3145 \frac{J}{mol * K}$$

$T = \text{inlet temperature} = 288$

$Y = \text{specific heat ratio of H}_2 = 1.41$

$M = \text{molecular mass H}_2 = 2.02 \text{ g/mol}$

$\eta_{ise} = \text{isentropic efficiency of the compressor} = 0.8$

$\eta_{mech} = \text{mechanical efficiency of the compressor} = 0.98$

$P1 = \text{inlet pressure (MPa)} = \text{Configuration specific}$

$P2 = \text{outlet pressure (MPa)} = \text{Configuration specific}$

$W_{COMP} = \text{rated capacity of the compressor (kW)}$

\dot{m} = mass flow rate of the gas ($\frac{kg}{s}$)

Reverse Osmosis

The reverse osmosis unit treats sea water for use in the electrolyzer. 1 kg of hydrogen needs 9 kg of water for electrolysis. The required rated water flow is therefore calculated by multiplying the rated hydrogen flow by 9 and expressing the flow in m³/day. The costs for an RO system is sensitive to the scale of the capacity. At capacities of 10000m³/day, the cost of such a system is 671.95(€/m³/day) (Ghaffour et al., 2013). This value was chosen for the production volumes necessary in the model configurations.

3.2.3. Transmission

AC cables

The cost of the 33kV AC cables are 206423.6 euro/km (Ioannou et al., 2018). To calculate the AC cable lengths, an algorithm was developed which first forms array strings comprising at most 5 turbines. This is 1 less than the maximum cable carrying capacity of each string assuming a 0.715 kA rated cable with a cross section of 630mm², calculated using the equation below. The assumption was made due to an already predefined maximum capacity cluster layout comprising 10 columns of 10 rows each. The strings are divided down the middle into sections of at most 5 turbines. The closest connection points from each string to the center of each cluster are then determined and the total lengths are calculated. Note that when exclusions are imposed or at locations close to shore with irregular layouts the algorithm sizes the strings dynamically and does not follow the standard 5.4GW layout. The calculated lengths are dependent on the depth profile of the site and are specific to the location of each turbine and also, the location of the platform. For the 4 turbines closest to the cluster, the depth at each turbine point is multiplied by a factor of 2, to represent the cable connection to and from each adjacent turbine in the string. For the turbine furthest from the cluster center and for the cluster center itself, a single connection to the sea-floor is assumed.

$$\begin{aligned} & \text{Maximum number of turbines per string} & (35) \\ & = \text{round down} \left(\frac{\sqrt{3} * I_{cab} * V_{cab} * \text{Power factor}}{T_{rated}} \right) \end{aligned}$$

Where:

I_{cab} = Rated capacity of cable (kA) = 0.715 (Rubí and González, 2018)

V_{cab} = Voltage rating = 33 kV

Power factor = 0.95

T_{rated} = Turbine rating = 6MW

DC cables

For the DC export cables, the rated capacity minus losses from the farms are divided by the assumed voltage of 525kV to calculate the number of cables required. Suitable cable capacities and cable numbers are then chosen using one of two cable types from the table below using a least cost decision algorithm.

Cross section (mm ²)	Current capacity (A)
2000	1900
3000	2600

Table 3.4. DC cable options(Rubí and González, 2018)

The cost is calculated using the ECN formula for DC export cables, sourced from (Rubí and González, 2018).

$$C_{DC} = 0.7353 * A_{Cab} + 0.7539 * V_{cab} - 257.2 \quad (36)$$

Where:

CDC= cost of the cables (k€/km)

Acab=area of the cables in mm²

Vcab= voltage =525kV

Pipelines

To size the pipeline, a simple approach was adopted where the rated flow rate at the inlet of a pipe is related to its volumetric flow rate and hence diameter, using the equation shown below. Where \dot{m} represents the mass flow rate of the gas, Q is the volumetric flow rate, A is the inner cross-section of the pipe and V is the assumed constant gas velocity of 25m/s.

$$\dot{m} = Q * A * V \quad (37)$$

Rearranging the terms and expressing the diameter as a function of the rated power of hydrogen flowing through the pipe results in the equation shown below. The approach was sourced from (Roobeek, 2020).

$$D = 2 * \sqrt{\frac{P}{\pi * V_{H2} * \rho * 39.41 * 3.6}} \quad (38)$$

Where:

D = the diameter of the pipeline in meters;

P= the rated power of hydrogen flowing through the pipe;

V_{H2}=the speed of the gas = 25m/s (Roobeek, 2020);

ρ = the density of hydrogen at the inlet temperature and pressure

For the offshore and In-Turbine cases, the length of the main transmission pipeline that delivers the hydrogen to shore is estimated as the closest distance to the nearest delivery location.

For the pipes within the cluster however, the network layout and methodology to estimate the pipeline lengths is described below. Operating pressure regimes have been discussed in chapter 2.

- The network in the cluster is assumed to be made up of 4 different pipeline classes.
- The hydrogen produced by each turbine is transported individually to the seafloor via pipeline class 1.
- The second pipeline type runs along each column of the farm and connects to each class 1 pipeline from each turbine.
- This means that at most, 10 turbines can connect to each type 2 pipeline in each column of a farm.
- The third pipe class runs along the spine, and center of each farm. This central pipeline connects to each type 2 pipeline in each column.
- Finally, the type 4 pipeline connects the center of each farm to the center of the cluster.

The costs for the pipelines are calculated using the equation shown below (Markus Reuß et al., 2019) . Where D is the diameter in meters.

$$C_{pipe} \left(\frac{\text{€}}{\text{m}} \right) = 1.05 * 278.24 * e^{1.6*D} \quad (39)$$

3.3. Other Capex

3.3.1. Installation

Without reference data for the installation of offshore wind farms of this scale, values found in literature for the installation times and costs were assumed to scale with the rated capacities of the deployed clusters. The goal of the analysis performed in this study was to capture the relationship with installation depth and transit distance to the nearest port. The values for the installation costs found in the literature were therefore weighted using factors that reflected the costs and in turn, the times spent either installing a component at a certain depth, or transiting back and forth from the installation site and nearest construction port. The rationale behind the calculation of these factors and the derivation of the component specific installation costs have been discussed in the following section.

The installation of each component type has been documented in the following order:

- 1) Fixed tower and rotor nacelle assembly (RNA)
- 2) Fixed monopile and transition piece installation for the turbines
- 3) Fixed substation installation
- 4) Floating turbine and platform installation
- 5) Floating substation installation
- 6) AC and DC cable installation
- 7) In-turbine pipelines

The sections have been presented with the following general format:

- 1) Description
- 2) Input tables
- 3) Output tables
- 4) Derived equations

Fixed tower and rotor nacelle assembly(RNA)

The reference data used for the derivation of the fixed turbine installation costs were sourced from (Ioannou et al., 2018). The reference depth and distance to port were 26m and 36km respectively. The reference farm comprised 140 3.6MW turbines. The analysis used a jack-up vessel with a holding capacity of 1 turbine per trip, which carries out both the transport as well as the installation of the turbine. The installation method used 3 lifts wherein the the RNA and two blades were pre-assembled onshore before transport to the site. The RNA and the two preassembled blades, the third blade and the tower therefore make up the three required lifts

The report did not explicitly state the costs of the installation cranes and the handling equipment. It was therefore assumed that these were accounted for in the charter rate of the vessel. The required number of trips to install 140 turbines for the vessel would be 140. With the speed of the vessel and the availability factor to account for downtime due to unfavourable weather, this translates to a total time of 54 (rounded-up) days spent in transit in between the site and the installation harbour, assuming a 12 hr work day and using the charter rate for the vessel this equates to a total cost of 6.69 M€.

The analysis performed in the report assumed that a 30 man crew would work on the installation of the turbine. An offshore-onshore work shift lasting 12 weeks on and 12 weeks off was assumed which is standard for offshore installation activities in the UK (Ioannou et al., 2018). The total installation time for 140 turbines was given as 264 days. This requires 4 crew shift transfers over the course of the installation of the 140 turbines, assuming a 5 day work-week and 12 hour work-day. Using the the day rate for the crew vessel and also the cost of labour in transit, the costs of crew transfer was calculated to be 19.64 k€. The inputs are given in Table 3.5. The outputs for the calculation of the transit fractions of the costs that depend on the distance from the closest port have been shown in Table 3.6.

Inputs			
General	Reference distance to port	36.00	km
	Reference depth	26.00	m
	Availability factor	0.85	
	Number of turbines	140.00	
	Work-hours per day	12.00	hrs
	Number of workers	30.00	
	Total time for installation	264.00	days
	Total costs for installation	68.88	M€
Jack-up installation	Capacity	1.00	unit/trip
	Charter rate	123.86	k€
	Vessel speed	18.52	kmph
	Jacking-up rate	30.00	m/h
	Jack-up height	30	m
Crew transfer	Capacity	12.00	people
	No of vessels	3.00	
	Crew transfer	10.73	k€/day
	Labour cost(1 person)	297.00	€/day

Vessel speed	48.15	kmph
Work week	5.00	days
Shift	12.00	weeks

Table 3.5. Inputs for the installation of fixed RNA and tower

Outputs (Transit fraction calculation)		
Jack-up installation	Jack-up travel time	54.00 days
	Calculated costs during transit	6.69 M€
Crew transfer	Number of trips for 3 vessels	5.00
	Crew transfer travel time	1.00 day
	Calculated vessel costs during transit	10.73 k€
	Calculated labour costs during transit	8.91 k€
	Total costs for crew transfer in transit	0.02 M€
Transit fraction for installation	Total costs in transit	6.71 M€
	Transit fraction	0.107

Table 3.6. Transit fraction calculation (Fixed turbine)

The main mechanism that affects the depth dependent time spent during the installation of the RNA and the tower are the jacking-up/down time at the turbine location. The calculation of the fraction of depth dependent costs for the installation have been shown in Table 3.7.

Outputs (Depth fraction calculation)		
Jack-up installation	Jack-up time at site	56.00 days
	Calculated costs for depth related activity	6.94 M€
Labour	Crew working time	56.00 days
	Calculated labour costs depth related activity	0.50 M€
Depth fraction for installation	Total costs for depth related activity	7.44 M€
	Depth fraction	0.119

Table 3.7. Depth fraction calculation (Fixed turbine)

The fraction of the costs that were dependent on distance to shore was therefore calculated to be 10.7% for the reference site. The influence of depth amounts to 11.9%. The derived equation for the costs of the installation of the tower and RNA is shown below. The factor 124.2 represents the installation costs from (Ioannou et al., 2018) in (€/kW).

$$\begin{aligned}
 & \text{Fixed tower and RNA installation cost} \left(\frac{\text{€}}{\text{kW}} \right) & (40) \\
 & = 124.2 * \left(1 - \alpha - \beta + \alpha * \frac{D_T}{D_{ref}} + \beta * \frac{t}{T_{ref}} \right)
 \end{aligned}$$

Where:

α = Fraction of installation costs dependent on depth at turbine =0.119

D_{ref} = Reference depth of 26m

D_T = Depth at turbine location (m)

β = Fraction of installation costs dependent on transit between port and site =0.107

T_{ref} = Reference distance to port of 36km

t = distance between configuration cluster and nearest port (km)

Fixed monopile and transition piece installation for the turbines

The analysis performed in (Ioannou et al., 2018) was used again to estimate the scaling factors for the installation of the fixed monopile foundations. A jack up installation vessel was again utilized with a carrying capacity of 4 piles. The transition pieces were assumed to be installed by the same vessel. A calculation similar to the installations of the RNA and tower was performed and the total time spent in transit was calculated.

For the depth related calculations, two additional cost elements reflecting the time required to drive the piles into the sea-bed and the time spent on scour protection using a rock dumping vessel were incorporated into the calculations. The sourced values and calculated cost/time fractions can be seen in the tables 3.8-3.10. The fraction of the installation costs of the monopiles that were incurred due to transit was found to be 1.9%. The depth contribution was 43%.

Inputs		
General	Reference distance to port	36.00 km
	Reference depth	26.00 m
	Availability factor	0.85
	Number of foundations	140.00
	Work-hours per day	12.00 hrs
	Number of workers	30.00
	Total time for installation	292.00 days
	Total costs for installation	102.22 M€
Jack-up installation	Capacity	4.00 units/trip
	Charter rate	123.86 k€/day
	Vessel speed	18.52 kmph
	Jacking-up rate	30.00 m/h
	Pile drive rate	0.65 hr/m
	Pile Embedment length	30.00 m
Crew transfer	Capacity	12.00 people
	No of vessels	3.00
	Crew transfer	10.73 k€/day
	Labour cost (1 person)	297.00 €/day
	Vessel speed	48.15 kmph
	Work week	5.00 days
	Shift	12.00 weeks
Scour protection	Vessel capacity	24.00 kton
	Required tonnage per turbine	6.89 kton/turbine
	Charter rate	15.18 k€/day
	Vessel speed	25.00 kmph

Table 3.8. Inputs for the installation of fixed foundations

Outputs (Transit fraction calculation)			
Jack-up installation	Jack-up travel time	14.00	days
	Calculated costs during transit	1.73	M€
Crew transfer	Number of trips for 3 vessels	5.00	
	Crew transfer travel time	1.00	day
	Calculated vessel costs during transit	10.73	k€
	Calculated labour costs during transit	8.91	k€
	Total costs for crew transfer in transit	19.64	k€
Scour protection	Vessel travel time	12	days
	Calculated costs during transit	182.16	k€
Transit fraction for installation	Total costs in transit	1.94	M€
	Transit fraction	0.019	

Table 3.9. Transit fraction calculation (Fixed turbine foundation)

Outputs (Depth fraction calculation)			
Jack-up installation	Jack-up time at turbine location	569.33	hours
	Pile driving time at turbine location	2730.00	hours
	Total effective time for depth related activity	324.00	days
	Calculated costs for depth related activity	40.13	M€
Labour	Crew working time	569.33	days
	Calculated labour costs for depth related activity	2.89	M€
Scour protection	Time spent rock-dumping	65.00	days
	Calculated scour costs for depth related activity	0.99	M€
Depth fraction for installation	Total costs for depth related activity	44.00	M€
	Depth fraction	0.430	

Table 3.10. Depth fraction calculation (Fixed turbine foundation)

The final relationship for the installation cost of the fixed monopiled of the turbines is given below

$$\begin{aligned} \text{Fixed turbine foundation installation cost} \left(\frac{\text{€}}{\text{kW}} \right) & \quad (41) \\ & = 202.78 * \left(1 - \alpha - \beta + \alpha * \frac{D_T}{D_{ref}} + \beta * \frac{t}{T_{ref}} \right) \end{aligned}$$

Where:

α = Fraction of installation costs dependent on depth at turbine = 0.1232

D_{ref} = Reference depth of 26m

D_T = Depth at turbine location (m)

β = Fraction of installation costs dependent on transit between port and site = 0.016

T_{ref} = Reference distance to port of 36km

t = distance between configuration cluster and nearest port(km)

Fixed substation installation

The calculation of the installation fractions for the substation follow the same rationale as the fixed turbine foundations, excluding the costs for scour protection, since this was not explicitly accounted for in the reference (Ioannou et al., 2018). An additional difference is that the sourced report did not account for the jacking-up/down time as a separate expense, and only mentioned the time spent for the installation activity at the site. This was assumed to be completely dependent on the depth at the site. The installation of the substation topside and jacket substructure was carried out using a heavy lift vessel. The input/output tables can be found below. The fraction of costs associated with transit was found to be 3.8% while that of the dependence on depth was 28.7%. All data was sourced from (Ioannou et al., 2018).

		Inputs	
General	Reference distance to port	36.00	km
	Reference depth	26.00	m
	Availability factor	0.85	
	Number of substations	2.00	
	Work-hours per day	12.00	hrs
	Number of workers	30.00	
	Total time for installation	26.00	days
	Total costs for installation	4.39	M€
	Jack-up installation	Capacity	1.00
Charter rate		123.86	k€/day
Vessel speed		18.52	kmph
Jacking-up rate		30.00	m/h
Pile drive rate		0.12	hr/m
Embed length		36.00	m
No of piles		4.00	
Crew transfer	Capacity	12.00	people
	No of vessels	3.00	
	Crew transfer	10.73	k€/day
	Labour cost(1 person)	297.00	€/day
	Vessel speed	48.15	kmph
	Work week	5.00	days
Shift	12.00	weeks	

Table 3.11. Inputs for the installation of fixed foundations

Outputs (Transit fraction calculation)		
Jack-up installation	Jack-up travel time	1.00 days
	Calculated costs during transit	0.15 M€
Crew transfer	Number of trips for 3 vessels	1.00
	Crew transfer travel time	1.00 day
	Calculated vessel costs during transit	10.73 k€
	Calculated labour costs during transit	8.91 k€
	Total costs for crew transfer in transit	19.64 k€
Transit fraction for installation	Total costs in transit	0.17 M€
	Transit fraction	0.038

Table 3.12. Transit fraction calculation (Fixed offshore substation)

Outputs (Depth fraction calculation)		
Jack-up installation	Installation time at turbine location	40.00 hours
	Pile driving time at turbine location	33.12 hours
	Total effective time for depth related activity	8.00 days
	Calculated costs for depth related activity	1.19 M€
Labour	Crew working time	8.00 days
	Calculated labour costs for depth related activity	0.07 M€
Depth fraction for installation	Total costs for depth related activity	1.26 M€
	Depth fraction	0.287

Table 3.13. Depth fraction calculation (Fixed offshore substation)

The derived relationships can be found below. The equation was applied to all three configuration types, without exception, however, for the onshore configuration, a cost of 27.5(€/kW) was added for the installation of the onshore substation (The Crown Estate, 2019).

$$\text{Fixed substation installation cost (Onshore config)} \left(\frac{\text{€}}{\text{kW}} \right) \quad (42)$$

$$= 38.5 * \left(1 - \alpha - \beta + \alpha * \frac{D_T}{D_{ref}} + \beta * \frac{t}{T_{ref}} \right) + 27.5$$

$$\text{Fixed substation installation cost (Offshore and In – Turbine configs)} \left(\frac{\text{€}}{\text{kW}} \right) \quad (43)$$

$$= 38.5 * \left(1 - \alpha - \beta + \alpha * \frac{D_T}{D_{ref}} + \beta * \frac{t}{T_{ref}} \right)$$

Where:

α = Fraction of installation costs dependent on depth at turbine =0.287

D_{ref} = Reference depth of 26m

D_T = Depth at turbine location (m)

β = Fraction of installation costs dependent on transit between port and site =0.038

T_{ref} = Reference distance to port of 36km

t = distance between configuration cluster and nearest port(km)

Floating turbine and platform installation

The analysis performed in (Maienza et al., 2020b) was utilized to derive the cost equations for the floating technologies. For the installation of the turbine, the analysis assumed that the turbine and platform are assembled onshore and transported to the site using a tug vessel. The costs for the installation were separated into the installation of the turbine+platform and the installation of the mooring system. The mooring system installation is carried out using an anchor handling vessel (AHV). The report made no explicit mention of the depth dependence of any of the costs. The installation of the mooring system was therefore assumed to be independent of depth. In reality the costs will depend on depth, however, the costs are expected to be dominated by the hydrodynamic conditions at the site which affect the positioning of the AHV. A availability factor of 0.75 was assumed in the study and was applied to calculated times wherever necessary. The sourced report did not separately state the mooring system installation costs of the turbines and the substation. Assuming that the costs relate to the length of the mooring lines. The costs were divided using ratios 25/26 and 1/26 for 25 turbines and 1 substation platform respectively.

Besides the difference in vessels/mechanisms and the assumptions made above, the rationale follows from calculations made for fixed foundations. The tabulated inputs and outputs can be found below. The calculated fractions due to transit for the platforms and the mooring systems are 33.8% and 18.6% respectively.

		Inputs	
General	Reference distance to port	165.00	km
	Reference depth	135.00	m
	Availability factor	0.75	
	Work-hours per day	12.00	hrs
	Number of workers	30.00	
	Number of turbines and platforms	25.00	
	Number of substations and platforms	1.00	
	Total time for installation floating turbines	300.00	hours
	Total costs for installation turbines and platforms	4.97	M€
	Total costs for mooring turbine platforms	8.14	M€
Tug boat	Vessel speed	12.960	kmph
	Cost	22.500	k€/day
AHV	Vessel speed	20.37	kmph
	Cost	90.75	k€/day
Crew transfer	Capacity	12.00	people
	No of vessels	3.00	
	Crew transfer	10.73	k€/day
	Labour cost(1 person)	297.00	€/day
	Vessel speed	48.15	kmph
	Work week	5.00	days
	Shift	12.00	weeks

Table 3.14. Inputs for the installation of floating technologies

Outputs (Transit fraction calculation)			
Tug Boat	Travel time	71.00	days
	Calculated costs during transit	1.60	M€
Crew transfer	Number of trips for 3 vessels	5.00	
	Crew transfer travel time	4.00	day
	Calculated vessel costs during transit	42.90	k€
	Calculated labour costs during transit	38.88	k€
	Total costs for crew transfer in transit	81.78	k€
Transit fraction for installation	Total costs in transit	1679280.00	M€
	Transit fraction	0.338	

Table 3.15. Transit fraction calculation (Floating offshore turbine and platform)

Outputs (Transit fraction calculation)			
Anchor handling vessel	Travel time	31.00	days
	Calculated costs during transit	1.52	M€
Transit fraction for installation	Total costs in transit	1.52	M€
	Transit fraction	0.186	

Table 3.16. Transit fraction calculation (Floating turbine platform mooring system)

The final equations are presented in equations 40 and 41.

$$\begin{aligned} \text{Floating Turbine and platform installation cost} \left(\frac{\text{€}}{\text{kW}} \right) & \quad (44) \\ & = 39.72 * \left(1 - \beta_{plat} + \beta_{plat} * \frac{t}{T_{ref}} \right) \end{aligned}$$

$$\begin{aligned} \text{Floating Turbine and platform mooring and anchoring installation cost} \left(\frac{\text{€}}{\text{kW}} \right) & \quad (45) \\ & = 65.05 * \left(1 - \beta_{moor} + \beta_{moor} * \frac{t}{T_{ref}} \right) \end{aligned}$$

Where:

β_{plat} = Fraction of platform installation costs dependent on transit between port and site = 0.329

β_{moor} = Fraction of mooring installation costs dependent on transit between port and site = 0.186

T_{ref} = Reference distance to port of 165km

t = distance between configuration cluster and nearest port(km)

Floating substation installation

The calculation for the costs for the floating substation are exactly the same as the ones for the floating turbines. The only difference is the total time of installation and associated sourced costs. The calculations have been tabulated below.

Outputs (Transit fraction calculation)		
Tug Boat	Travel time	3.00 days
	Calculated costs during transit	0.07 M€
Crew transfer	Number of trips for 3 vessels	1.00
	Crew transfer travel time	1.00 day
	Calculated vessel costs during transit	10.73 k€
	Calculated labour costs during transit	9.72 k€
	Total costs for crew transfer in transit	20.45 k€
Transit fraction for installation	Total costs in transit	87945.00 M€
	Transit fraction	0.020

Table 3.17. Transit fraction calculation (Floating offshore turbine and platform)

Outputs (Transit fraction calculation)		
Anchor handling vessel	Travel time	2.00 days
	Calculated costs during transit	0.10 M€
Transit fraction for installation	Total costs in transit	0.10 M€
	Transit fraction	0.300

Table 3.18. Transit fraction calculation (Floating turbine platform mooring system)

The equations are presented below.

$$\begin{aligned} \text{Floating Turbine and platform installation cost} \left(\frac{\text{€}}{\text{kW}} \right) & \quad (46) \\ & = 35.04 * (1 - \beta_{plat} + \beta_{plat} * \frac{t}{T_{ref}}) \end{aligned}$$

$$\begin{aligned} \text{Floating Turbine and platform mooring and anchoring installation cost} \left(\frac{\text{€}}{\text{kW}} \right) & \quad (47) \\ & = 2.71 * (1 - \beta_{moor} + \beta_{moor} * \frac{t}{T_{ref}}) \end{aligned}$$

Where:

β_{plat} = Fraction of platform installation costs dependent on transit between port and site = 0.02

β_{moor} = Fraction of mooring installation costs dependent on transit between port and site = 0.3

T_{ref} = Reference distance to port of 165km

t = distance between configuration cluster and nearest port(km)

AC and DC cable installation

The installation of the AC and DC cables employ the use of a cable laying vessel and a remotely operated vehicle. An analysis similar to the previous components was performed for the reference values in (Ioannou et al., 2018). The derived equations have been shown below. For the DC cables the variable distance to the nearest port is reflected in the total length of the export cables. The study decomposed the costs of the DC cable into those of mobilization costs of the vessels and the cable laying itself. For the AC cables, the costs of transit are also accounted for. The contributions of the mobilization/de-mobilization and in the AC case, the transit costs were subThe costs of labour transfer were not calculated since it was not mentioned in the report.

Inputs		
General	Reference distance to port	36.00 km
	Reference depth	26.00 m
	Availability factor	0.85
	Total AC cable length	147.70 km
	Total DC cable length	108.00 km
	Mobilization/de-mobilization costs	0.49 M€
	Total costs for installation AC	96.47 M€
ROV	speed	20.37 kmph
	Cost	90.75 k€/day
CLV	Vessel speed	25.93 kmph
	Cost DC	110.00 k€/day
	Cost AC	88.00 k€/day

Table 3.19. Inputs for the installation of AC and DC cables

Outputs - Cables (Length fraction calculation)		
ROV and CLV	Mobilization fraction	0.03
	Length fraction	0.97

Table 3.20. Length fraction calculation (DC cables)

Outputs - AC cables (Transit fraction calculation)		
ROV	Travel time	4.00 days
	Calculated costs during transit	0.36 M€
CLV	Travel time	3.00 days
	Calculated costs during transit	0.26 M€
Transit fraction for installation	Total costs in transit	0.63 M€
	Transit fraction	0.006
Outputs - Cables (Length fraction calculation)		
ROV and CLV	Mobilization fraction	0.01
	Length fraction	0.98

Table 3.21. Transit and Length fraction calculation (DC cables)

For the AC cables the the cost relationship was derived by dividing the costs into those incurred due to transit and those incurred actually laying the cables at the farm location. These were 8.24% and 50.17% respectively. No explicit mention was made for the use and cost of a rock dumping vessel for the installation of either cables.

$$DC \text{ cable installation cost}(M\text{€}) = 27.3 * (1 - \beta_{Len} + \beta_{Len} * \frac{L_{DC}}{L_{ref}}) \quad (48)$$

Where:

β_{Len} = Fraction of platform installation costs dependent on transit between port and site = 0.496

L_{ref} = Reference export cable length = 108 km

L_{DC} = Total length of DC export cables (km)

$$AC \text{ cable installation cost}(M\text{€}) = = 87.7 * (1 - \beta_T + \beta_T * \frac{t}{T_{ref}} + \beta_{Len} + \beta_{Len} * \frac{L_{AC}}{L_{ref}}) \quad (49)$$

Where:

β_{plat} = Fraction of platform installation costs dependent on transit between port and site = 0.082

β_{moor} = Fraction of mooring installation costs dependent on transit between port and site = 0.502

T_{ref} = Reference distance to port of 36km

t = distance between configuration cluster and nearest port(km)

L_{ref} = Reference AC cable length = 147.7 km

L_{AC} = Total length of AC cables (km)

In- turbine pipelines

The installation costs of the pipelines are internalized in the equation presented for pipeline costs in section 3.2.3. For the installation of the networked pipeline layout in the in-turbine case though, the installation would require transit to a cluster at a certain location. It was however, difficult to find a representative installation project with reliable data to account for the scaling process. The previous analysis of the AC cable installation showed a minimal dependence on transit distance of 0.6%. After considering the fact that modern pipeline laying vessels can lay up to 9km of pipeline per day compared to 0.6km/day for an AC cable laying vessel, it was assumed that the costs associated due to transit would be minimal for the pipelines. No calculation was therefore performed for the networked pipeline layout for the in-turbine configuration.

3.3.2. Decommissioning

The costs of decommissioning are expressed as a factor of the installation costs, shown in the table below. The rationale follows from the fact that for fixed structures, the decommissioning procedures follow similar timelines and require similar procedures as those of installation. For floating platforms, the platform and structures that they house can be towed back to port and dismantled onshore. The mooring systems need to be disconnected from the sea floor. Industry practice for cables is to cut the cables up in sections that can be retrieved using cheap service operation vessels. As much as 50% of total cable length may be left un-retrieved on the sea-floor, reflecting the low value of 0.1 in the assumption below (Ioannou et al., 2018)

Fixed Turbines and foundations	0.5	(Ioannou et al., 2018)
Fixed substation and offshore structure	0.3	(Ioannou et al., 2018)
Floating turbine and platform	0.7	(Maienza et al., 2020a)
Mooring systems	0.9	(Maienza et al., 2020a)
AC cables	0.1	(Maienza et al., 2020a)
DC cables	0.1	(Maienza et al., 2020a)

Table 3.22. Decommissioning assumptions

3.3.3. Soft capex

The assumptions for the remaining elements of the capex are tabulated below. These costs are applied to all the configurations since they relate to financing, development and logistics of an offshore project. (The Crown Estate, 2019)

Logistics (euro/kW)	
Sea-based support	3.83
Marine coordination	
Weather forecasting and metocean data	
Development, consenting and Management(euro/kW)	
Conenting surveys	131.43
Environmental assessments	
Resource and metocean assessments	
Geological and hydrological surveys	
Engineering and consultancy	
Other project expenses	
Insurance , Contingency, Project management(euro/kW)	232.19

Table 3.23. Soft CAPEX assumptions

3.4. Operation and maintenance

The cost for operations are assumed to be the same for all three configurations (The Crown Estate, 2019).

Operations (euro/kW)	27.5
Training	
Onshore logistics	
Offshore logistics	
Health and safety inspections	
Other (insurance, environmental studies and compensation payments)	

The costs for maintenance are expressed as a fixed percentage of the component capex costs, shown below. The floating sustructure assumptions are derived by multiplying the assumptions for fixed structures with a factor of 0.75. This is to reflect the fact that floating structures could be towed to the nearest harbour for necessary corrective or preventitive maintenance. This avoids the costs incurred due to unfavourable weather and also higher charter and hiring rates for offshore activities.

Configuration Type	Onshore	Offshore	In Turbine	Source
Turbine RNA	2%	2%	2%	(Rubí and González, 2018)
Foundation (Fixed)	2%	2%	2%	(Rubí and González, 2018)
Foundations (Floating)	1.5%	1.5%	1.5%	(Katsouris and Marina, 2016)
Substations incl platforms(Fixed)	2%	3%	4%	(Jepma et al., 2018)
Substations incl platforms(Floating)	1.5%	2.25%	3%	(Katsouris and Marina, 2016)
Electrolyzer	2%	2%	2%	(FCHJU, 2017)
Compressor	3%	3%	3%	(Jepma et al., 2018)
RO unit	3%	3%	3%	(Jepma et al., 2018)
AC cables	2%	2%	0%	(Rubí and González, 2018)
DC cables	2%	0%	0%	(Rubí and González, 2018)
Pipelines	4%	4%	4%	(Reuß et al., 2017)

Table 3.24. Operation and maintenance cost percentages

3.5. Lifetimes and losses

The lifetimes assumed for the annualization of the capex are shown below. The soft capex is annualized with a time period of 25 years.

Lifetime (Years)		Source
Turbines	25	(Rubí and González, 2018)
AC cables	25	(Rubí and González, 2018)
DC cables	25	(Rubí and González, 2018)
Substation/platform	40	(Jepma et al., 2018)
RO unit	20	(Jepma et al., 2018)
Electrolyzer	20	(Jepma et al., 2018)
Compressor	15	(Reuß et al., 2017)
Pipelines	40	(Reuß et al., 2017)

Table 3.25. Component lifetimes

All process losses for each of the three configurations have been tabulated below. In terms of conversion chain differences between turbines for the different configurations, the only difference lies between the case where hydrogen is converted within the turbine. With the removal of the LVAC to MVAC conversion step, the losses in the conversion chain within the turbine stand at 2% as opposed to the conventional 4.92% (Jepma et al., 2018). A wake loss of 5% for an assumed power density of 3.6 MW/km² has been sourced from (Nyserda, 2018). The wake loss does not account for the effects of other OWF configurations that may surround a given cluster, i.e., inter-farm wake losses. The ‘other losses’ are cumulative losses associated with Icing/Blade soiling, Low/High Temp Shutdown, Lightning Loss, on-board equipment load and Rotor Misalignment (Musial et al., 2020).

Component/element	Process	Configuration			Source
		1	2	3	
Turbine	(LVAC-LVDC)	2.00%	2.00%	2.00%	(Jepma et al., 2018)
	(LVDC-LVAC)	2.00%	2.00%	-	(Jepma et al., 2018)
	(LVAC-MVAC)	1.00%	1.00%	-	(Jepma et al., 2018)
	wake loss	5.00%	5.00%	5.00%	(Nyserda, 2018)
	other loss	2.80%	2.80%	2.80%	(Musial et al., 2020)
AC cables	-	32,33 (W/m/phase)	32,33 (W/m/phase)	-	(Arrambide et al., 2017)
Substation electric	MVAC-HVAC	0.40%	-	-	(Jepma et al., 2018)
	HVAC-HVDC	1.10%	-	-	(Jepma et al., 2018)
	MVAC-MVDC	-	1.10%	-	(Jepma et al., 2018)
DC cables	-	0.015% /km	-	-	(NSWPH, 2020)
ALK electrolyser	incl electricity	25.00%	25.00%	25.00%	(IEA, 2019)
Compressor	Electric	Variable	Variable	Variable	Calculated
	Leakage	0.50%	0.50%	0.50%	(Reuß et al., 2017)
RO	Electric	3.25 MWh/2000m3	3.25 MWh/2000m3	3.25 MWh/2000m3	(Amin et al., 2020)
Pipelines	Leakage	0.002% /km	0.002% /km	0.002% /km	(NSWPH, 2020)

Table 3.26. Component specific loss assumptions

3.6. Assumptions for future developments

Future reductions in price and improvements in efficiency till 2050 have been considered to account for technological development and learning. Future costs and improvements in efficiency were sourced from the literature as either absolute values or as a percentage of current baseline values. When in absolute form, the projected development was reduced to either a percentage reduction or a percentage improvement factor, relative to the assumed baseline in 2020. The percentages were then fit using exponential functions to generate expressions for all simulation years i.e., 2020-2050.

The assumptions made for the commercial availability of turbines in the NREL study (source 1 in table 3.10) for both fixed and floating foundations have been shown below. For this analysis it is assumed that the operational years are 2020,2025,2030 and 2035 respectively. This represents a conservative estimate for developments up until 2035.

Technology	Commercial Operation Dates			
	2019	2022	2027	2032
Turbine Rated Power (MW)	6	10	12	15
Turbine Rotor Diameter (m)	155	178	222	248
Turbine Hub Height (m)	100	114	136	149
Turbine Specific Power ¹³ (W/m ²)	318	410	310	311

Figure 3.4. Turbine details from (Musial et al., 2020)(Musial et al., 2019)

In Table 3.27 below, ‘x’ indicates no source data for the specified year. Data pertaining to source 1 below were already expressed as a percentage relative to the baseline year which was 2019 in the sourced study (Musial et al., 2020). The factors however, related to potential reductions in floating turbines and farms. For fixed structures, the projections made in (Valpy et al., 2017) were used. The NREL document notes that the floating specific costs and the projections mentioned in the report also apply to the array cables and future reductions in maintenance, however this distinction between fixed and floating technologies was not made for simplicity.

The electrolyzer capex reduction was derived using the assumption of a 500 euro/kW_e base line cost, a reduction to 400 euro/kW_e in 2030 and a price of 200 euro/kW_e by 2050 (IEA, 2019). The compressor is assumed to reduce by a compounded factor of 0.98 per 5 year step since mechanical compressors are a mature technology, however, future developments may see significantly cheaper electrochemical compressors. The conversion efficiency of the electrolyzer is assumed to increase from 75% in the baseline to 0.8% and 0.85% in 2030 and 2050 respectively.

Factors as %	Foundation type	2025	2030	2035	2040	2045	2050	Source
DEV	-	96.21%	93.32%	88.25%	x	x	x	(Musial et al., 2020)
RNA	-	99.39%	90.55%	75.00%	x	x	x	
Substructure	Float	99.23%	88.08%	68.48%	x	x	x	
Foundation	Float	99.39%	90.53%	74.94%	x	x	x	
Turbine installation	Float	99.95%	91.98%	78.80%	x	x	x	
Substructure and foundation installation	Float	99.91%	85.89%	62.67%	x	x	x	
Array cable	-	85.88%	74.03%	53.19%	x	x	x	
DC cab	-	85.17%	72.66%	50.64%	x	x	x	
Operations	-	77.68%	71.73%	58.07%	x	x	x	
Maintenance	-	75.24%	68.59%	53.31%	x	x	x	
Wind turbine yield	-	101.75%	102.40%	105.72%	x	x	x	
Substructure	Fix	84.27%	72.38%	x	x	x	x	(Valpy et al., 2017)
Foundation	Fix	84.27%	72.38%	x	x	x	x	
Turb install	Fix	84.27%	72.38%	x	x	x	x	
Substructure and foundation installation	Fix	61.44%	48.07%	x	x	x	x	
Electrolyzer	-	x	80.00%	x	x	x	40.00%	(IEA, 2019)
Compressor	-	95.00%	x	x	x	x	x	Assumption
Electrolyzer yield	-	x	106.67%	x	x	x	113%	

Table 3.27. Assumptions for future developments

4. Results

The following chapter presents the model results and will help to answer the 4 research sub-questions. Each sub-section is therefore structured to address each corresponding sub-question.

4.1. Configuration comparison (Hypothetical results)

All results in section 4.1 have been calculated with generalized cluster cases and are not specific to the North Sea. In these clusters, the depth within the cluster, i.e., for each turbine is constant at an assumed value. The notations D and T have been used to denote the Depth and transmission length values of a certain case. All hypothetical cases in section 4.1 are calculated using a gross capacity factor of 0.55 which does not include losses and availability factors. All results shown in this sub-section are for the year 2020 unless specified otherwise. The rest of the assumptions and equations used to derive these results are the same as the main model applied to the study space.

The first two subplots in Figure 4.1 compare the specific capex and specific yields of each of the three configuration types for three different representative sites. The abbreviations ON, OFF and IN represent the onshore, offshore and in-turbine cases respectively. From figure 1, the specific capex of the onshore configuration is the highest over all three reference depth and transmission lengths. The In-Turbine configuration has the lowest specific capex.

Subplot 2 shows a specific yield comparison for the reference cases. The results are as expected with the IN turbine type generating the highest yield, followed by the offshore and onshore cases. The third subplot shows the LCOH contribution per subsystem type. Generation or wind turbines, make up more than half of the costs for all three configurations. The label 'other' represents fixed project costs which includes the cost for fixed annual operations and soft capex.

System Comparison for Hypothetical cases - 2020 (5.4 GW_{OWF}, Gross capacity factor=0.55)

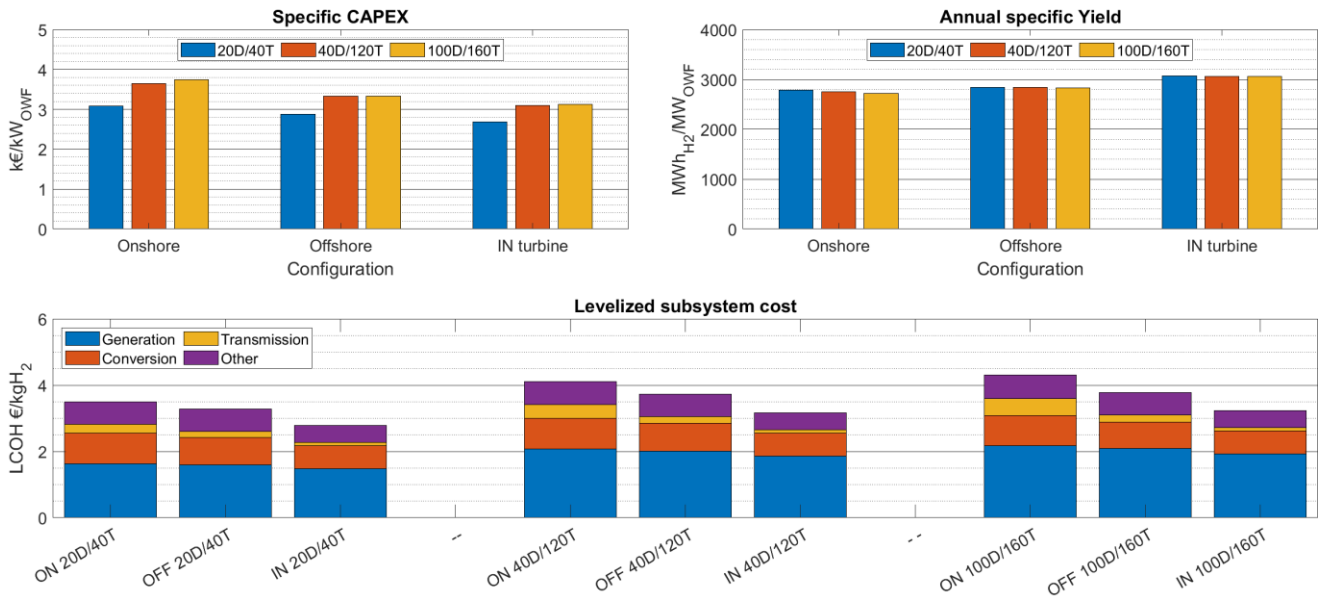


Figure 4.1. System comparison for Hypothetical cases- 2020

LCOH breakdown per configuration type

Figure 4.2 below shows component specific levelized cost contributions for each of the three configuration types for the same three reference cases. The most significant contribution comes from the turbines, costing at least more than twice every other component. The cost contribution from the turbines for the 100D case decreases when compared to the fixed counterparts. The fixed project costs make up the second largest contribution for the onshore and offshore configurations, followed by the electrolyzers. Higher pipeline costs in the In turbine case compared to the offshore configuration is a result of a larger number of smaller diameter pipelines in the wind farm and cluster network, as opposed to the single large platform to shore pipeline used in the offshore case. The difference between AC and DC cable cost contributions as opposed to pipeline costs is significant. The assumed values for fixed and floating platforms result in lower costs for floating platforms. This indicates an ideal transition point between fixed and floating that is lower than the chosen value of 40m depth.

Levelized component cost comparison for Hypothetical cases - 2020 (5.4 GW_{OWF}, Gross capacity factor=0.55)

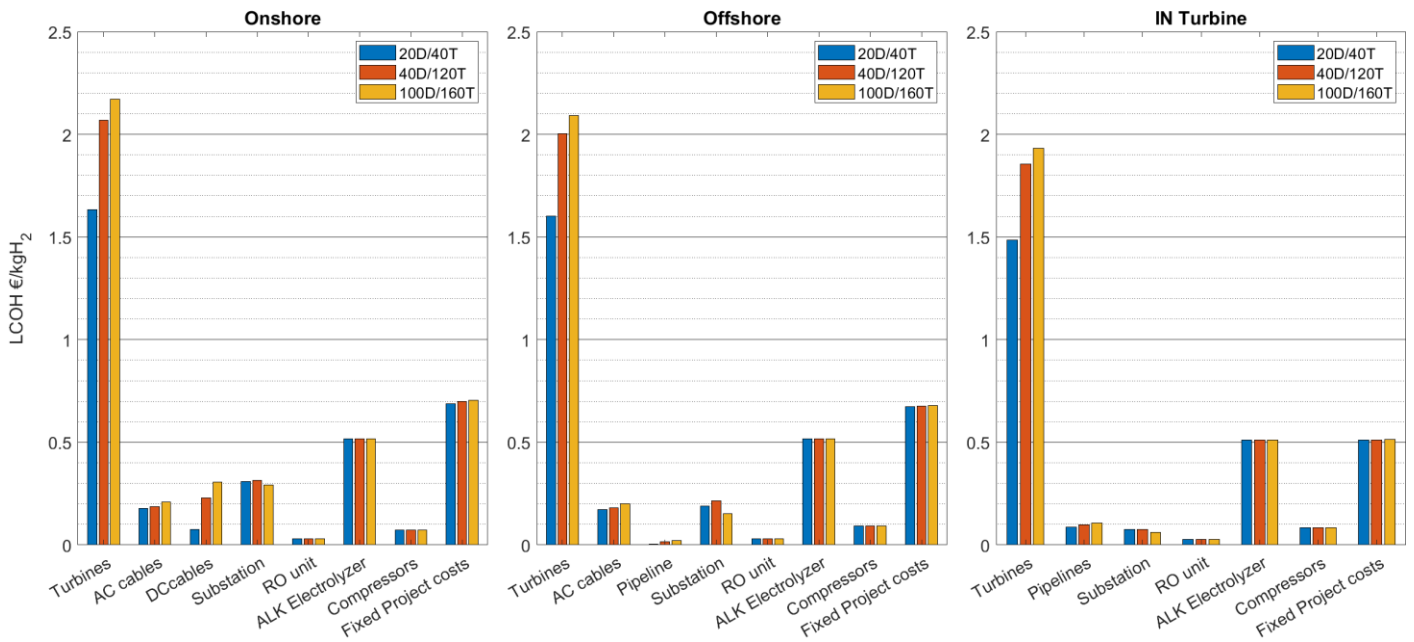


Figure 4.2. Levelized component cost comparison for Hypothetical cases - 2020

LCOH comparison between the three configurations for a range of Depths and transmission lengths

LCOH contours - 2020 (5.4 GW_{OWF}, Gross capacity factor=0.55)

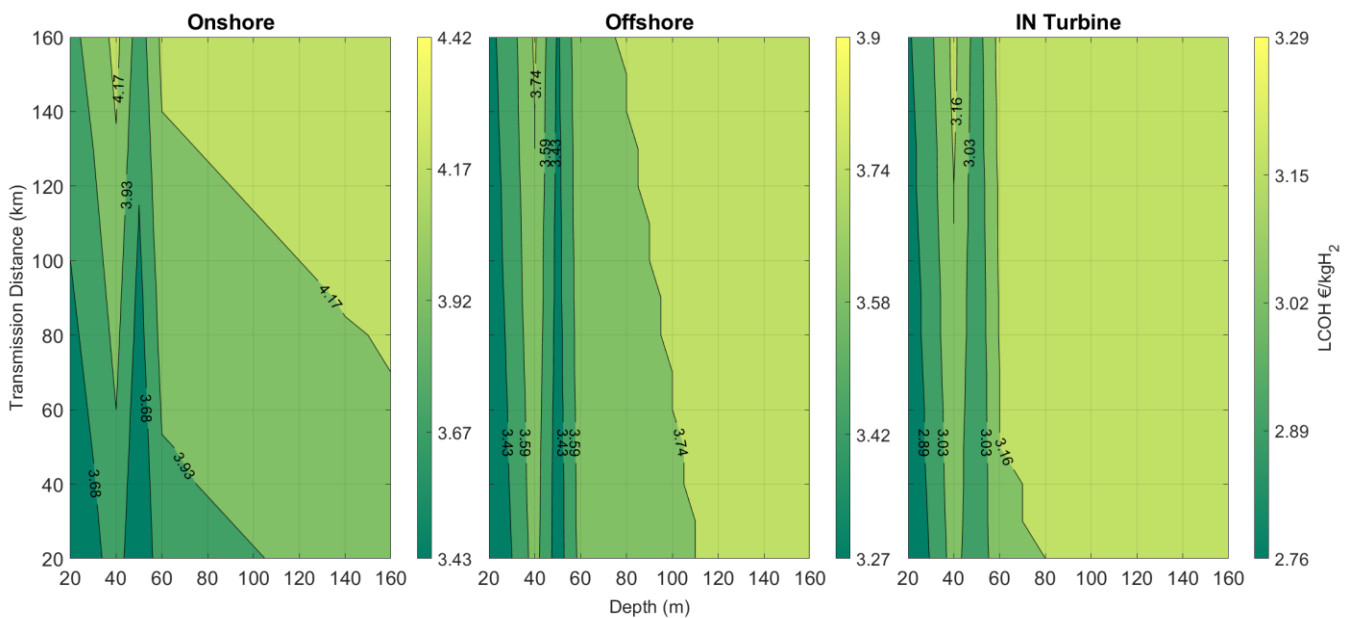


Figure 4.3. LCOH contour plots - Hypothetical - 2020

Figure 4.3 above shows the LCOH sensitivity to depth and transmission length for each of the 3 configuration types. The results were calculated for a reference cluster capacity of 5.4 GW and a gross capacity factor of 0.55. All 3 configurations exhibit a higher sensitivity to depth than transmission distance but the sensitivity is higher for the onshore case due to higher DC cable costs and losses. The LCOH for the onshore case therefore also increases more rapidly for higher depths and transmission lengths.

The influence of the transition depth at 40m is seen as the gradients flip either side of the point. Costs up till the 40m point rise steeply and this sensitivity decreases for floating technologies at higher depths. A decomposition of all cost elements as a function of depth and transmission distance revealed that the difference between the fixed and floating substations are the main reason for the abrupt change and corresponding behaviour in between 40-60m depth. This is because the chosen transition point does not equate to the ideal transition point for the substations for all three configurations. This transition for substations ideally, occurs lower than 40m with the current assumptions for cost.

Both the offshore and in-turbine configurations are relatively independent of depth. The reason the offshore case displays a pattern that is slightly different after the transition point is because the factors used to estimate the costs for the offshore substation, offer it the highest reduction relative to its closest fixed counterpart.

Temporal LCOH developments for Hypothetical cases

Figure 6 below shows the results of the assumptions made for component cost reductions and yield improvements over all simulation steps. The results of 2 extreme reference cases have been shown. The differences between the costs of the three types is reduced as we move along each 5 year step. For the higher extreme case in waters requiring floating foundations, a marginally steeper price reduction is seen as we move from 2020-2050.

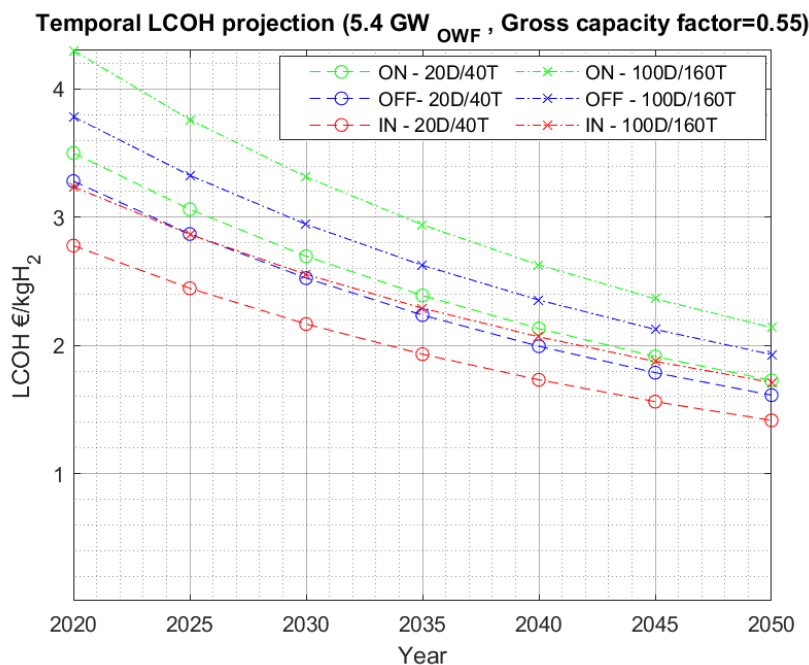


Figure 4.4. Temporal LCOH projection – Hypothetical

4.2. LCOH distribution in the North Sea over time and space (Without spatial exclusions)

The previous results in section 4.1 were for hypothetical cases with constant depth and transmission distance to shore/nearest port. The figures from this point on present model results specific to the North Sea. Section 4.2.1 first presents statistics that show the spread of the calculated results in the study space. Sections 4.2 and 4.3 then present supply curves and LCOH maps respectively.

Note that all results are plotted after removing values greater than 5 €/kgH₂. This was done to allow for sufficient visualization of the spread of the results. The values that were removed were mainly locations off the Norwegian coast which had poor wind resources at locations with depths >500m.

4.2.1. Statistical LCOH distribution in the North Sea (Current prices – 2020)

Depths and transmission lengths wherever mentioned in section 4.2.1, refer to values measured at the center of each cluster platform. The component specific sizing and costs however, do reflect explicit depth and transmission inputs from the study area. Outliers off the cost of Norway have been discarded to prevent skewing the outputs. Results shown in 4.2.1 refer to year 2020.

The subplot in Figure 4.5 below shows the statistical spread of the calculated LCOH values in the study space for each of the three configurations. Geographically, global transmission distances and depths vary between 0-300km and 0-400m respectively, with most of the depth values falling between 0-150m depth. The effects of lower component cost variance is seen in the range of values in the colorbar and the histogram for each of the three types. The spread of the LCOH values is the highest for onshore results and is followed by types 2 and 3.

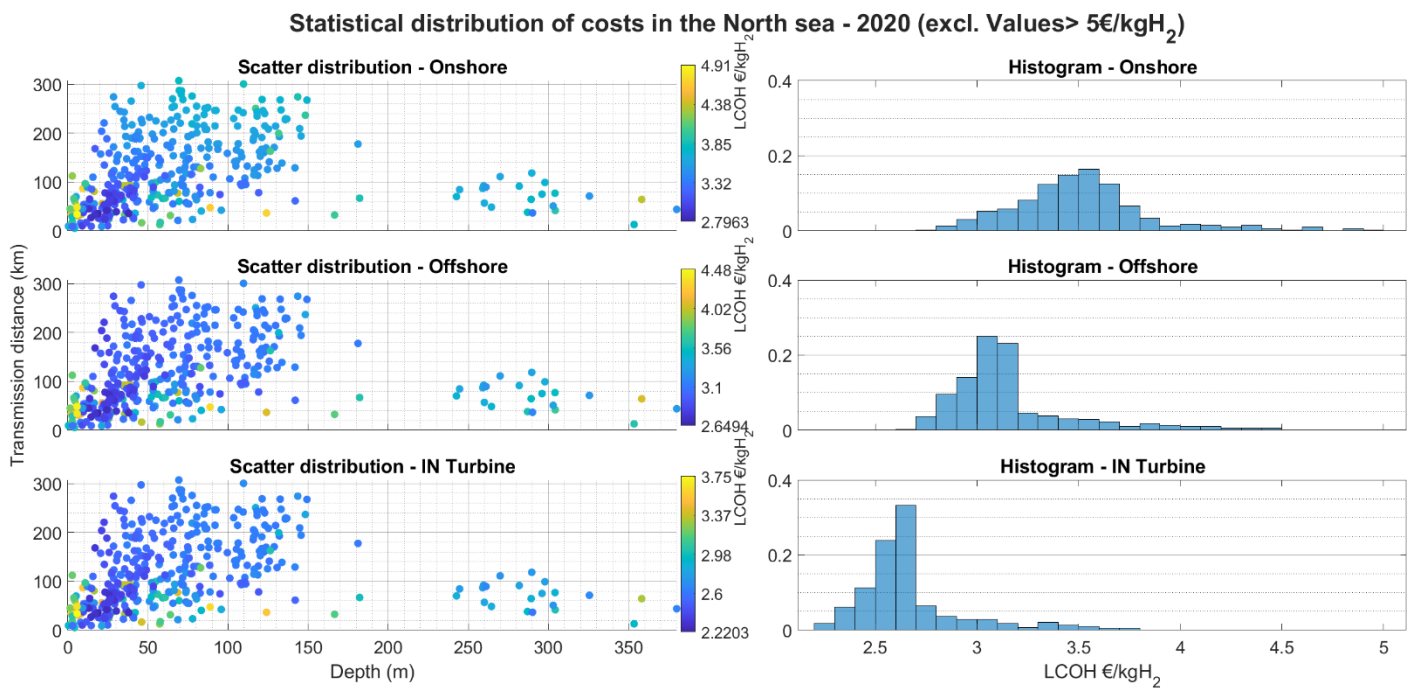


Figure 4.5. Statistical distribution of LCOH clusters in the North Sea - 2020

4.2.2. Supply curves

The distribution of the LCOH values shown in the previous sub-section is shown in the form of supply curves in the subplot below. Again, a few outliers off the coast of Norway were excluded for representation. Figure 4.6 below compares the global unrestricted supply curves between each type and depicts how the curves change for years 2020, 2030, 2040 and 2050.

There is a clear hierarchy for cheapest supply pathways between the three configurations, across all years. For 2020 the difference between all three curves is the highest and is reduced progressively as we move through time. In general all 3 configuration types experience a sloping due to lower component costs and higher yields, however, the effect on the onshore configuration is the most stark in comparison to the other two configurations. The flat supply curves reflect the extremely low spatial distribution of calculated costs in the North Sea.

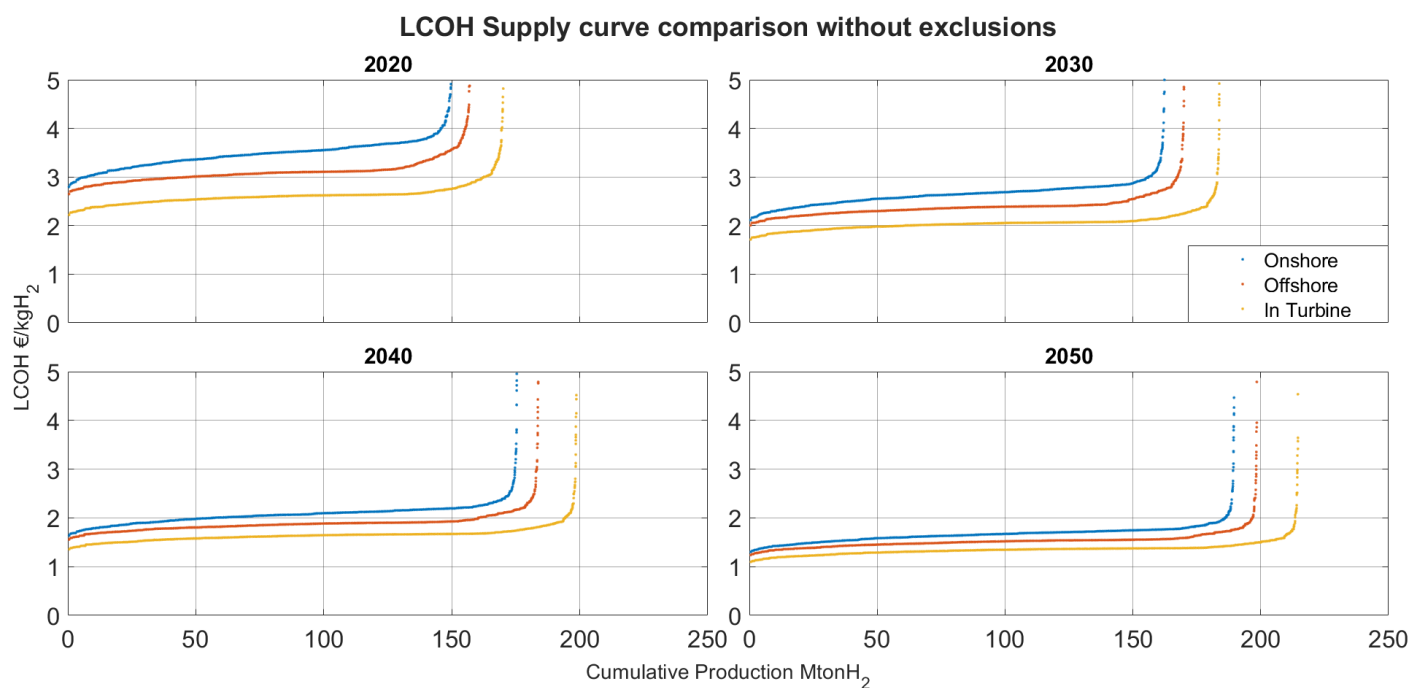


Figure 4.6. LCOH supply curves for the North Sea across time

4.2.3. Maps

LCOH maps for the North Sea

The next 3 figures plot the LCOH maps for the North Sea for the 3 configuration types. Figure 4.7 below shows the results for the onshore configuration across years 2020-2050. The range of values becomes smaller from 2020-2050 as seen before in the supply curves. For the onshore clusters, the costs are the lowest off the coasts of the Dutch, Danish and German shores, with low values also seen in the southern part of the North Sea, of the coast of the UK.

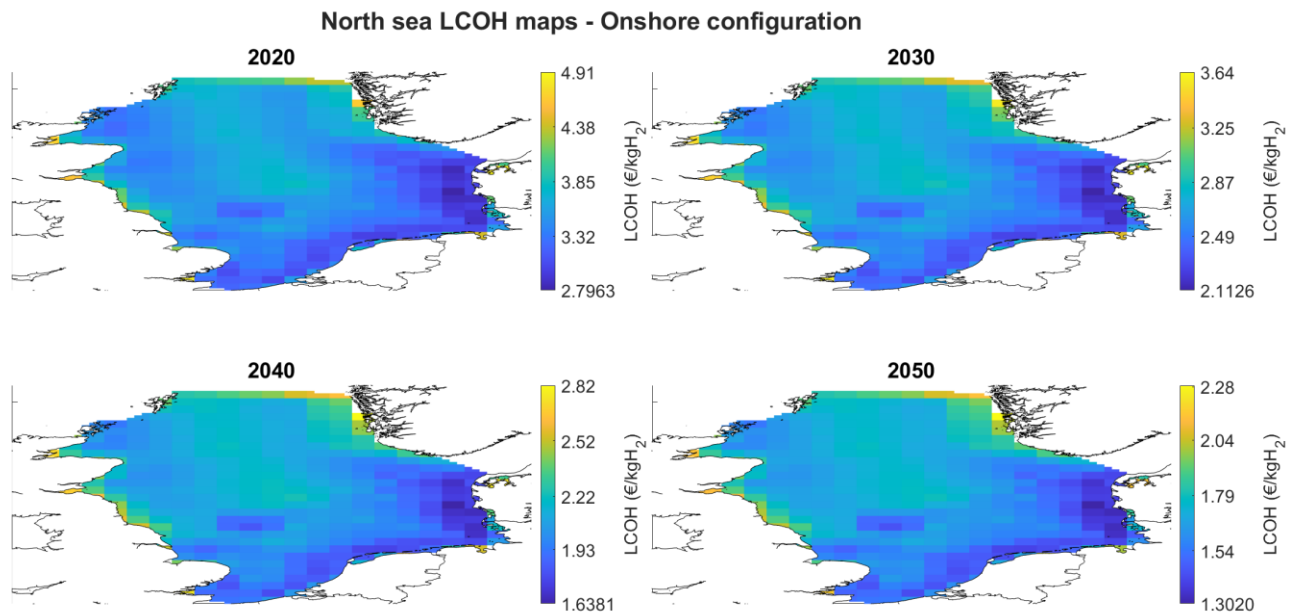


Figure 4.7. LCOH maps for the onshore configuration across time

Figure 4.8 and Figure 4.9 show maps that have patterns that are similar to each other for the offshore and In-turbine configurations. The range of data is however reduced and lower cost locations are spread more evenly, owing to a lower sensitivity to transmission distance. The observed, low variance of the capacity factors in the North Sea mean that in the north and north-west parts of the North Sea, the influence of the assumed costs for floating platforms over-ride potential benefits from transmission via pipelines. These values remain more or less constant across the study area.

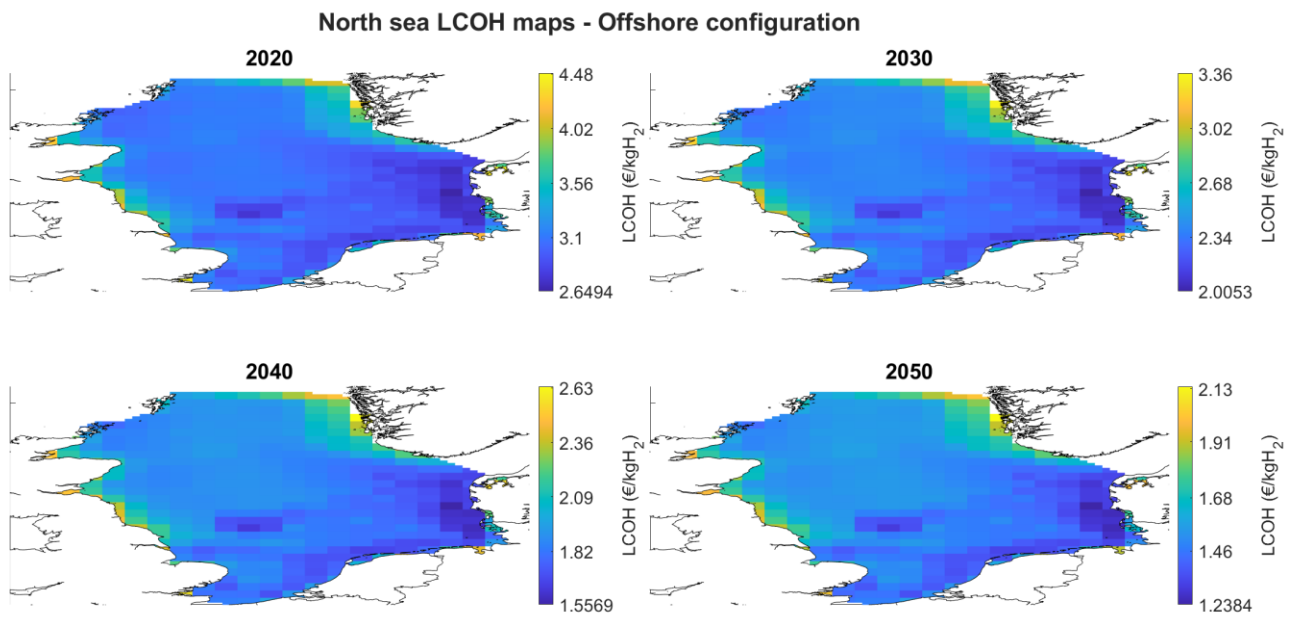


Figure 4.8. LCOH maps for the offshore configuration accross time

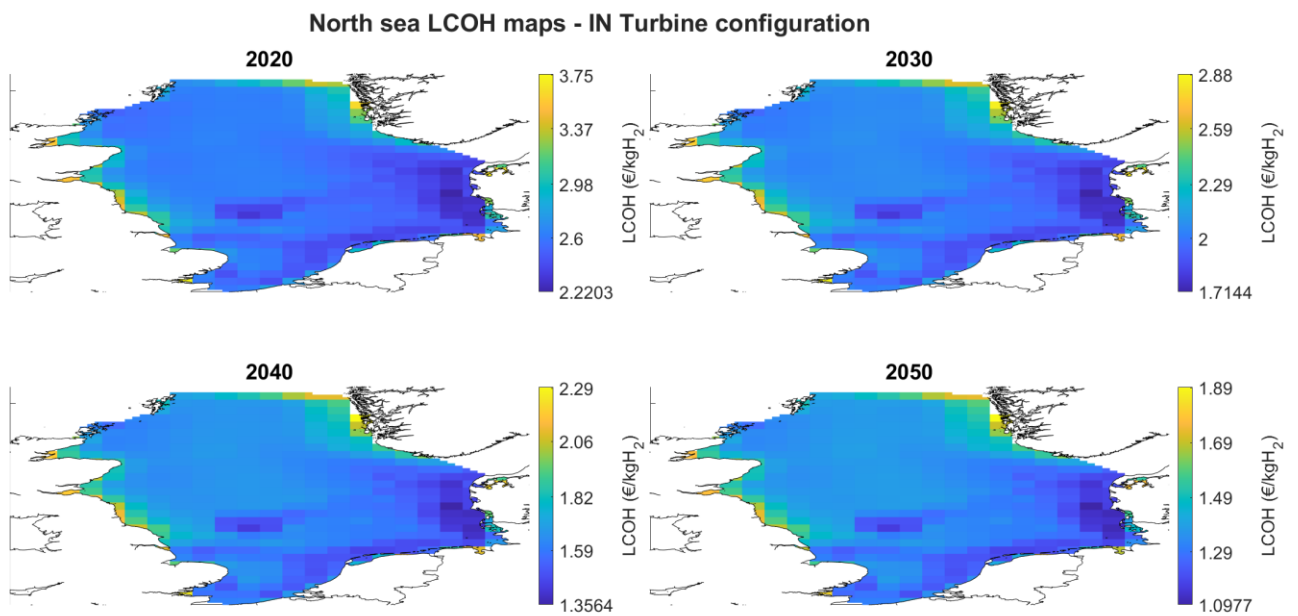


Figure 4.9. LCOH maps for the In Turbine configuration accross time

Spatial LCOH cost comparison

The next 3 figures show how the LCOH maps for each type compare with each other. Figure 4.10 shows this comparison between the offshore and onshore configurations. The maximum cost difference and the range of potential benefits of offshore over onshore are lowered across time. All locations of the offshore configuration are cheaper than the onshore case across all years but this difference is between 3.5-3.9% close to shore and can increase up to 18.7-13.6% in the center of the North Sea across 2020-2050.

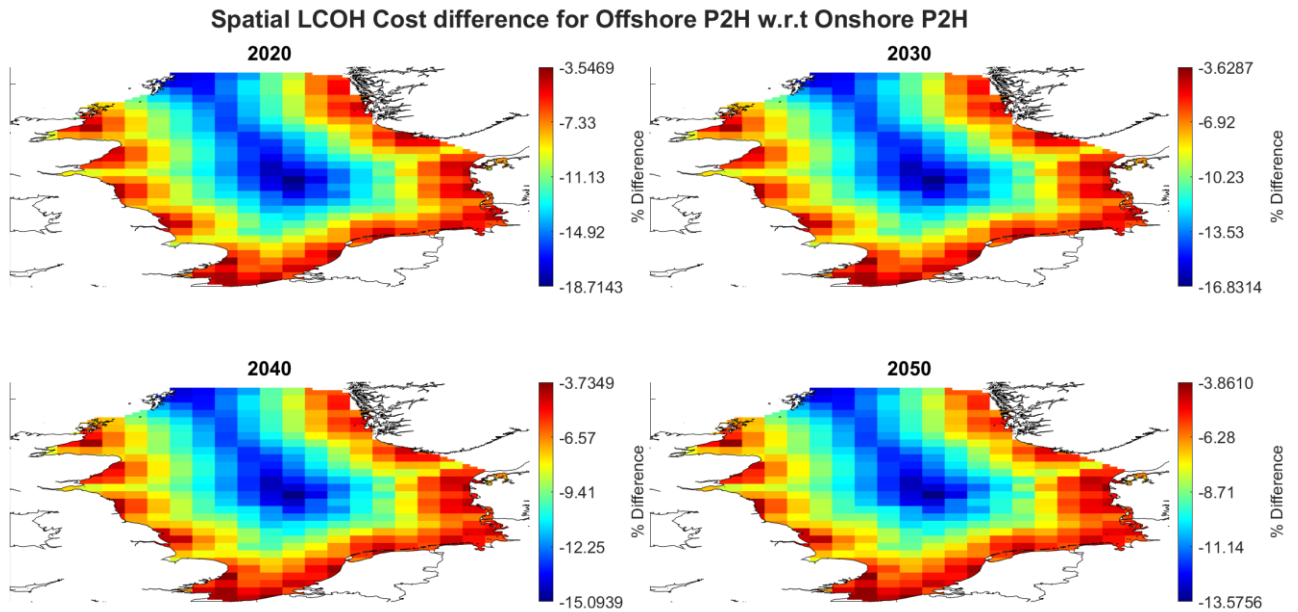


Figure 4.10. LCOH comparison maps for the offshore vs onshore configuration across time

Figure 4.11 shows how the In-turbine configuration compares with the onshore case. The maximum difference is significant and is 30.8% between offshore and onshore for the year 2020. Again the range and extremes are lowered across time but still reach a maximum benefit of 22.8% in 2050.

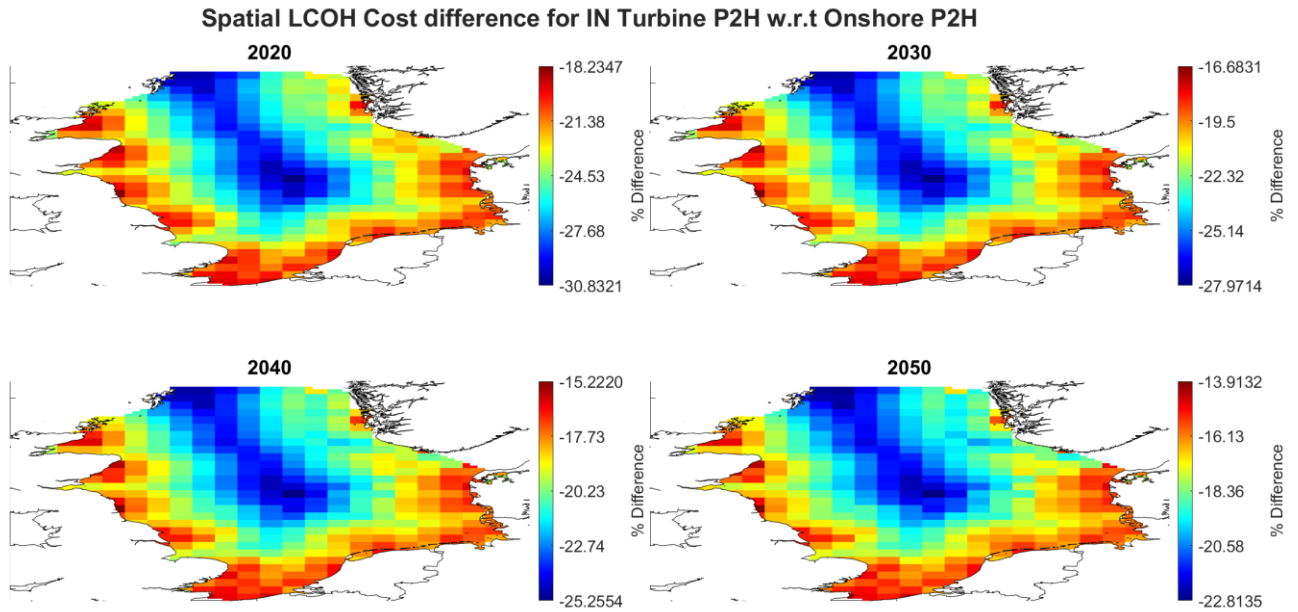


Figure 4.11. LCOH comparison maps for the In Turbine vs onshore configuration accross time

The difference between the in-turbine and offshore cases in Figure 4.12 are significant as well but lie in between the first two comparisons, following a slower benefit reduction over time. The spatial variance in this case follows the depth profile and capacity factor distribution of the study space, reflecting the effect of array cable costs and losses. The deepest locations off the norwegian coast are the most expensive offshore locations when compared to the in-turbine case.

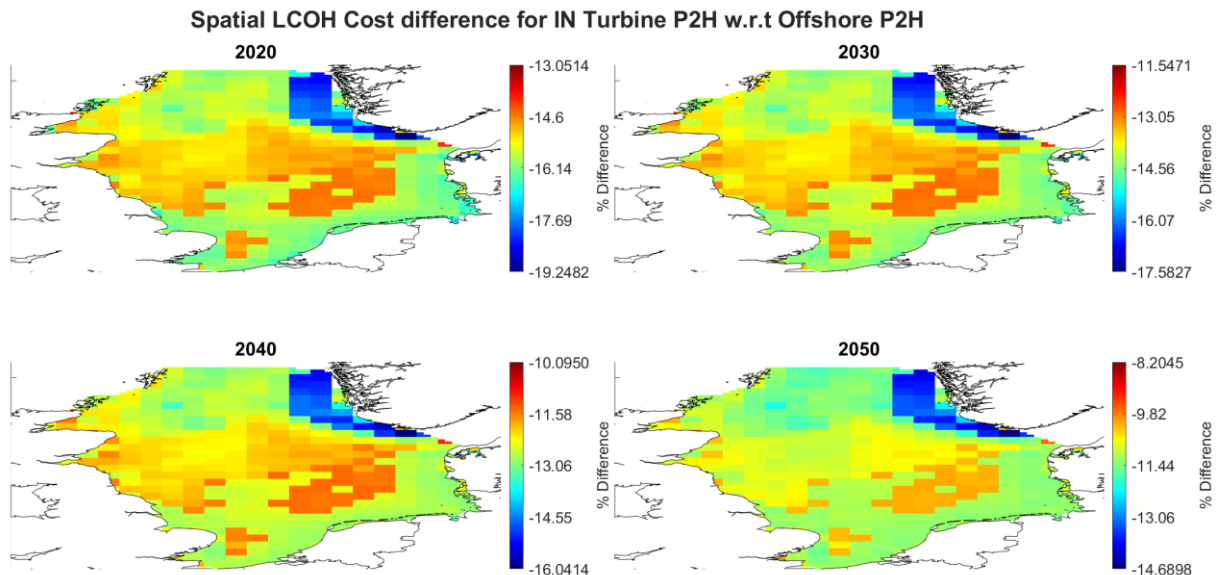


Figure 4.12. LCOH comparison maps for the In Turbine vs offshore configuration accross time

4.3. Exclusionary effects on supply pathways

The results in this section show how spatial constraints could affect the supply potentials in the North Sea. Figure 4.13 below first shows the unrestricted capacity potential in the North Sea. The results are in keeping with observed maritime areas for each country. The UK has an unrestricted capacity potential of more than twice every other country in the North Sea. The calculated values are representative for a power density of 3.6 MW/km².

Maximum unrestricted capacity potential per country 1900 GW

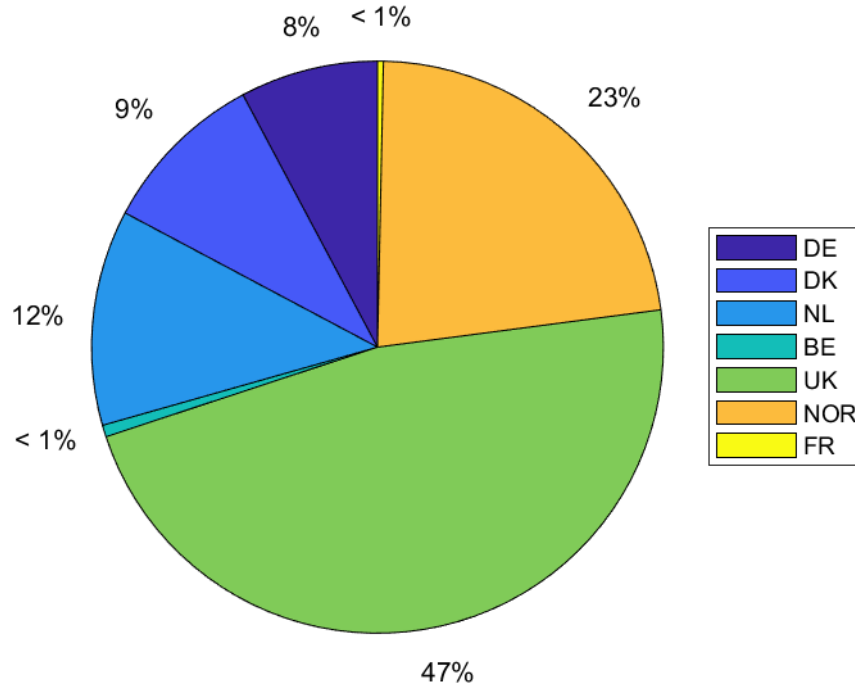


Figure 4.13. Pie chart of the maximum unrestricted GW capacity potentials in the North Sea

Power density (3.6 MW/km²)

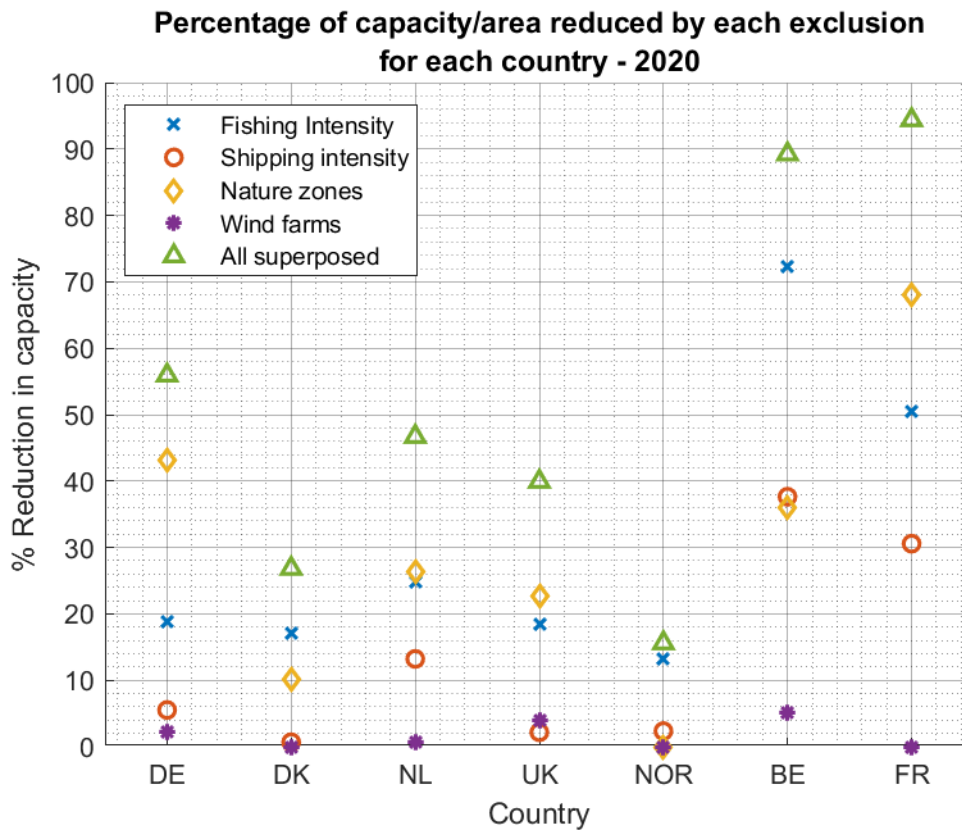


Figure 4.14. Exclusionary effects on the power capacity of each country - 2020

Figure 4.14 above shows how each exclusion affected the potential area/capacity of each country in the North Sea. Fishing and nature zones have the most effect on all countries. Belgium and France are affected the most owing to smaller North Sea maritime areas and having heavily utilized marine spaces in the southern North Sea. For the other 5 countries, Germany has the most conserved or designated protected marine space, taking up close to 45% of its total area. Fishing intensity reductions fall between 15-30% for the 5 larger NSC countries. Shipping takes up lesser space with the Netherlands being affected the most at about 15%. Germany, Netherlands and the UK face the most significant superposed exclusionary capacity reductions besides Belgium and France.

The effects of the exclusions on the yield per country has been shown below in Figure 4.15. The horizontal bars represent the 2050 H₂ demand for each country. The values for the 2050 demand for each country have been calculated by scaling the 2050 H₂ demand of 2251 TWh from (Fuel Cells and Hydrogen Joint Undertaking (FCH), 2019), using the TFE contribution by each country to EU TFE in 2019. The HHV value of 39.41 kg/kWh was used. Note that the demand for France was not accounted for and not plotted. When taken in isolation, the exclusions only affect Germany, Belgium and France, and results in a potential that is lower than the national demand. This is mainly due to fishing and nature zones. All other countries have more than enough potential yield capacities to satisfy 2050 national hydrogen demand.

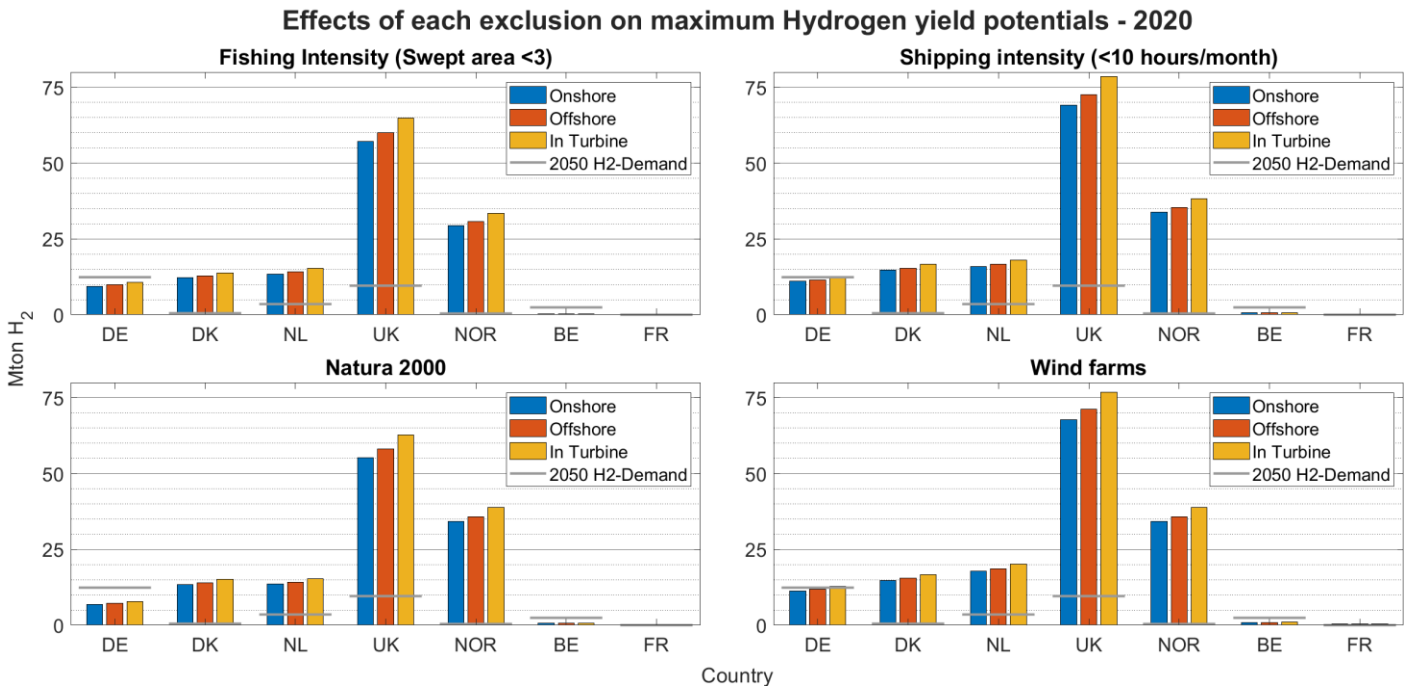


Figure 4.15. Effects of each exclusion on the theoretical yields for each country - 2020

Figure 4.16 below compares maximum restricted and unrestricted potentials for all the countries. Superposed exclusions have the most effect on the UK, Germany and the Netherlands. However again, only Germany, Belgium and France have lower potentials in this extreme case.

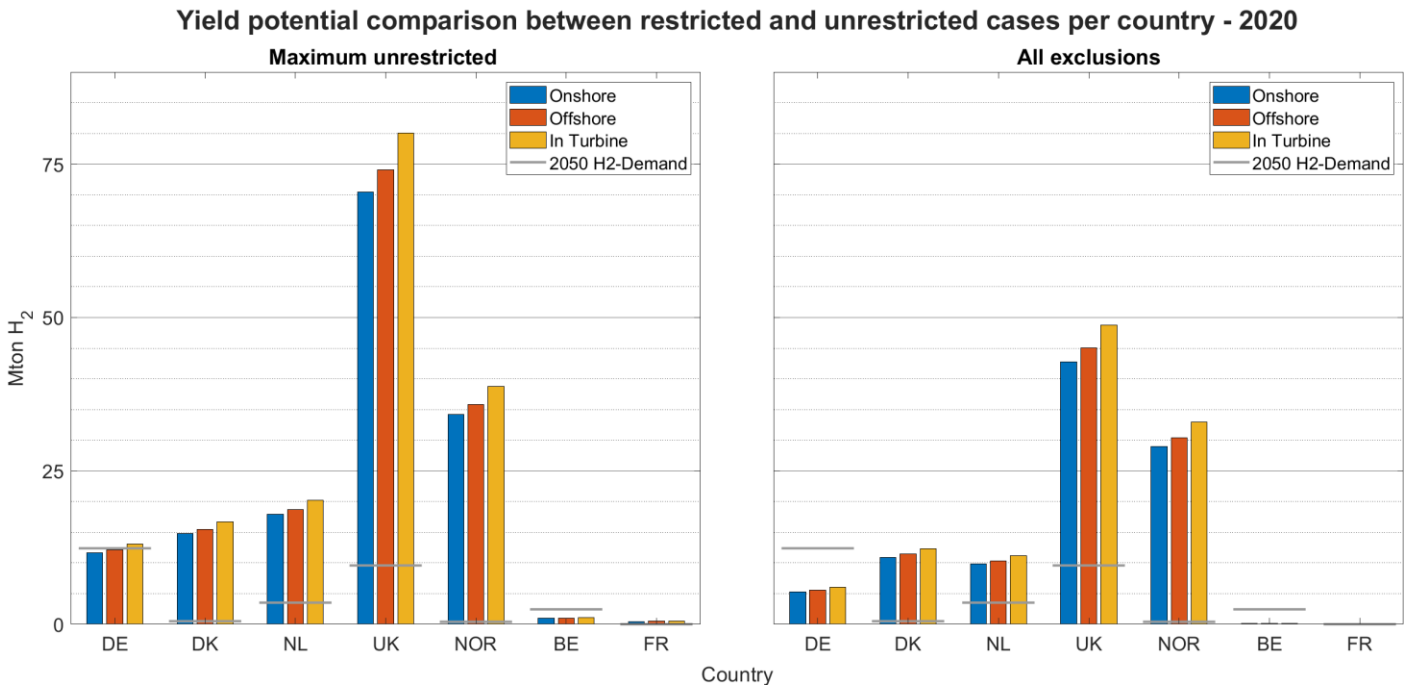


Figure 4.16. Comparison between maximum restricted and unrestricted H₂ yield potentials in the North Sea - 2020

Finally, Figure 4.17 below shows the exclusionary effects on supply curves for each configuration type for 2020. The exclusions cause the curves to shift up and to the left. The onshore supply pathway is affected the most due to a steeper slope, i.e, wider spread of costs that increase as we move away from shore and into deeper waters. This difference though is in the order of only 1 €/kgH₂ at most for the region before the curve shoots up for more expensive fringe locations. Both the in-turbine and offshore configurations are almost unaffected by the exclusions owing to a flatter curve and resulting lower dependence on cheaper but heavily utilized near-shore locations.

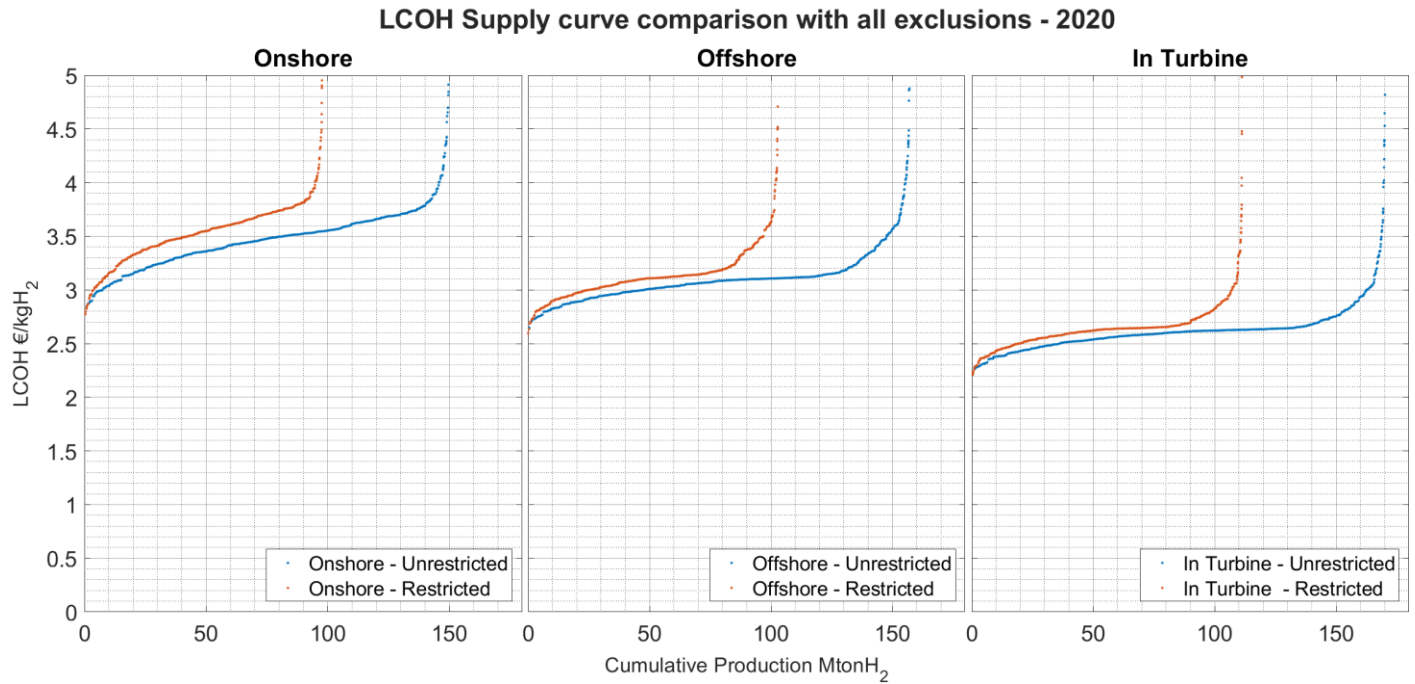


Figure 4.17. Comparison between restricted and unrestricted supply curves for each configuration type - 2020

4.4. Spatial comparison between Electricity and Hydrogen production

This section presents a comparison between hydrogen and conventional HVDC electricity supply costs in the North Sea. Hydrogen produced was converted to MWh using the HHV of hydrogen to offer a comparison between the two carriers. The first two figures offer a cost per unit of energy comparison between the offshore and the In-Turbine configurations w.r.t electricity. The next two then present a yield comparison between the same.

Figure 4.18 shows that hydrogen is more expensive than electricity for all years between 2020-2040. Between 2040-2050, locations in the center and north-western part of the North Sea become up to 7.5% cheaper for the offshore case.

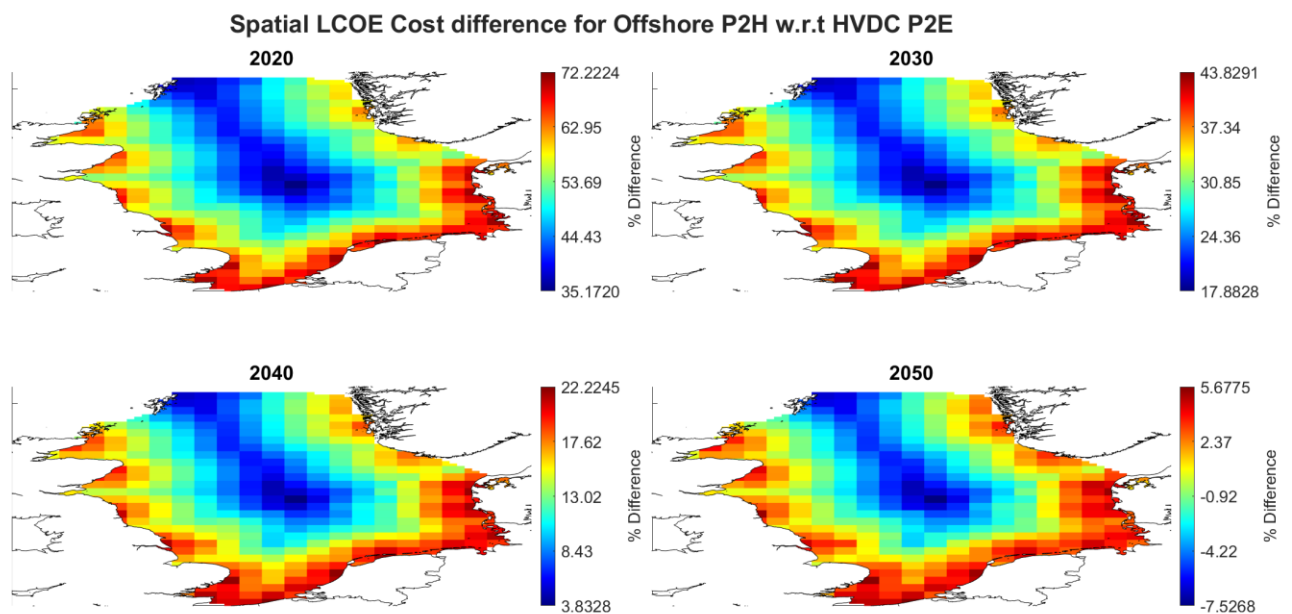


Figure 4.18. LCOE comparison maps for offshore P2H vs HVDC P2E accross time

Figure 4.19. shows that the In turbine configuration breaks even with HVDC costs between 2030-2040, with locations closer to shore being about 7% more expensive. More and more locations become cheaper over time and by 2050, all locations in the North Sea are revealed to be cheaper than conventional electricity production.

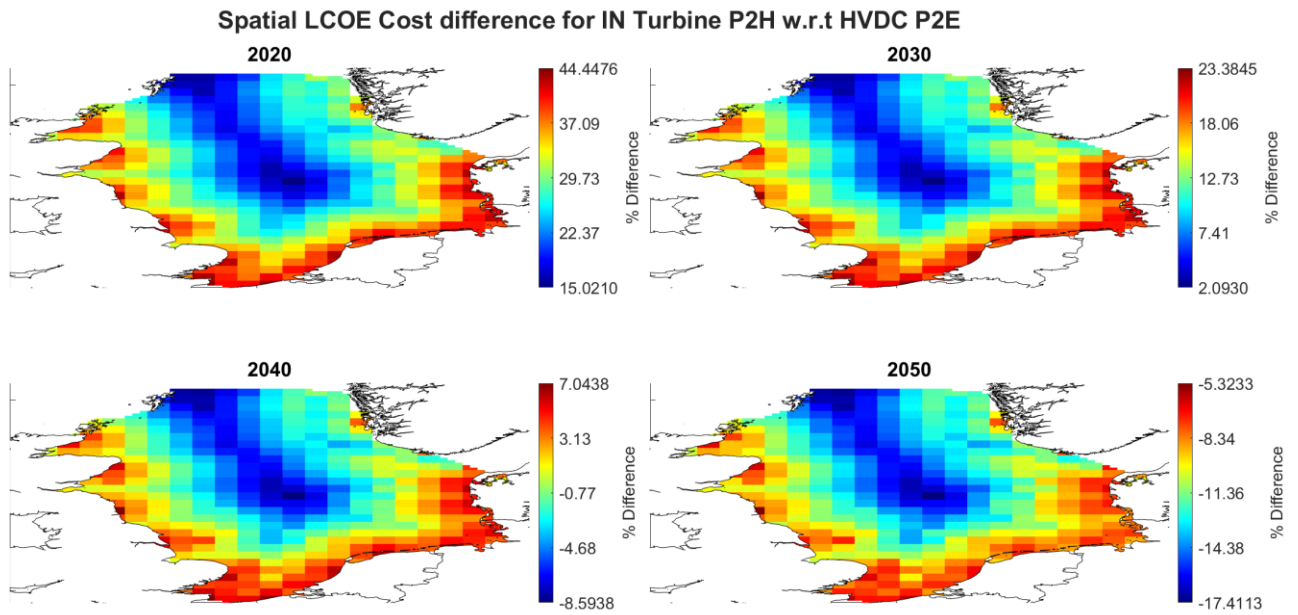


Figure 4.19. LCOE comparison maps for In Turbine P2H vs HVDC P2E accross time

Figure 4.20 and Figure 4.21 below compare how the energy extracted by the two P2H configuration types compare with electricity in the North Sea. All cases show a lower yield which is expected due to more steps in the conversion chain. The difference is lowered as we move through time and is a direct consequence of the improvements in electrolyzer conversion efficiency.

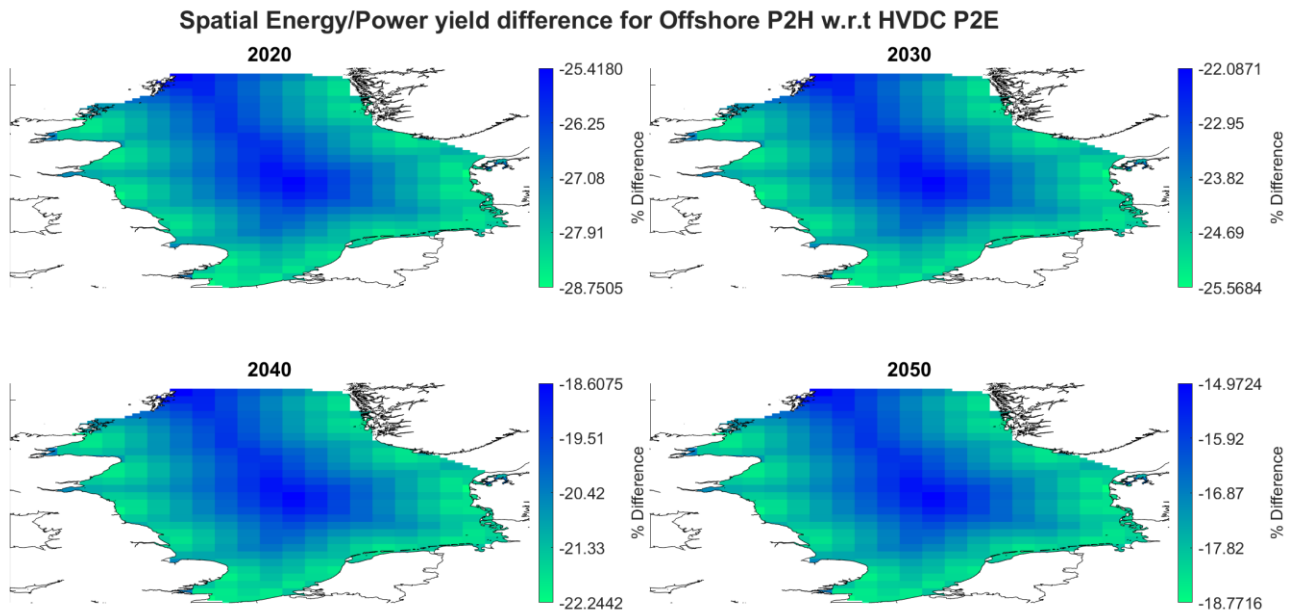


Figure 4.20. Yield comparison maps for offshore P2H vs HVDC P2E accross time

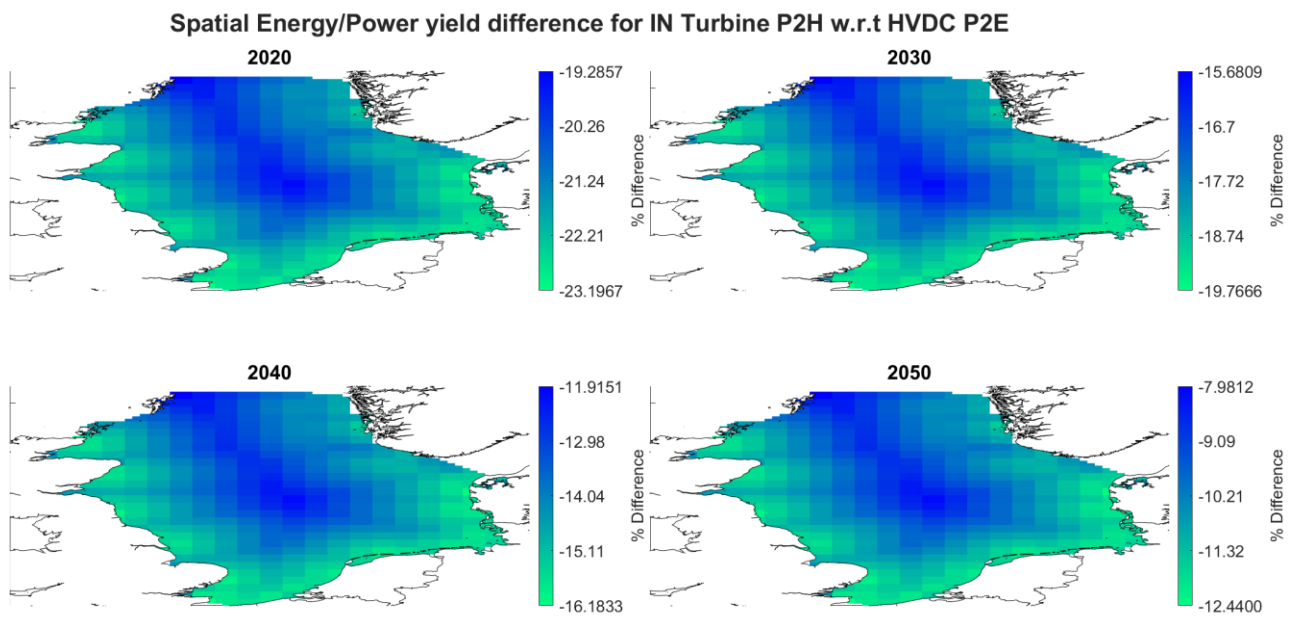


Figure 4.21. Yield comparison maps for In Turbine P2H vs HVDC P2E accross time

5. Discussion

This section draws on from models results in the previous section. Section 5.1 first notes the key limitations of the study. Section 5.2 tries to address some of the discussed limitations using a sensitivity analysis. Section 5.3 then weighs the calculated costs against the EU and the North Sea countries' projected hydrogen and electricity demands in 2050.

5.1. Limitations and Critique

Assumptions for the installation module

The assumptions for the installation module may be a possible source of error since the installation costs were assumed to scale with rated capacity. The installation costs of the turbine and the foundations could be lowered by using larger vessels with higher transfer capacities. On the other hand, the installation costs do not account for possible logistical barriers associated with transporting and installing offshore substations and platforms of this scale. Current installation vessels could possibly install substations in the order of 1.5GW. The number of substations and the corresponding vessels to install them would cause the costs to differ from those estimated in this study, which used values pertaining to reference farms with substations of 2x252MW and 125 MW for the fixed and floating cases respectively.

In general, the proportionality constants that were derived to express the dependence on transportation distance and depth, were derived using a highly simplistic analysis. The constants may have not accurately reflected the costs as a function of the depth and transit distance gradients in the North Sea.

Assumptions for floating technologies

The transition point between fixed and floating technologies was selected by comparing the total cost of the substructures. Differences in baseline costs would shift this transition point. Jacket structures could possibly shift this point to higher values.

Whether or not pipeline transmission becomes cheaper further from shore in the north-central and north-west high capacity factor regions, depends heavily on the costs for floating foundations, since the costs of turbines and foundations in general, are the most significant cost contributing elements. The current results indicate that the yield benefits are offset by the costs for these high capacity regions. However, if floating technologies become cheaper, this could potentially invert the spatial pattern observed in the offshore and In-Turbine LCOH maps.

No consideration was made for the transition point between fixed and floating substation platforms. A consideration for this design choice would result in smoother transitions between fixed and floating. Current abrupt transitions are mainly due to a simplified standard transition point for all foundation technologies.

Possible errors in GIS data pre-processing

The extraction and pre-processing of the GIS inputs took up the most amount of time during initial model runs. Instead of automating the extraction and pre-processing of the sourced GIS files, it was therefore decided to

save, or assign the sourced inputs to the closest grid point in a dummy reference grid. . The initial extracted values were interpolated and extrapolated linearly to newer grids that were defined during the course of the thesis. This reduces the spatial explicitness of the analysis. However, for an analysis of a spatial region of this scale, this approach was adopted for simplicity.

The fishing intensity and shipping intensity input datasets were gridded cells and geotiff images respectively. It was necessary to convert these into a format in a way that made generating spatial exclusion masks easy. The approach adopted was to convert the input cells or pixel data to points. These data values were then assigned to the dummy grid mentioned before using interpolation. This again, reduced the explicitness of the model. An alternative option would have been to generate polygon boundaries around exclusionary data points with values higher than selected limits. These would then serve as an input to MATLAB masking functions.

Simplistic design for array cable layouts

The algorithm used to generate the cable layouts was highly approximate. Ideally, optimized layouts would be designed using a combination of minimum graph trees and power flow equations. The array strings have been sized to accommodate 1 turbine less than the maximum possible cable capacity. This introduces an overestimation of calculated cable lengths for a given cluster.

Lack of spatial exclusionary dynamics

The model does not account for spatial dynamics which will change eligible locations. For example, a change in designated fishing zones due to the need to move activities elsewhere to allow the aquatic population to replenish itself. The assumptions made for the fishing intensity and shipping intensity limits need further investigation as well. No accounting was also made for designated military and oil and gas zones which occupy a considerable amount of space in the North Sea.

No accounting for effects of scale

No explicit assumptions were made to account for scale benefits, besides the costs of the electrolyzer and the RO unit. The analysis assumed a constant baseline value of 500 €/kW_e for the alkaline electrolyzer in 2020. This value is expected for electrolyzers of scales in the order of 100MW. This however, may not apply to the in-turbine case and the analysis therefore makes an optimistic assumption.

A lack of foresight in relation to the development of future costs and technologies

The assumptions for reductions in costs were, in most cases, projected using reference estimates from sources up until 2030. The long term reduction potentials between 2030-2050 may therefore be underestimated. The assumptions made for future projections were also derived using curve fits which add to the uncertainty in future developments.

5.2. Sensitivity analysis

Some of the limitations discussed in the previous section will be discussed in this section.

The four main tests performed were :

1. Supply curve sensitivity to WACC rates in the North Sea
2. LCOH sensitivity to WACC rates and capacity factors
3. LCOH comparative sensitivity to the In-turbine electrolyzer cost
4. Yield and capacity potential sensitivity to varying power densities

5.2.1. Supply curve sensitivity to WACC rates

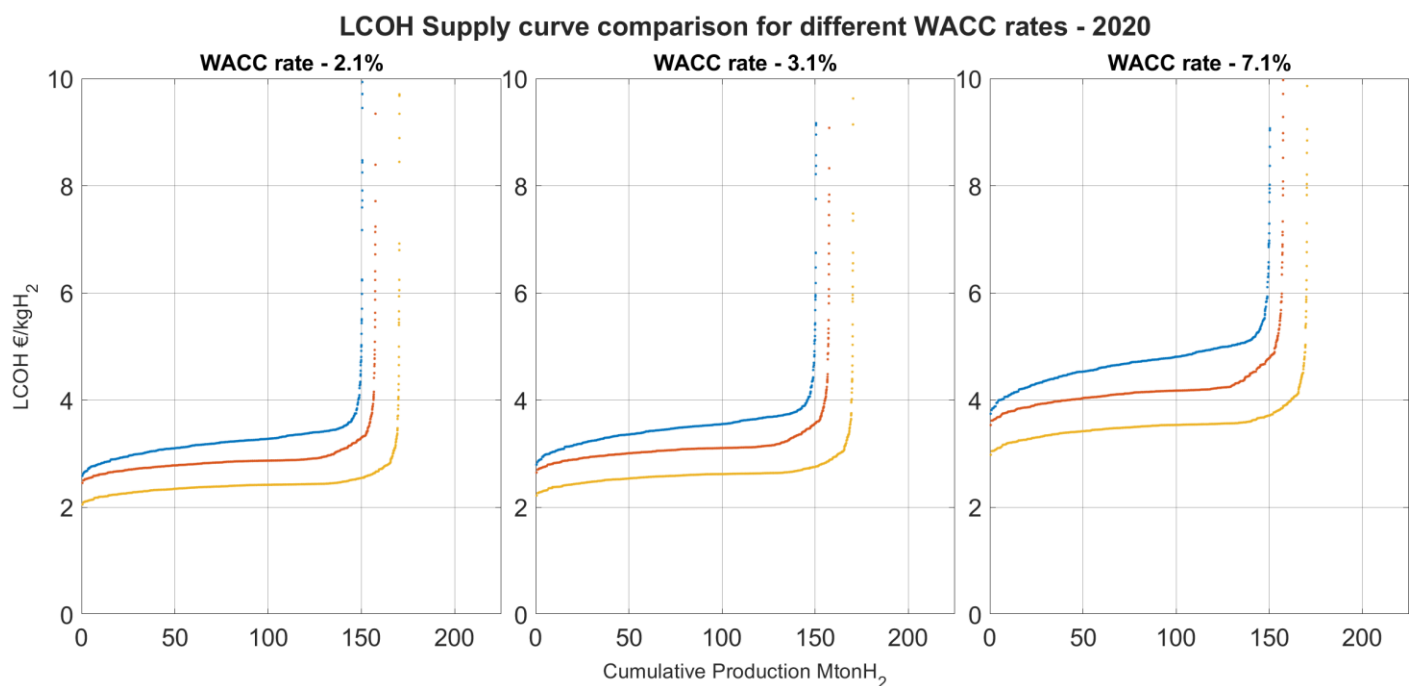


Figure 5.1. Supply curve sensitivity to WACC rates - 2020

The supply curves for 2020 were plotted using a WACC rate of 2.1% and 7.1% to show the variation in prices compared to the baseline 3.1% case. For the case with a WACC rate of 7.1%, the lowest prices increase to 3, 3.62 and 3.81 for the In-Turbine, offshore and onshore cases respectively. The higher WACC rate, as seen before in the supply curves for HVDC, cause the curves to become steeper. The in-turbine and offshore configurations though show a lower sensitivity to a higher WACC rate for more expensive locations in the North Sea. Even with the higher more realistic WACC rate, the model results show favourable results for the In-turbine configuration.

5.2.2. LCOH sensitivity to WACC rates and capacity factors

The next 3 plots present sensitivity tiles for each configuration, for the three reference depths and transmission distances discussed previously. The values are calculated for the Hypothetical cases in 2020.

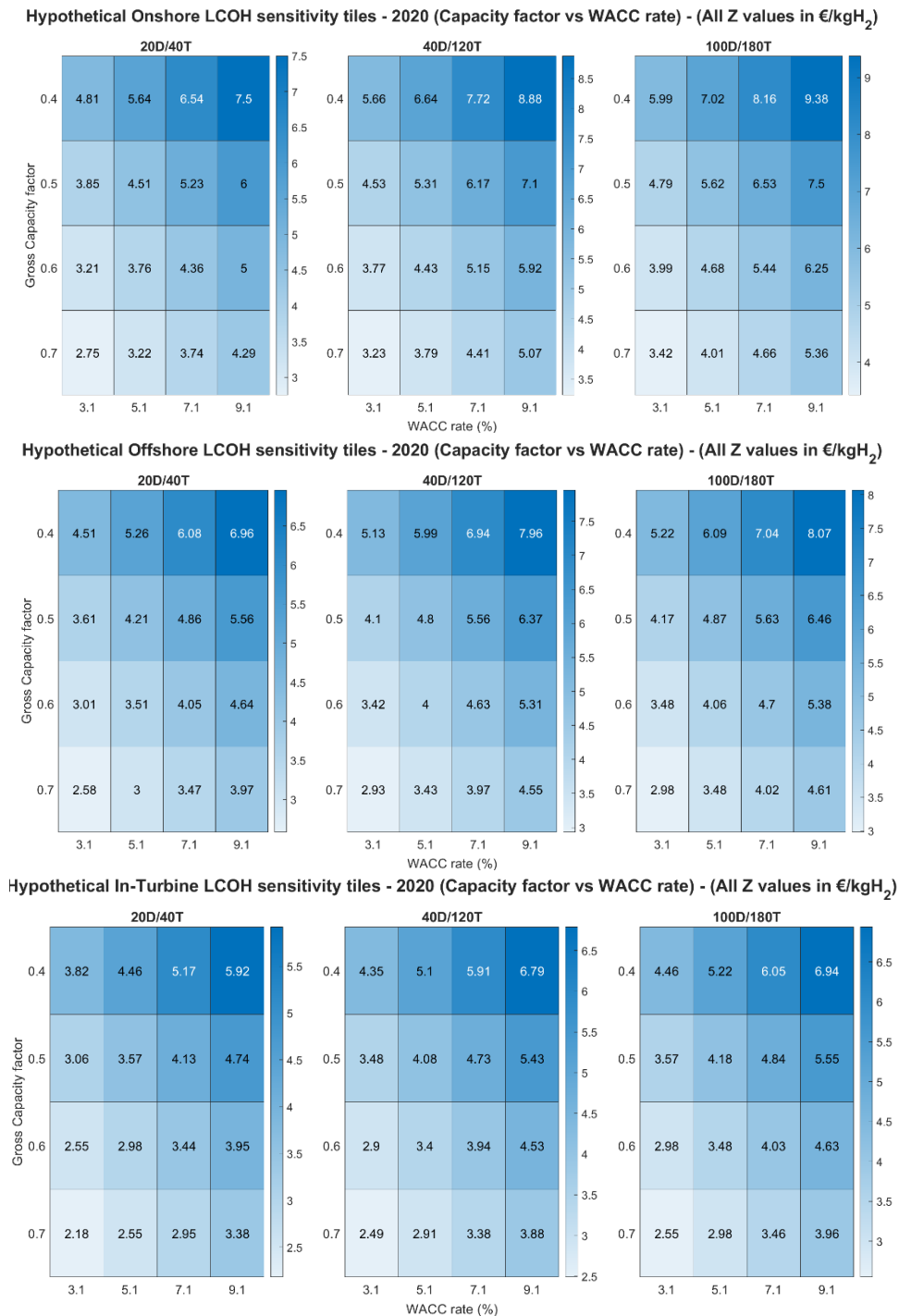


Figure 5.2. LCOH sensitivity to gross capacity factor and WACC rates for the three configurations (Hypothetical cases - 2020)

5.2.3. LCOH comparison sensitivity to cost of In-Turbine electrolyzer

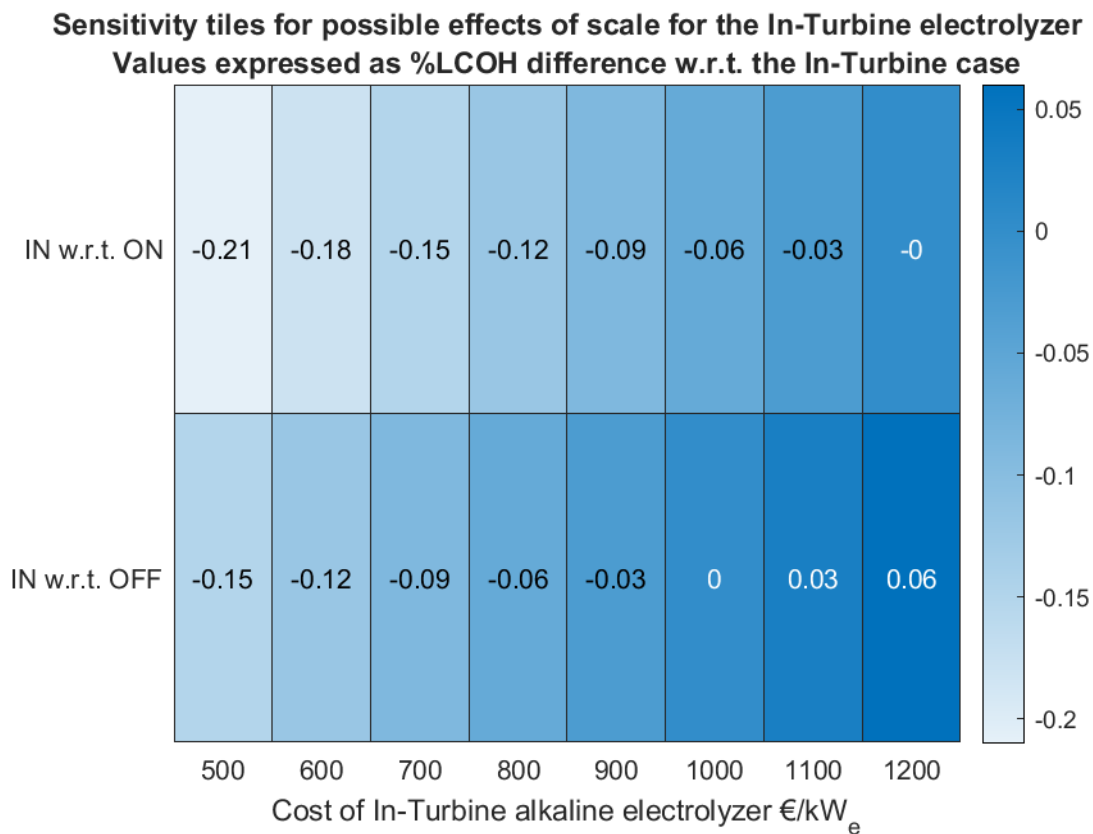


Figure 5.3. Relative LCOH sensitivity comparison for variable In-Turbine electrolyzer costs

For the in-turbine case with a smaller electrolyzer, the possible consequences of higher electrolyzer costs were calculated for an hypothetical case at (20D/40T), and compared to the LCOH values of the onshore and offshore configurations which use a fixed baseline cost of 500€/kW_e.

For a gross capacity factor of 0.55, the tiles in the plot above show that the limiting cost at which the LCOH for the in-turbine configuration becomes equal to the onshore case is 1200 €/kW_e. The limiting cost w.r.t the offshore case is 1000 €/kW_e. The limiting cost will however, shift higher or lower depending on the value of the gross capacity factor.

5.3. Model results in a wider context

The results from the previous section will now be put into perspective by estimating how future demand targets can be met. The 2050 H₂ demands for the North Sea countries, the EU and either 50% or 40% of 2050 EU TFEC were superposed on the supply curves presented in sections 4.2 and 4.3. The demands have been tabulated in table 5.1 below. The limiting values for costs to satisfy these demands were used to plot boxcharts to estimate the range of costs needed to satisfy each 2050 demand under different conditions.

2050 Demands (TWh)			
NSC H2	EU H2	40% EU TFEC	50% EU TFEC
1136.88	2251	3720	4650

Table 5.1. Projected 2050 TFEC demands in Europe

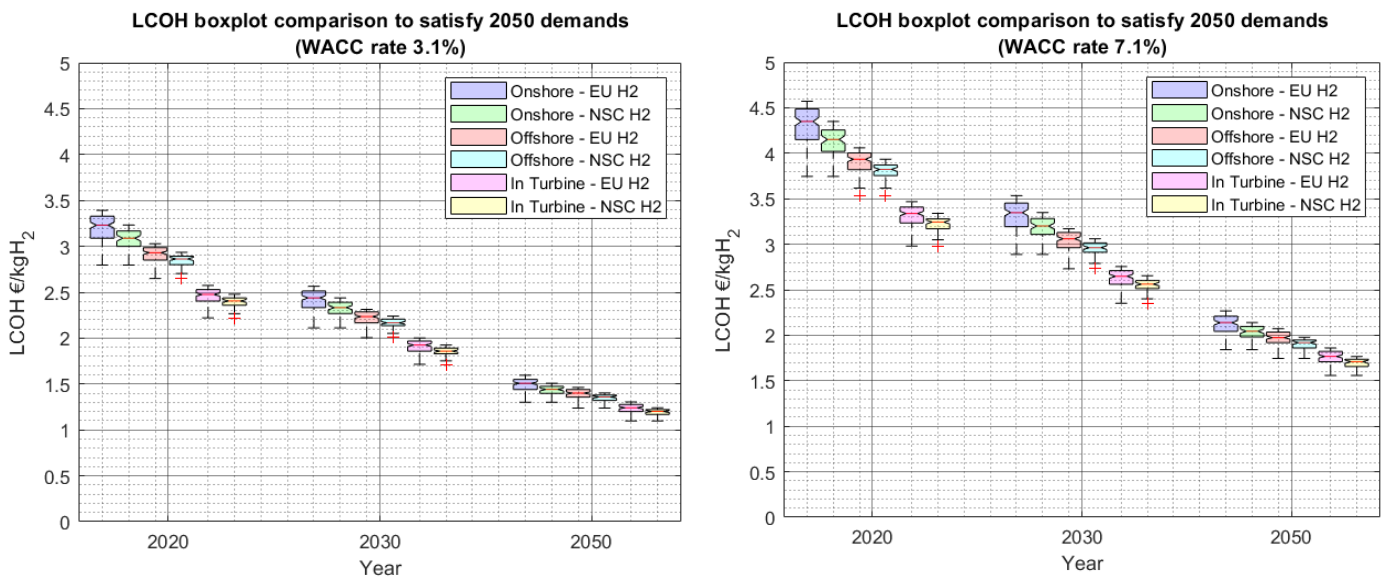


Figure 5.4. LCOH boxplot comparing the range of costs to satisfy 2050 H₂ demands

(a. WACC rate = 3.1% ; b). WACC rate=7.1%)

The range of costs to satisfy the EU and NSC H₂ demands are first shown in Figure 5.4 above using a box plot. The observed hierarchy between the three configuration types and the developments over time are seen in the plot again. Flattening of the supply curves cause the range of the boxes to be more compact than they already are over time. Between 2030-2050 we see more favorable spreads for offshore relative to the In-turbine case. By 2050, medians for all types are under 1.5 €/KgH₂ and 2.25 €/KgH₂ for WACC rates of 3.1 and 7.1 respectively.

As mentioned before, wind europe predicts 212GW of offshore wind to be deployed in the North Sea by 2050. The effects of this potential spatial competition with future North Sea offshore wind farms on H₂ supply pathways has been shown in Figure 5.5 below. The minimum values are not affected but we see a stretching out of all the distributions with medians shifting up by about 0.25 €/KgH₂ and 0.5 €/KgH₂ for WACC rates of 3.1% and 7.1% respectively. However, as seen before, the In turbine configuration feels the effects the least

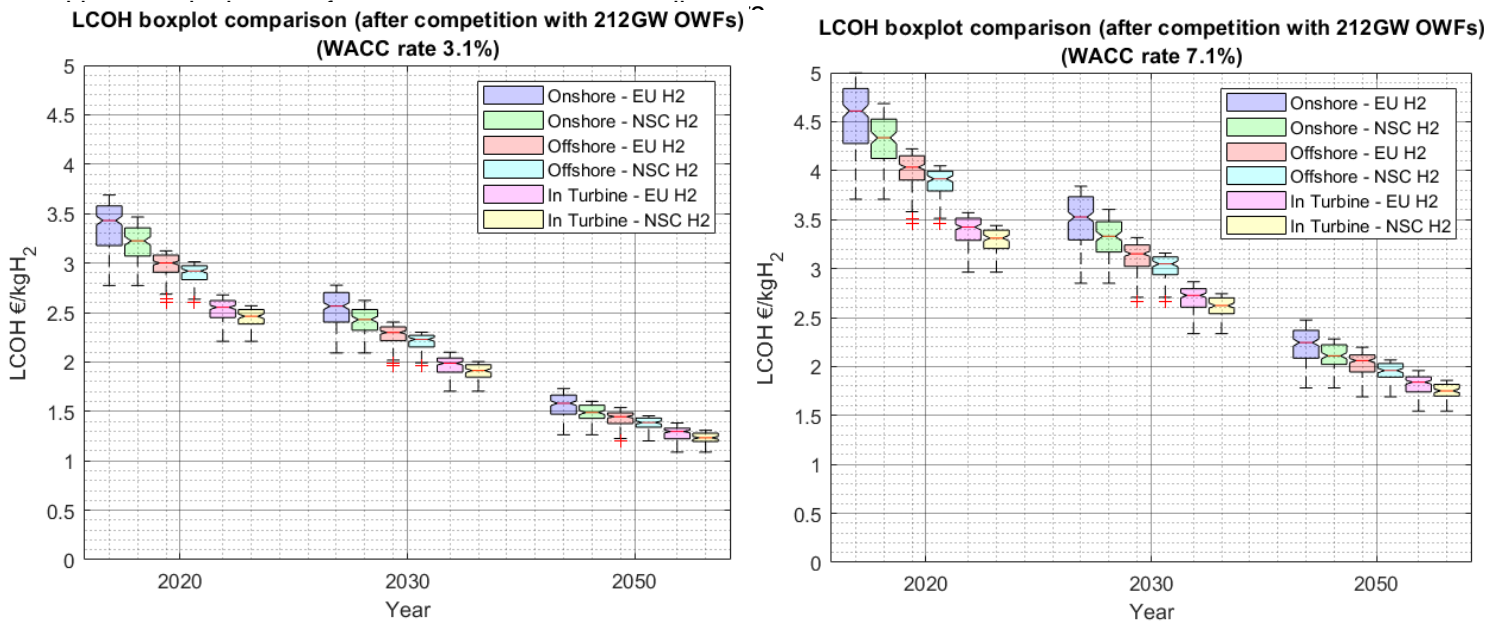


Figure 5.5. LCOH boxplot comparing the range of costs to satisfy 2050 H₂ demands after competition with 212GW OWFs

Next, the box plot in Figure 5.6 makes a comparison between the three P2H configurations with HVDC electricity added in as well. The comparison is made in relation to satisfying 50% of EU TFEC in 2050. Like the maps, we see that hydrogen becomes more competitive with electricity as we move through time for the In Turbine configuration. Between 2040 and 2050, we see a new hierarchy w.r.t the the In Turbine configuration and electricity. Minimum values between the offshore configuration and electricity differ by about 5 €/MWh while the medians differ by 10 €/MWh in 2050 for a WACC rate of 3.1%. The difference is lower for a WACC rate of 7.1%

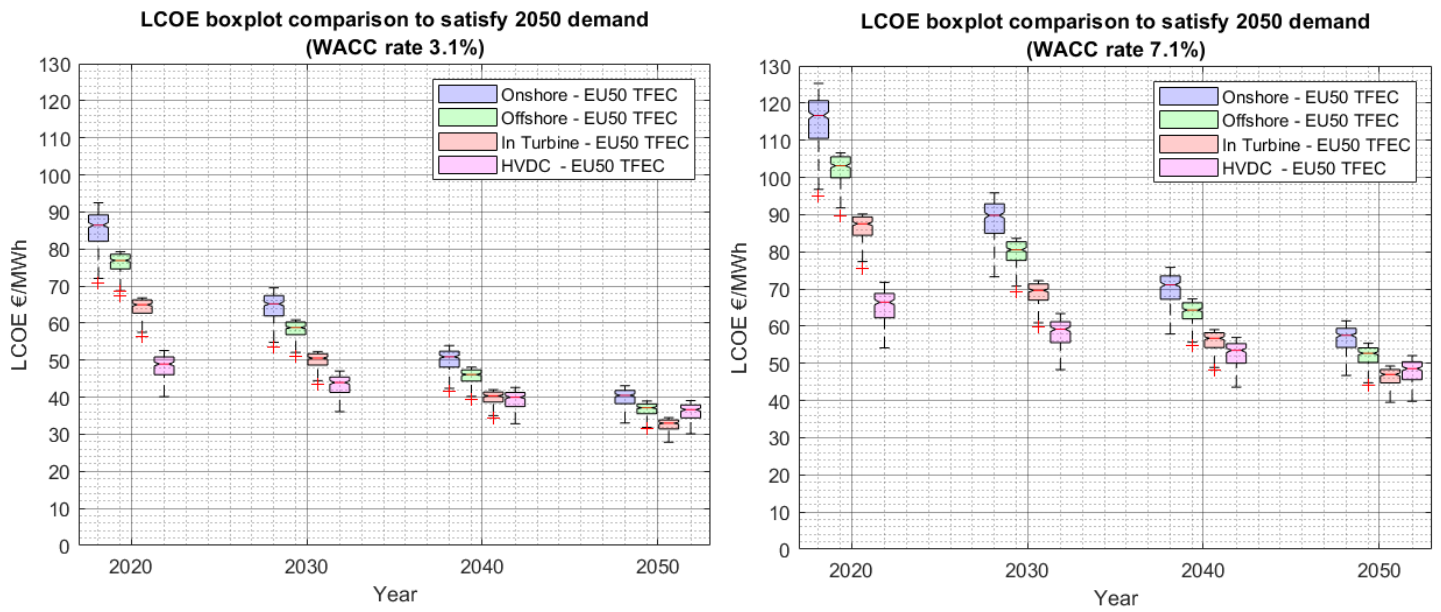


Figure 5.6. LCOE boxplot comparing the range of costs to satisfy EU-2050 TFEC demand

Finally, Figure 5.7 plots the same results but with the extreme case where all spatial exclusions are imposed on the North Sea. While the resilience of the In turbine configuration w.r.t the other two P2H configurations when subjected to the extreme case with all exclusions was already clear, the figure shows that this resilience extends to the comparison with HVDC P2E as well.

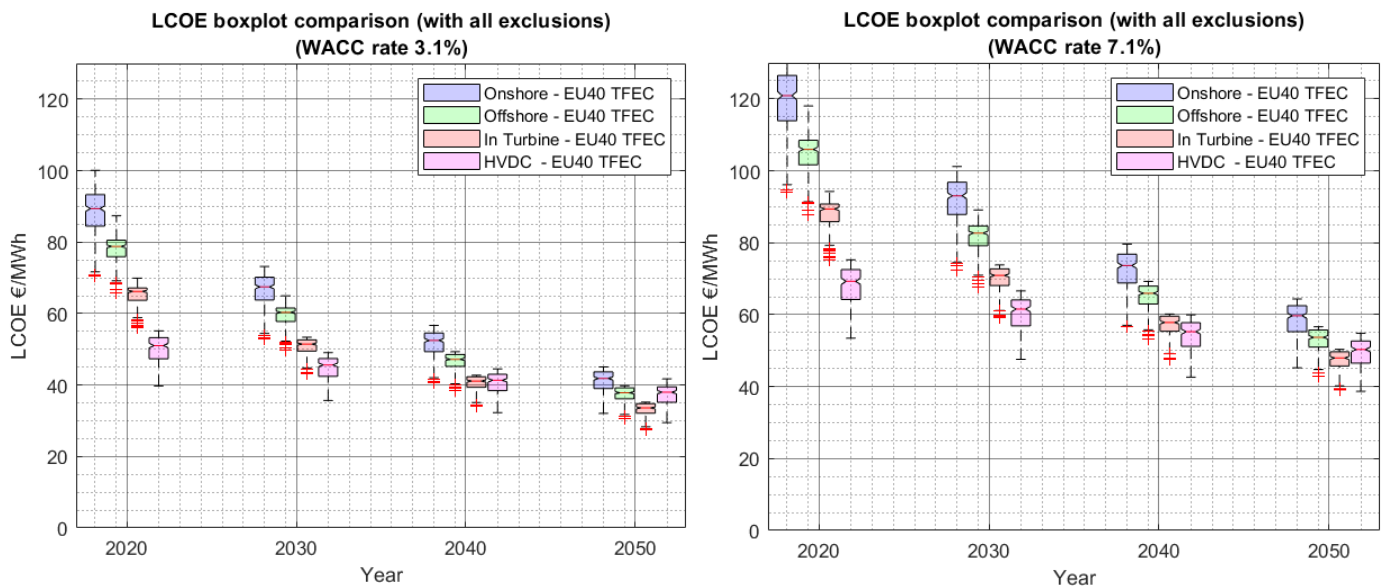


Figure 5.7. LCOE boxplot comparing the range of costs to satisfy EU-2050 TFEC demand with all exclusions

6. Conclusions

The findings of the study will now be summarized while addressing the research questions that were defined in chapter 1.

Sub-question 1: How do the three generation-conversion and transmission system configurations compare for a dedicated P2H system

The three configurations, namely: the onshore, offshore and In Turbine configurations, were tested for both Hypothetical and real world scenarios. The analysis shows that the configurations in all cases perform with the following hierarchy ON<OFF<IN. This has to mainly do with the benefits in hydrogen yield that also follows the same hierarchical order. The specific costs, follow the order IN< OFF<ON. This difference is made clearer as we move to higher depth and transmission distances for reference sites. The costs of the turbines and foundations make up up to 50% of the costs for all configurations. All configurations also show a higher sensitivity to depth than transmission distance.

Sub-question 2: How do the P2H supply paths vary in the North Sea over time and space

All configurations showed relatively flat supply curves and low spatial variance in the study area. Present day minimum costs were 2.8 €/kgH₂, 2.65 €/kgH₂ and 2.22 €/kgH₂ for the onshore, offshore and in-turbine configurations respectively. This reduced to 1.3 €/kgH₂, 1.24 €/kgH₂ and 1.1 €/kgH₂ in 2050. The offshore and in-turbine configurations when compared to the onshore case, offer maximum LCOH benefits between 19-13% and 31-22.8% across years 2020-2050 respectively. These maximum benefit locations are located in the centre and north west regions of the North Sea.

Sub-question 3: Which geographic exclusionary constraints and human activities have the most impact on the cost of the transition

The Fishing and nature zones have the most effect on the available space. Belgium and France feel the effects of spatial exclusions the most due to busier maritime waters in the southern North Sea. As far as the other five major countries go, hydrogen yield potentials in the unrestricted case are more than sufficient to meet national hydrogen demand targets in 2050. The total unrestricted and restricted hydrogen yield potentials for the In-turbine case in the North Sea are 15.8 and 24.18 EJ respectively. This represents 47% and 72% of 2050 EU TFE.

While the exclusionary effects did affect the onshore supply curve the most. This difference compared to the unrestricted case was at most 1€/kgH₂.

Sub-question 4: How does P2H in the North Sea compare with conventional HVDC P2E supply pathways

The offshore and In turbine configurations break even with HVDC P2E by 2050 and 2040 respectively. This is for some of the most expensive P2E locations at the center of the North Sea at the largest transmission distances from shore.. The maximum costs benefit for the offshore and onshore cases when compared to HVDC P2E in 2050 was found to be 7.5% and 17.4% respectively. For the In-turbine case all North Sea locations in 2050 are cheaper, with a minimum value of 5.3% closest to shore.

“What is the future potential of P2H in the North Sea , from a spatially explicit, techno-economic perspective”

The North Sea Harbours an enormous latent potential to satisfy the demands of not only the countries that surround it but also a significant portion of EU TFEC in 2050. The premise of the thesis was therefore based on exploring this potential benefit that may be possible in an hypothetical scenario in which dedicated, large scale P2H production facilities are a norm in the future North Sea area.

The thesis concludes that the In-turbine configuration is the cheapest hydrogen supply route in the North Sea in the present day. The in-turbine configuration is followed by the offshore conversion configuration. While uncertainties about scale and future prices exist, the analysis presented in this thesis showed that hydrogen may be the preferable, most cost effective energy carrier between 2040-2050, especially further offshore in the North Sea.

Bibliography

- Amin, I., Ali, M.E.A., Bayoumi, S., Oterkus, S., Shawky, H., Oterkus, E., 2020. Conceptual Design and Numerical Analysis of a Novel Floating Desalination Plant Powered by Marine Renewable Energy for Egypt. *J. Mar. Sci. Eng.* 8, 95. <https://doi.org/10.3390/jmse8020095>
- Arrambide, I., García, P.M., Ugartemendia, J.J., Zubia, I., 2017. Evaluation of electrical losses in MVAC collector systems in offshore wind farms. *Renew. Energy Power Qual. J.* 1, 287–292. <https://doi.org/10.24084/repqj15.296>
- Blanco, H., Nijs, W., Ruf, J., Faaij, A., 2018. Potential for hydrogen and Power-to-Liquid in a low-carbon EU energy system using cost optimization. *Appl. Energy* 232, 617–639. <https://doi.org/10.1016/j.apenergy.2018.09.216>
- Cavazzi, S., Dutton, A.G., 2016. An Offshore Wind Energy Geographic Information System (OWE-GIS) for assessment of the UK's offshore wind energy potential. *Renew. Energy* 87, 212–228. <https://doi.org/10.1016/j.renene.2015.09.021>
- Cleijne, H., 2021. ALGEMEEN 1–25.
- Cockerill, T.T., Kühn, M., Van Bussel, G.J.W., Bierbooms, W., Harrison, R., 2001. Combined technical and economic evaluation of the Northern European offshore wind resource. *J. Wind Eng. Ind. Aerodyn.* 89, 689–711. [https://doi.org/10.1016/S0167-6105\(01\)00066-6](https://doi.org/10.1016/S0167-6105(01)00066-6)
- Commission, E., 2019. STUDY ON BALTIC OFFSHORE WIND Final Report. <https://doi.org/10.2833/864823>
- Crivellari, A., Cozzani, V., 2020. Offshore renewable energy exploitation strategies in remote areas by power-to-gas and power-to-liquid conversion. *Int. J. Hydrogen Energy.* <https://doi.org/10.1016/j.ijhydene.2019.11.215>
- dNVGL, 2018. Power-to-Hydrogen IJmuiden Ver Final report for TenneT and Gasunie 79.
- Ebl, A., 2020. J.J.A. Eblé.
- EMODnet_bath, 2020. Bathymetric dataset - <https://portal.emodnet-bathymetry.eu/>.
- EMODnet, 2020. Human activities - <https://www.emodnet-humanactivities.eu/view-data.php>.
- EU COM, 2020. the hydrogen strategy for a climate-neutral Europe 53, 1689–1699. <https://doi.org/10.1017/CBO9781107415324.004>
- EU COM, 2019. Hybrid projects : How to reduce costs and space of offshore developments North Seas Offshore Energy Clusters study. <https://doi.org/10.2833/416539>
- EU COM, 2018. IN-DEPTH ANALYSIS IN SUPPORT OF THE COMMISSION COMMUNICATION COM (2018) 773 A Clean Planet for all A European long-term strategic vision for a prosperous , modern , competitive and Table of Contents.
- EU COM, 2016. Study on regulatory matters concerning the development of the North Sea offshore energy potential. <https://doi.org/10.2833/987989>

European Commission, 2019. The EU Blue Economy Report.

European Commission, 2017. Environmental Baseline Study for the Development of Renewable Energy Sources, Energy Storages and a Meshed Electricity Grid in the Irish and North Seas. <https://doi.org/10.2833/720927>

FCHJU, 2017. Early business cases for H2 in energy storage and more broadly power to H2 applications, Final Report, Fuel cells and hydrogen joint undertaking, P2H-BC/4NT/0550274/000/03, 2017.

Fuel Cells and Hydrogen Joint Undertaking (FCH), 2019. Hydrogen Roadmap Europe. <https://doi.org/10.2843/249013>

Ghaffour, N., Missimer, T.M., Amy, G.L., 2013. Technical review and evaluation of the economics of water desalination: Current and future challenges for better water supply sustainability. *Desalination* 309, 197–207. <https://doi.org/10.1016/j.desal.2012.10.015>

Gusatu, L.F., Yamu, C., Zuidema, C., Faaij, A., 2020. A spatial analysis of the potentials for offshore wind farm locations in the North Sea region: Challenges and opportunities. *ISPRS Int. J. Geo-Information* 9. <https://doi.org/10.3390/ijgi9020096>

IEA, 2019. The future of fuel: The future of hydrogen. *Fuel Cells Bull.* 2012, 12–15. [https://doi.org/10.1016/S1464-2859\(12\)70027-5](https://doi.org/10.1016/S1464-2859(12)70027-5)

Ioannou, A., Angus, A., Brennan, F., 2018. A lifecycle techno-economic model of offshore wind energy for different entry and exit instances. *Appl. Energy* 221, 406–424. <https://doi.org/10.1016/j.apenergy.2018.03.143>

Jepma, C., Kok, G.-J., Renz, M., van Schot, M., Wouters, K., 2018. North Sea Energy D3.6 Towards sustainable energy production on the North Sea-Green hydrogen production and CO₂ storage: onshore or offshore? 79.

Katsouris, G., Marina, A., 2016. Cost Modelling of Floating Wind Farms 36. <https://doi.org/10.1207/s15324834basp0902>

KNMI, 2020. DOWA Dataset - <https://dataplatfom.knmi.nl/open-data-info/index.html>.

Knoope, M.M.J., 2015. Costs, safety and uncertainties of CO₂ infrastructure development 359.

Koornneef, J., 2020. North Sea Energy Technical assessment of Hydrogen transport , compression , processing offshore As part of Topsector Energy :

Legorburu, I., Johnson, K.R., Kerr, S.A., 2018. Multi-use maritime platforms - North Sea oil and offshore wind: Opportunity and risk. *Ocean Coast. Manag.* 160, 75–85. <https://doi.org/10.1016/j.ocecoaman.2018.03.044>

Maienza, C., Avossa, A.M., Ricciardelli, F., Coiro, D., Troise, G., Georgakis, C.T., 2020a. A life cycle cost model for floating offshore wind farms. *Appl. Energy* 266, 114716. <https://doi.org/10.1016/j.apenergy.2020.114716>

Maienza, C., Avossa, A.M., Ricciardelli, F., Coiro, D., Troise, G., Georgakis, C.T., 2020b. A life cycle cost model for floating offshore wind farms. *Appl. Energy* 266, 114716. <https://doi.org/10.1016/j.apenergy.2020.114716>

- Maness, M., Maples, B., Maness, M., Maples, B., 2017. NREL Offshore Balance-of- System Model NREL Offshore Balance-of- System Model.
- Markus Reuß; Lara Weldera; Johannes Thußrauf; Jochen Linßena;Thomas Grubea; Lars Schewed; Martin Schmidte;, 2019. Modeling hydrogen networks for future energy systems: A comparison of linear and nonlinear approaches.
- Möller, B., Hong, L., Lonsing, R., Hvelplund, F., 2012. Evaluation of offshore wind resources by scale of development. *Energy* 48, 314–322. <https://doi.org/10.1016/j.energy.2012.01.029>
- Möller Bernd, B., 2011. Continuous spatial modelling to analyse planning and economic consequences of offshore wind energy. *Energy Policy* 39, 511–517. <https://doi.org/10.1016/j.enpol.2010.10.031>
- Musial, W., Beiter, P., Nunemaker, J., 2020. Cost of Floating Offshore Wind Energy Using New England Aqua Ventus Concrete Semisubmersible Technology 43.
- Musial, W., Beiter, P., Nunemaker, J., Heimiller, D., Ahmann, J., Busch, J., Musial, W., Beiter, P., Nunemaker, J., Heimiller, D., Ahmann, J., Busch, J., 2019. Oregon Offshore Wind Site Feasibility and Cost Study Oregon Offshore Wind Site Feasibility and Cost Study.
- Myhr, A., Bjerkseter, C., Ågotnes, A., Nygaard, T.A., 2014. Levelised cost of energy for offshore floating wind turbines in a lifecycle perspective. *Renew. Energy* 66, 714–728. <https://doi.org/10.1016/j.renene.2014.01.017>
- NSEC, 2020. Joint Statement of North Seas Countries and the European Commission.
- NSWPH, 2020. Integration routes North Sea offshore wind 2050. North Sea Wind Power Hub.
- NSWPH, 2019. Cost Evaluation of North Sea Offshore Wind Post 2030.
- Nyserda, 2018. Analysis of Turbine Layouts and Spacing Between Wind Farms for Potential New York State Offshore Wind Development.
- Peters, J.L., Remmers, T., Wheeler, A.J., Murphy, J., Cummins, V., 2020. A systematic review and meta-analysis of GIS use to reveal trends in offshore wind energy research and offer insights on best practices. *Renew. Sustain. Energy Rev.* 128, 109916. <https://doi.org/10.1016/j.rser.2020.109916>
- Reuß, M., Grube, T., Robinius, M., Preuster, P., Wasserscheid, P., Stolten, D., 2017. Seasonal storage and alternative carriers: A flexible hydrogen supply chain model. *Appl. Energy* 200, 290–302. <https://doi.org/10.1016/j.apenergy.2017.05.050>
- Roobeek, R.E., 2020. Shipping Sunshine A techno-economic analysis of a dedicated green hydrogen supply chain from the Port of Sohar to the Port of Rotterdam.
- Rubí, L., González, R., 2018. 2050:Power-to-hydrogen opportunities for far off-shore wind farms.
- Schillings, C., Wanderer, T., Cameron, L., van der Wal, J.T., Jacquemin, J., Veum, K., 2012. A decision support system for assessing offshore wind energy potential in the North Sea. *Energy Policy* 49, 541–551. <https://doi.org/10.1016/j.enpol.2012.06.056>
- Shafiee, M., Brennan, F., Espinosa, I.A., 2016. A parametric whole life cost model for offshore wind farms. *Int. J. Life Cycle Assess.* 21, 961–975. <https://doi.org/10.1007/s11367-016-1075-z>

The Crown Estate, 2019. A Guide to an Offshore Wind Farm. Power 1–70.

Valpy, B., Hundleby, G., Freeman, K., Roberts, A., Logan, A., 2017. Future renewable energy costs: offshore wind. *Futur. Renew. energy costs* 80. <https://doi.org/10.1016/j.jembe.2010.04.022>

van Schot, M., Jepma, C., 2020. North Sea Energy: A vision on hydrogen potential from the North Sea.

van Wijk, A., Hellinga, C., 2018. Hydrogen, the key to the energy transition. *Water* 10–12.

Wijk, A. van, Chatzimarkakis, J., 2020. Green Hydrogen for a European Green Deal 39.

Wijnant, I.L., Ulft, B. Van, Stratum, B. Van, Barkmeijer, J., Onvlee, J., Valk, C. De, Knoop, S., Kok, S., Marseille, G.J., Baltink, H.K., Stepek, A., 2019. The Dutch Offshore Wind Atlas (DOWA): description of the dataset. DOWA Proj.

Wind Europe, 2019. Our Energy Our Future.